FACULDADE DE MEDICINA

PROGRAMA DE PÓS-GRADUAÇÃO EM PATOLOGIA MOLECULAR

Alterações Proteômicas e Bioquímicas Envolvidas nas Respostas Febris Induzidas por LPS e PGE_2 em Ratos

Marina Firmino Lima de Oliveira

Orientador: Prof. Dr. Marcelo Valle de Sousa

Co-orientadora: Profa. Dra. Fabiane Hiratsuka Veiga de Souza

Brasília

2018

FACULDADE DE MEDICINA

PROGRAMA DE PÓS-GRADUAÇÃO EM PATOLOGIA MOLECULAR

Marina Firmino Lima de Oliveira

Tese de Doutorado

Alterações Proteômicas e Bioquímicas Envolvidas nas Respostas Febris Induzidas por LPS e PGE_2 em Ratos

Tese apresentada ao programa de Pós-Graduação em Patologia Molecular como requisito parcial para obtenção do título de Doutor.

Orientador: Prof. Dr. Marcelo Valle de Sousa

Co-orientadora: Profa. Dra. Fabiane Hiratsuka Veiga de Souza

Brasília

2018

“Dias inteiros de calmaria, noites de ardentia,

dedos no leme e olhos no horizonte,

descobri a alegria de transformar distâncias em tempo.

Um tempo em que aprendi,

a entender as coisas do mar,

a conversar com as grandes ondas

e não discutir com o mal tempo.

A transformar o medo em respeito,

o respeito em confiança.

Descobri como é bom chegar quando se tem paciência.

E para se chegar onde quer que seja,

aprendi que não é preciso dominar a força, mas a razão.

É preciso antes de mais nada querer.”

Amyr Klink

Dedicatória

Aos meus pais,

pelo ombro, pelo choro,

pelo sorriso, pelo abraço,

pelo amor incondicional que une nossa família.

Agradecimentos

À Deus que me ampara, protege e guia sempre.

Ao meu querido orientador Prof. Marcelo, por toda generosidade, compreensão, pelo incentivo e pela paciência comigo. Por ter me dado oportunidades únicas, que eu jamais pensei que teria. Por acreditar em mim, apesar das minhas falhas e dificuldades. Por ser muito mais que um orientador, mas um exemplo, pessoal e profissional.

À Profa. Fabiane, pela co-orientação. Por me permitir fazer parte do seu grupo de pesquisa, por todo conhecimento compartilhado e pela oportunidade de crescimento.

À todos os professores e colaboradores do Laboratório de Bioquímica e Química de Proteínas: Prof. Sebastien, Profa. Mariana, Prof. Luís, Seu Antônio e Nuno. Em especial, ao Prof. Wagner pelas aulas de bioquímica e espectrometria de massas, por sua disponibilidade e boa vontade em ajudar. Ao Prof. Carlos André, nosso querido C.A., por sempre se preocupar com todos no lab, e sempre arrumar um tempinho para perguntar: “E ai Marina?, como anda o seu trabalho?”. À Profa. Consuelo, mãezona querida, por todos os conselhos e sua magnânima sabedoria e bondade. Saibam que tenho profunda admiração pelo trabalho, dedicação e competência de todos vocês.

À Profa. Tatiana, pela disponibilidade e auxílio nas análises por citometria de fluxo.

Ao Prof. Paulo Souza, por sempre arrumar soluções criativas para nossos problemas operacionais, por todos os ensinamentos, pela simpatia e amizade.

À todos os colegas do laboratório e do grupo de febre. Em especial, à Bruna por me ajudar em tantos experimentos ao longo desses anos e ao Alan pelo auxílio nas sofridas análises estatísticas.

Aos meus antigos e queridos amigos, Agenor, Micaela, e Aline por todos os momentos compartilhados. Ao Jaques, pela presença, por todo apoio e amizade, por fazer parte da minha rotina, por me deixar ser “tia” do Pedro. À Simone, por todas as horas de ensinamento, por me

fazer pensar, interpretar meus resultados, escrever meus artigos, por me incentivar a ser sempre melhor, por me ensinar a amar a ciência e além de tudo obrigada pelo carinho e amizade. Jaques e Simone vocês são irmãos científicos para mim!

À minha pequena e unida família. Meus queridos pais, Márcia e Carlos André, minha irmã Gabriela, meus tios, avós, sogros e agregados. Obrigada por me apoiarem e por acreditarem que um dia eu chegaria lá! Amo vocês mais do que tudo nesta vida!

Ao meu marido, meu companheiro, meu amor, Diego. Obrigada pelo bom humor constante, por me apoiar e por estar ao meu lado nos momentos mais difíceis. Te amo muito!

Aos funcionários do biotério e ao Jivago por tornar a nossa pesquisa viável.

Ao CNPq pela bolsa concedida, à CAPES e à FAPDF.

Sumário

Apresentação

Esta tese está organizada em tópicos, a saber: **Introdução**, **Objetivos**, **Capítulos** (1 – referente ao manuscrito submetido a revista *Journal of Proteomics*; 2 – referente ao manuscrito a ser submetido a revista *Neuroscience Letters* e 3 – referente a resultados não publicados), **Discussão**, **Conclusões**, **Perspectivas**, **Referências Bibliográficas** e **Anexos**.

A **Introdução** apresenta o embasamento teórico que nos levou a formular a proposta de trabalho. Os **Objetivos** – geral e específicos – estão dispostos no corpo da tese e em maiores detalhes inseridos dentro de cada capítulo. Os **Capítulos** contêm os manuscritos e mais alguns resultados não publicados, mas realizados durante o período do doutorado. As análises farmacológicas, bioquímicas e proteômicas foram desenvolvidas no Laboratório de Bioquímica e Química de Proteínas (Departamento de Biologia Celular, Universidade de Brasília - UnB). As análises por citometria de fluxo foram realizadas no Laboratório de Imunologia Celular (Faculdade de Medicina, Universidade de Brasília – UnB).

O tópico **Discussão** apresenta uma interpretação geral dos resultados obtidos nos diferentes trabalhos. Nas seções **Conclusões** e **Perspectivas** há uma abordagem geral das conclusões da tese e as possibilidades de futuros trabalhos a partir dos resultados obtidos na presente tese.

As **Referências Bibliográficas** contêm somente as referências dos trabalhos citados nos tópicos **Introdução** e **Discussão**.

O **Anexo 1** contém a declaração de aprovação pelo comitê de ética no uso animal (CEUA) do Instituto de Ciências Biológicas da UnB. O **Anexo 2** contém o aceite do manuscrito, apresentado no capítulo 1, com *minor revision*, pela revista *Journal of Proteomics*. O **Anexo 3** traz a publicação de parte dos dados desta tese nos anais do congresso PPTR, e o **Anexo 4** contém o artigo científico que foi realizado durante o período do doutorado e tem conteúdo associado ao tema da tese.

As tabelas suplementares deste trabalho poderão ser obtidas mediante solicitação via e-mail encaminhado ao seguinte correio eletrônico: marinafirminolima@gmail.com

Lista de Figuras

Lista de Tabelas

Lista de Abreviaturas e Siglas

β_3-AR: *β3-adrenergic Receptor*; Receptor β_3 Adrenérgico

AC: Adenilil Ciclase

AH/POA: *Preoptic Area in the Anterior Hypothalamus*; Área Pré-óptica do Hipotálamo Anterior

AINEs: Antiinflamatórios não esteroidais

AMPc: adenosina 3',5'-monofosfato cíclico

AP-1: *Activator Protein 1*; Proteína Ativadora 1

ATGL: *Adipose Triglyceride Lipase*; Lipase de Triglicerídeos do Tecido Adiposo

BAT: *Brown Adipose Tissue*; Tecido Adiposo Marrom

BMCP: *Brain Mitochondrial Carrier Protein*

Ca^{2+}: Cálcio

cPGES: *Cytosolic Prostaglandin E Synthase*; Prostaglandina E sintase citosólica

cPLA2-α: *Cytosolic Phospholipase A2-α*; Fosfolipase A2 citosólica α

COX: Cicloxigenase

CREB1: *cAMP-Responsive-Element-Binding protein 1*; Proteína de Ligação ao Elemento de Resposta do AMPc

DMH: *Dorsomedial Hypothalamus*; Núcleo Dorsomedial do Hipotálamo

EP: *Prostaglandin E_2 Receptor* ; Receptor de Prostaglandina

ERK: *Extracellular Signal-regulated Kinase*; Cinases Reguladas por Sinais Extracelulares

FFAs: *Free Fatty Acids*; Ácidos Graxos Livres

Gi: Proteína G inibitória

Gs: Proteína G estimulatória

H-89: *N-[2-(p-Bromocinnamylamino)ethyl]-5-isoquinolinesulfonamide*

HSL: *Hormone Sensitive Lipase*; Lipase Hormônio-sensível

HSP: *Heat-Shock Proteins*; Proteínas de choque-térmico

HT: Hipotálamo

IFN-α: Interferon α

IL-1β: *Interleukin 1β*; Interleucina 1β

IL-6: *Interleukin 6*; Interleucina 6

IML: *Intermediolateral Nucleus*; Núcleo Intermediolateral

IP3: Fosfatidilinositol trifosfato

IRAK: *IL-1R-associated Kinases*; Cinase Associada ao Receptor IL-1

IRF: *Interferon Regulatory Factors*; Fatores Regulatórios de Interferon

JNK: *c-Jun N-terminal Kinase*; Cinase c-Jun N-terminal

LBP: *LPS Binding Protein*; Proteína de Ligação ao LPS

LC-MS/MS: Cromatografia Líquida Acoplada a Espectrometria de Massas em Tandem

LPS: Lipopolissacarídeo Bacteriano

MAL: *MyD88-adaptor-like*; Proteína Adaptadora Semelhante a MyD88

MAPK: *Mitogen-activated Protein Kinase*; Proteína Cinase Ativada por Mitógenos

MAPKK: *Mitogen-activated Protein Kinase Kinase*

MAPKKK: *Mitogen-activated Protein Kinase Kinase Kinase*

MD2: *Myeloid Differentiation Protein 2*; Proteína de Diferenciação Mielóide 2

MDP: Muramil-dipeptídeo

MnPO: *Hypothalamic Median Preoptic Nucleus*; Núcleo Mediano Pré-óptico

MPA: *Medial Preoptic Area*; Área Pré-óptica Medial

mPGES-1: *Microsomal Prostaglandin E* Synthase; Prostaglandina E Sintase Microssomal

MyD88: *Myeloid Differentiation Primary Response Protein 88*; Fator 88 de Diferenciação Mielóide

NFκB: *Nuclear Factor κB*; Fator Nuclear Kappa B

NF-IL6: *Nuclear Factor Interleukin-6*; Fator Nuclear Interleucina 6

OVLT: *Organum Vasculosum Laminae Terminalis*; Órgão Vascular da Lamina Terminal

PAMPs: *Pathogen-associated Molecular Pattern;* Padrões Moleculares Associados a Patógenos

PGs: Prostaglandinas

PGE_2: Prostaglandina E_2

PGG_2: Prostaglandina G_2

PGH_2: Prostaglandina H_2

PKA: Proteína cinase dependente de AMP cíclico

PKC: Proteína cinase C

Poli I:C: Ácido Poliinosínico:policitidílico

Prkcsh: *PKC substrate 80 K-H*

PuNu: *Purine Nucleotides*; Nucleotídeos de Purina

ROS: *Reactive Oxygen Species*; Espécies reativas de oxigênio

rRPa: *Rostral Raphe Pallidus*; Núcleo Pálido da Rafe

SPNs: *Sympathetic Preganglionic Neurons*; Neurônios Pré-ganglionares Simpáticos

STAT3: *Signal Transducer and Activator of Transcription*; Fator Ativador de Transcrição de Sinal e Transdutor de Ativação

TAK1: *Transforming Growth Factor β-activated Kinase 1*; Cinase 1 Ativadora do Fator Transformador de Crescimento β

TGL: *Triglycerides*; Triglicerídeos

TLR4: *Toll Like Receptor 4*

TRAF3: *TNF-receptor-associated Factor* 3; Fator 3 Associado ao Receptor do TNF

TRAF6: *TNF-receptor-associated Factor 6*; Fator 6 Associado ao Receptor do TNF

TRAM: *TRIF-related Adaptor Molecule*; Molécula Adaptadora Relacionada a TRIF

TRIF: *TIR-domain-containing Adaptor Protein Inducing IFN-β*; Domínio TIR Contendo Adaptador indutor de IFN-β

TNF-α: *Tumor Necrosis Factor α*; Fator de Necrose Tumoral α

UCPs: *Uncoupling proteins*; Proteínas desacopladoras

VH: *Ventral Horn*; Corno Ventral

WAT: *White Adipose Tissue*; Tecido adiposo branco

W-S: *Warm-sensitive*; Termo sensíveis

Resumo

A febre é uma antiga e bem caracterizada resposta de defesa do hospedeiro, em geral iniciada pela produção de prostaglandina E_2 (PGE_2) na área pré-óptica do hipotálamo anterior (AH/POA) em resposta a mediadores químicos, produzidos durante processos infecciosos ou inflamatórios. A sinalização desencadeada na AH/POA induz a ativação de mecanismos para produção e conservação de calor como, por exemplo, a termogênese no tecido adiposo marrom (BAT) e nos músculos esqueléticos, por meio de tremores, e vasoconstricção periférica. Na presente tese, investigamos as alterações proteômicas e bioquímicas, bem como as vias de sinalização envolvidas na gênese da resposta febril induzida pelos estímulos lipopolissacarídeo (LPS) e PGE_2. Um total de 1.388 proteínas diferencialmente expressas foram identificadas no grupo LPS e 895, no grupo PGE_2. De maneira geral, observamos que ambos os estímulos induzem alterações significativas no proteoma hipotalâmico, sendo que estão relacionadas principalmente a vias inflamatórias e metabólicas. Considerando as vias metabólicas, observamos que os ratos expostos aos estímulos pirogênicos apresentaram redução na abundância relativa de várias proteínas inseridas nas vias da glicólise, pentoses-fosfato e ciclo de Krebs, além de promover a redução na abundância de diversas proteínas dos complexos mitocondriais, sendo os complexos I e IV os mais impactados. Tendo em vista que a mitocôndria é a principal fonte de produção de calor na célula, e as significativas alterações na abundância de proteínas dos complexos mitocondriais, investigamos também os efeitos da resposta febril induzida por LPS sobre a função mitocondrial, no hipotálamo (HT) e BAT. No BAT, observamos que a resposta febril induz redução no fluxo de elétrons entre os complexos I e III, sem alterar o potencial de membrana mitocondrial. Acredita-se que esta redução possa contribuir para o maior escape de elétrons e formação de espécies reativas de oxigênio, que, por sua vez, contribuem com o desenvolvimento de febre. Por outro lado, no HT, apesar da redução na abundância de proteínas mitocondriais, não houve comprometimento da atividade dos complexos, nem do potencial de membrana mitocondrial. Por fim, investigamos o efeito da inibição farmacológica das proteínas cinases A e C (PKA e PKC), com a finalidade de compreender como estas proteínas se relacionam com o desenvolvimento da febre. O inibidor de PKC promoveu redução parcial da resposta febril induzida por LPS e PGE_2, enquanto que o inibidor de PKA foi capaz de reduzir apenas a febre induzida pelo LPS. Acredita-se que o conhecimento das vias metabólicas envolvidas na resposta febril é importante não somente para melhor compreender os mecanismos pelos quais esta resposta se desenvolve, mas também para avaliar efeitos metabólicos decorrentes dela. A caracterização destas vias pode ainda acelerar o desenvolvimento de agentes terapêuticos mais específicos e com menor incidência de efeitos colaterais.

Abstract

Fever is an ancient host-defense response generally initiated by the production of prostaglandin E_2 (PGE_2) within preoptic area in the anterior hypothalamus (AH/POA) in response to inflammatory mediators, released during infection or inflammation. The signaling triggered in AH/POA induces the activation of mechanisms for heat production, such as shivering, brown adipose tissue (BAT) thermogenesis and cutaneous vasoconstriction among them. In this thesis, proteomic and biochemical alterations induced by both lipopolysaccharide (LPS) and PGE_2 stimuli were investigated as well as the signaling pathways related to the initiation of the febrile response. A total of 1,388 and 895 differentially abundant proteins were found in LPS and PGE_2 groups respectively. In general, it was observed that both stimuli induced significant alterations in the hypothalamic proteome, and these alterations are mainly related to inflammatory and metabolic pathways. Considering metabolic pathways, rats exposed to LPS or PGE_2 presented lower relative abundance of proteins involved in glycolysis, pentose-phosphate pathway and tricarboxylic acid cycle. Mitochondrial function might also be altered by both stimuli because significant downregulation of several proteins was found, mainly in complexes I and IV. Considering that mitochondria are the main source of heat production in cell, and that significant changes in abundance of mitochondrial proteins occurred, we also investigated the effects of LPS-induced fever on mitochondrial function in hypothalamus (HT) and BAT. Inhibition in electron transport chain complex I-III activity was observed in BAT, without impairment of mitochondrial membrane potential. On the other hand, no changes were detected in the HT neither in mitochondrial complexes activities nor in membrane potential at the time point observed. These findings suggest that fever induced by LPS caused a mild inhibition in BAT mitochondrial function that possibly contribute for reactive oxygen species production and fever generation. Finally, the pharmacological inhibition effect of protein kinases A and C (PKA and PKC) were also investigated, in order to understand how these proteins are related to fever development. PKC inhibitor promoted a partial reduction on febrile response induced by LPS and PGE_2, whereas PKA inhibitor was able to reduce only the LPS-induced fever. It is believed that the identification of the metabolic pathways involved in fever response is important not only to better understand the mechanisms for the development of this response, but also to assess the metabolic effects arising from it. The characterization of these pathways may also foster the development of more specific therapeutic agents, with less incidence of side effects.

1. Introdução

1.1 Febre: Definição e Bases Fisiológicas

A febre é uma resposta complexa, caracterizada pelo aumento da temperatura corporal, e controlada por um circuito fisiológico e neuronal integrado. Ocorre como parte da resposta de defesa do organismo, geralmente durante processos infecciosos e inflamatórios (EVANS; REPASKY; FISHER, 2015; OGOINA, 2011; ROTH; BLATTEIS, 2014; ZEISBERGER, 1999). A resposta febril é acompanhada de várias alterações comportamentais, bem como de alterações metabólicas, bioquímicas e fisiológicas necessárias para o aumento da temperatura corporal (DANTZER, 2004; HASDAY; THOMPSON; SINGH, 2014; TANSEY; JOHNSON, 2015).

Uma imensa diversidade de substâncias pode desencadear respostas de defesa no hospedeiro. Considerando os conceitos clássicos relacionados ao desenvolvimento da resposta febril, chamamos de pirogênios as substâncias capazes de induzir febre, sendo estes classificados em exógenos e endógenos dependendo de sua origem. Os pirogênios exógenos estão presentes no ambiente e geralmente compreendem microrganismos e seus subprodutos, porém, qualquer estímulo capaz de induzir uma resposta inflamatória e consequentemente levar à febre pode ser considerado um pirogênio exógeno. Uma vez presentes no hospedeiro, os pirogênios exógenos estimulam as células do sistema imune a produzir e secretar mediadores inflamatórios, conhecidos como pirogênios endógenos (DINARELLO, 2004; EVANS; REPASKY; FISHER, 2015; ROTH; BLATTEIS, 2014; ROTH; DE SOUZA, 2001) (**Figura 1**).

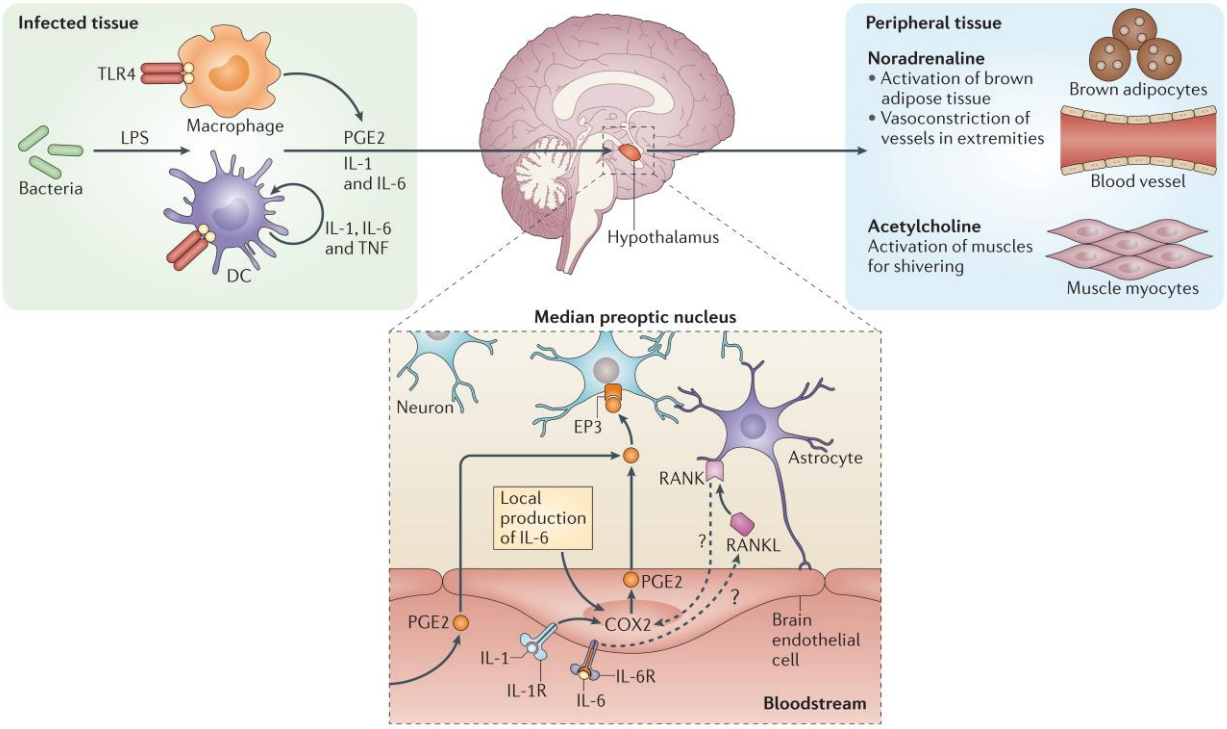

Figura 1: Indução de febre durante processos infecciosos. Extraído de: (EVANS; REPASKY; FISHER, 2015).

Atualmente, sabe-se que estes mediadores sintetizados em resposta à presença de pirogênios exógenos pertencem a uma classe de pequenos peptídeos imunorregulatórios conhecidos como citocinas. Estas moléculas possuem uma potente atividade biológica e algumas delas são intrinsicamente pirogênicas, isto é, quando presentes são capazes de induzir febre dentro de poucos minutos. Dentre elas, o fator de necrose tumoral α (TNF-α), as interleucinas 1β (IL-1β) e 6 (IL-6) e o interferon α (IFN-α) são as principais citocinas envolvidas no desenvolvimento da resposta febril (DINARELLO, 2004; HARDEN et al., 2006; KLUGER, 1991; LUHESHI; ROTHWELL, 1996) (**Figura 1**). Apesar da importância destes mediadores endógenos devemos ainda considerar a ação direta (independente dos pirogênios endógenos) dos pirogênios exógenos que podem se ligar a receptores específicos presentes nas células endoteliais, localizadas na AH/POA, e desencadear a sinalização necessária para a produção de PGE_2 e desenvolvimento da resposta febril (DINARELLO, 2004).

Diversos modelos experimentais são utilizados para estudar o desenvolvimento, caracterização e controle da resposta febril. Dentre os pirogênios exógenos utilizados nestes modelos, podemos citar o muramil-dipeptídeo (MDP) (ROTH et al., 1997), o lipopolissacarídeo bacteriano (LPS) (BLATTEIS, 2006; DERIJK et al., 1993; FRAIFELD; KAPLANSKI, 1998), o ácido poliinosínico:policitidílico (Poli I:C) (BASTOS-PEREIRA et al., 2015; FORTIER, 2004), o *Estafilococos aureus* (*S. aureus*) (MARTINS et al., 2012) e o zymosan - um polissacarídeo preparado a partir da parede celular de leveduras (KANASHIRO et al., 2009). Apesar desta grande diversidade, a maior parte dos estudos utiliza o modelo clássico de indução de febre, onde o LPS é utilizado como estímulo pirogênico e os roedores como espécie animal. Em razão disso, a maior parte do conhecimento a respeito da fisiologia da resposta febril é sustentado por este modelo experimental (ROTH; BLATTEIS, 2014; ZAMPRONIO; SOARES; SOUZA, 2015).

O LPS é o principal constituinte estrutural da parede celular de bactérias gram-negativas, composto por um domínio hidrofóbico, o lipídio A (também conhecido como endotoxina), um cerne polissacarídico e um polissacarídeo O (DEMON; VANDE WALLE; LAMKANFI, 2014; TORTORA; FUNKE; CASE, 2017) (**Figura 2**). O sistema imune do hospedeiro reconhece a presença do LPS por meio da ligação do lipídeo A ao receptor *Toll Like 4* (TLR4) encontrado na superfície de diversas células, como por exemplo, em macrófagos, neutrófilos, neurônios, micróglia, astrócitos e células endoteliais cerebrais (AKIRA; TAKEDA, 2004; AKIRA; UEMATSU; TAKEUCHI, 2006; KONG; LE, 2011; VAURE; LIU, 2014). Desta forma, acredita-se que o lipídio A seja o principal componente responsável por desencadear as manifestações próprias dos processos inflamatórios decorrentes de infecções por bactérias gram-negativas, como por exemplo a febre (RAETZ et al., 2007; ROTH; BLATTEIS, 2014; TORTORA; FUNKE; CASE, 2017; WANG; QUINN, 2010). O cerne polissacarídico encontra-se ligado ao lipídeo A e desempenha uma função estrutural,

contribuindo para manutenção da integridade e viabilidade da bactéria. Por fim, o polissacarídeo O funciona como antígeno sendo útil para diferenciar espécies de bactérias gram-negativas (TORTORA; FUNKE; CASE, 2017). Os componentes polissacarídicos contribuem ainda para resistência contra a ação de antibióticos, ataques do sistema imune e outros estresses ambientais (RAETZ; WHITFIELD, 2002) (**Figura 2**).

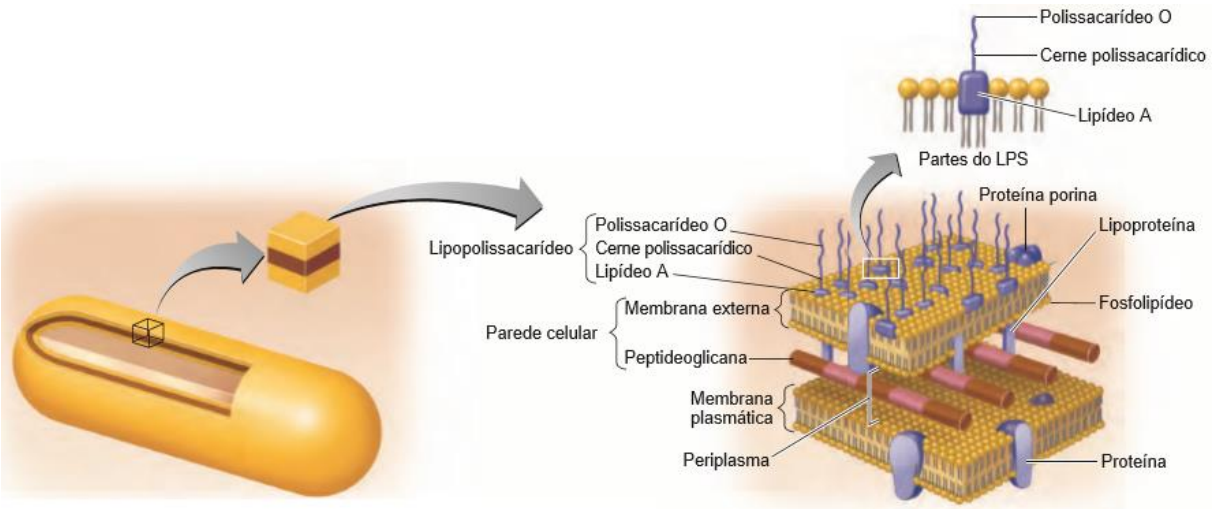

Figura 2: Estrutura do LPS. Extraído de: TORTORA; FUNKE; CASE, 2017.

Uma vez estimuladas pelo LPS, as células do sistema imune induzem a rápida transcrição de diversos genes essenciais para o desenvolvimento da resposta inflamatória, incluindo os genes necessários para síntese de citocinas, quimiocinas, receptores e enzimas inflamatórias (MEDZHITOV; HORNG, 2009; RUMMEL, 2016). Esta resposta é controlada por fatores de transcrição constitutivamente expressos em vários tipos celulares, como o fator nuclear kappa B (NFκB), o fator ativador de transcrição de sinal e transdutor de ativação (STAT3), o fator nuclear interleucina 6 (NF-IL6), o fator regulador de interferon (IRF), a proteína de ligação ao elemento de resposta ao AMPc (CREB1) e proteína ativadora 1 (AP-1) (MEDZHITOV; HORNG, 2009; RAHIMIFARD et al., 2017; RUMMEL, 2016).

Diversos estudos demonstram que as respostas febris produzidas por pirogênios, sejam eles exógenos ou endógenos, dependem da ação central de prostaglandinas (PGs), principalmente a PGE_2, considerada o mediador final da febre (IVANOV; ROMANOVSKY, 2004; ROTH; BLATTEIS, 2014; SAPER; ROMANOVSKY; SCAMMELL, 2012; ZAMPRONIO; SOARES; SOUZA, 2015) (**Figura 1**).

1.2 Termorregulação e Febre

O sistema termorregulatório é formado por três componentes integrados: a porção sensorial aferente, a porção integradora e a porção de respostas eferentes. A área pré-óptica do hipotálamo anterior funciona como um centro termorregulatório (BOULANT, 2000) sendo, portanto, responsável por integrar as informações provenientes de termorreceptores centrais e periféricos aferentes e desencadear respostas eferentes apropriadas para o controle da temperatura corporal (NAKAMURA, 2011). Acredita-se que a regulação da temperatura corporal pela AH/POA baseia-se na existência de um mecanismo similar a um termostato, que foi denominado de ponto de equilíbrio térmico "*balance point*" (BOULANT, 2000; BOULANT; DEAN, 1986; BOULANT; SILVA, 1988; ROTH; BLATTEIS, 2014; TANSEY; JOHNSON, 2015).

Durante a febre, mediadores centrais como a PGE_2, alteram a frequência de disparo dos neurônios que regulam a temperatura corporal na AH/POA, de forma que o ponto de regulagem hipotalâmico é alterado para valores superiores de temperatura. Essa alteração leva a ativação de respostas termorregulatórias de produção e conservação do calor ao mesmo tempo em que ativa mecanismos para inibição da perda de calor (EVANS; REPASKY; FISHER, 2015; NAKAMURA, 2011; ROTH et al., 2009; TANSEY; JOHNSON, 2015) (**Figura 1**).

O local de produção da PGE_2 que atua sobre a AH/POA produzindo febre é ainda um tema controverso. Alguns autores acreditam que durante a fase inicial da resposta febril a PGE_2 seja produzida na periferia, por macrófagos pulmonares e hepáticos ativados, e posteriormente transportada pela corrente sanguínea para a AH/POA (LI et al., 2006; NAKAMURA, 2011; ROTH et al., 2009; ROTONDO et al., 1988). Outros dados sugerem que a produção de PGE_2 ocorreria em locais mais próximos anatomicamente da AH/POA, como por exemplo no órgão vascular da lamina terminal (OVLT) (STITT, 1991), pela micróglia e macrófagos perivasculares cerebrais (SCHILTZ; SAWCHENKO, 2002) e células endoteliais cerebrais (ENGSTRÖM et al., 2012). Dados recentes sugerem ainda que células endoteliais hipotalâmicas seriam essenciais para produção de PGE_2 durante a febre induzida por LPS (ESKILSSON et al., 2017).

Segundo Morrisson (2016), processos infecciosos estão associados à presença de PGE_2 na AH/POA **(Figura 3)**. Uma vez presente neste local, a PGE_2 se liga aos receptores de prostaglandina (EP3) e provoca a atenuação da atividade de neurônios inibitórios (sensíveis ao calor) que apresentam projeções descendentes para o núcleo dorsomedial do hipotálamo (DMH) e núcleo pálido da rafe (rRPa). A atenuação da inibição destes neurônios causa a desinibição de neurônios pré-motores no DMH e rRPa. Estes por sua vez, se comunicam com neurônios pré-ganglionares simpáticos (SPNs), presentes no núcleo intermediolateral (IML), e com motoneurônios (α e γ), no corno ventral (VH), desencadeando assim mecanismos efetores para aumentar a termogênese e a temperatura corporal (MORRISON, 2016; NAKAMURA, 2011; TANSEY; JOHNSON, 2015; TUPONE; MADDEN; MORRISON, 2014). Dentre os mecanismos relacionados ao aumento da temperatura corporal podemos citar: aumento da termogênese no tecido adiposo marrom, no músculo esquelético por meio de tremores, e aumento da vasoconstrição periférica de forma a conservar a temperatura corporal e evitar a

perda de calor para o ambiente (MORRISON, 2016; TUPONE; MADDEN; MORRISON, 2014) (**Figuras 1 e 3)**.

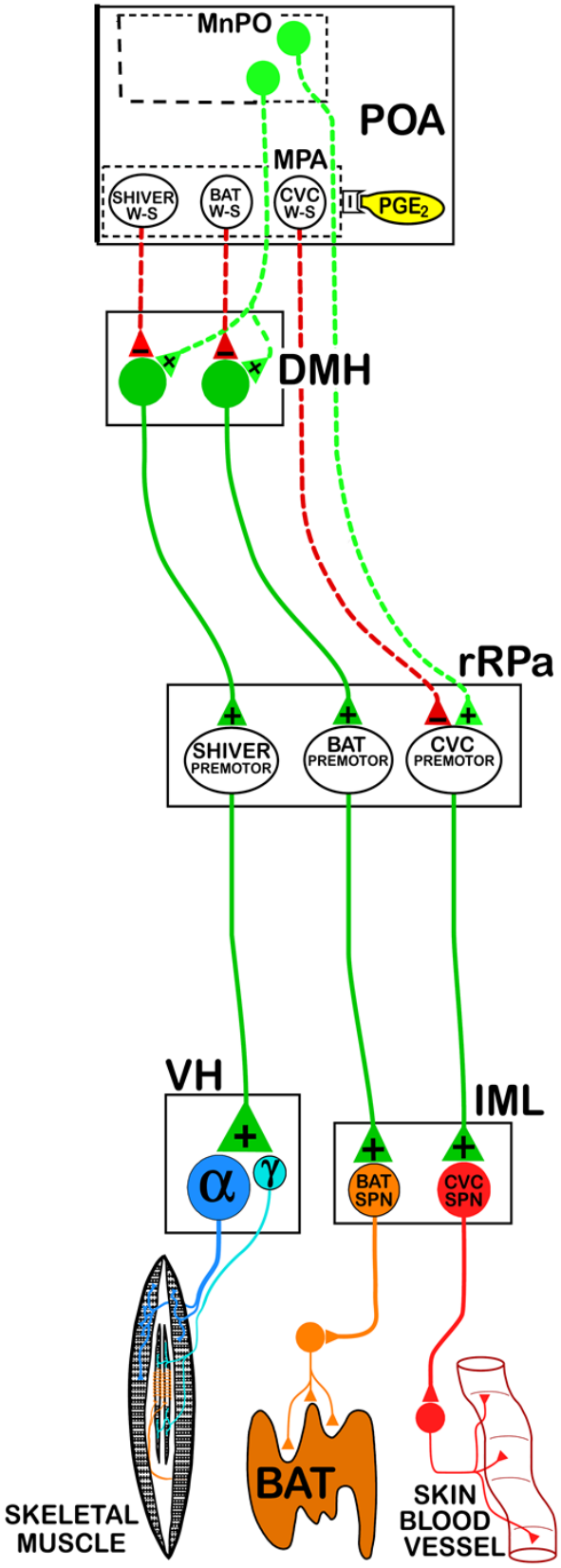

Figura 3: Modelo proposto por Morrison para ativação pirogênica da vasoconstrição cutânea e termogênese do músculo esquelético e tecido adiposo marrom (BAT). Área pré-óptica do hipotálamo anterior (AH/POA); núcleo mediano pré-óptico (MnPO); área pré-óptica medial (MPA); núcleo dorsomedial do hipotálamo (DMH); núcleo pálido da rafe (rRPA); núcleo intermediolateral (IML); corno ventral (VH); tecido adiposo marrom (BAT). Adaptado de: MORRISON, 2016.

1.3 Vias de Sinalização Intracelular

1.3.1 Lipopolissacarídeo

O LPS exerce seus efeitos inflamatórios pela ligação a receptores do tipo *Toll-like*, mais especificamente, pelo TLR4. Os receptores do tipo *Toll* pertencem a uma família altamente conservada de receptores capazes de reconhecer padrões moleculares associados a patógenos (PAMPs) e, portanto, representam a primeira linha de defesa do organismo contra a invasão por patógenos infecciosos (AKIRA; TAKEDA, 2004; BROWN et al., 2011; KAWASAKI; KAWAI, 2014). O TLR4 está presente na superfície de diversos tipos celulares como em macrófagos (DANTZER, 2004), células endoteliais (TAYLOR et al., 2004), micróglia (KONG; LE, 2011) e adipócitos (TAO et al., 2017).

A especificidade da ligação entre o LPS e este receptor pode ser influenciada por moléculas acessórias (**Figura 4**). Na superfície celular encontra-se, associada ao TLR4, uma proteína extracelular denominada proteína de diferenciação mielóide (MD2) que contribui para o reconhecimento do LPS sendo essencial para desencadear uma sinalização eficiente (NAGAI et al., 2002). Uma vez presente no organismo, o LPS se liga à proteína de ligação ao LPS (LBP) geralmente presente na fase aguda da infecção. A proteína LBP é sintetizada no fígado e liberada na corrente sanguínea onde pode se associar ao lipídeo A do LPS. A alta afinidade desta ligação parece contribuir para a distribuição do LPS pela superfície celular, assim como para sua interação com o receptor (DEMON; VANDE WALLE; LAMKANFI, 2014;

PÅLSSON-MCDERMOTT; O'NEILL, 2004). Outra proteína essencial para esta sinalização é a CD14 que, por sua vez, favorece a comunicação entre os complexos LPS/LBP e TLR4/MD2 (ZANONI et al., 2011).

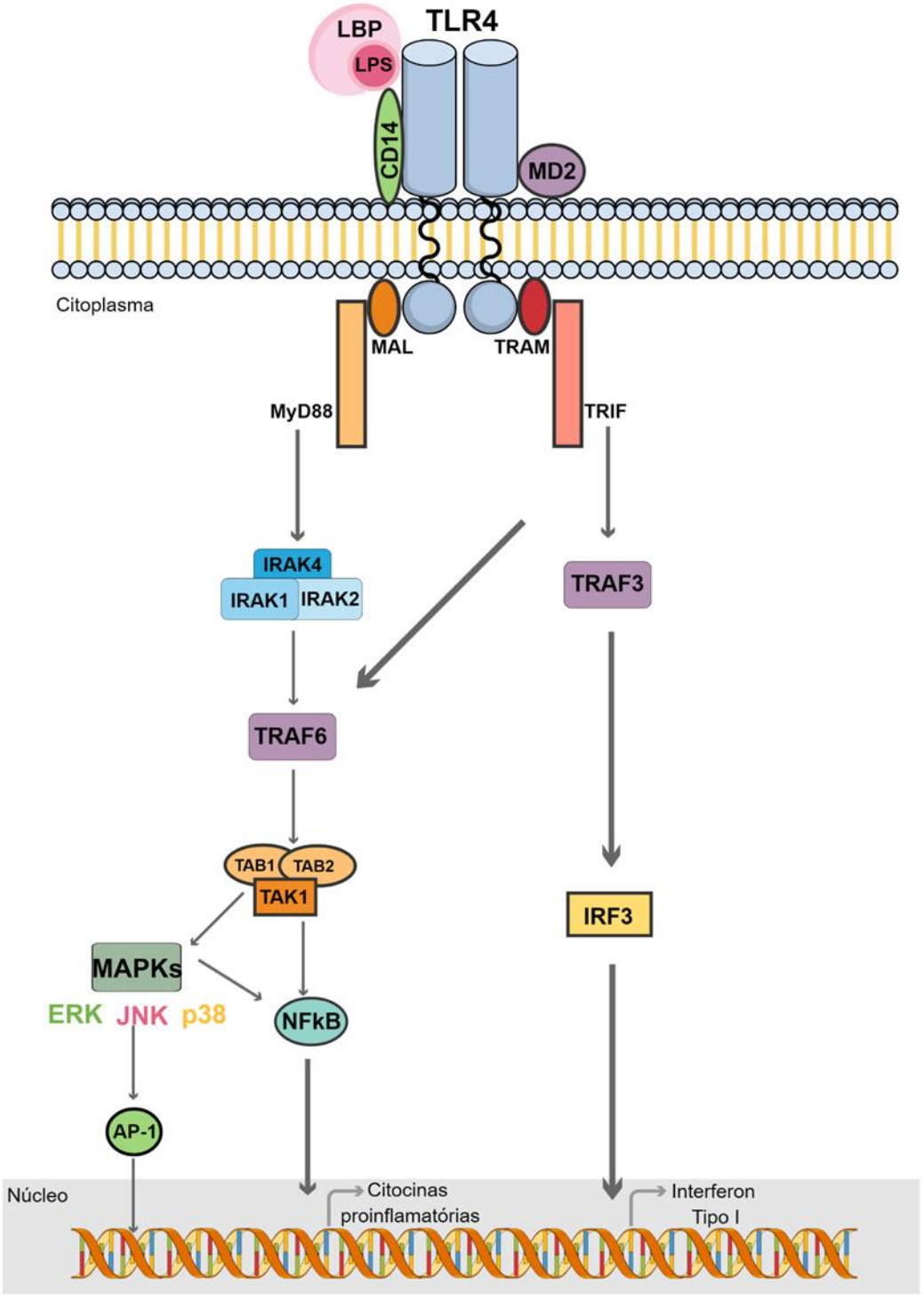

Figura 4: Sinalização desencadeada pela ligação do LPS ao seu receptor TLR4.

A ligação do LPS ao receptor TLR4 promove o recrutamento de proteínas adaptadoras que induzem a ativação de duas vias de sinalização intracelular distintas: a via dependente e a via independente da proteína adaptadora denominada fator 88 de diferenciação mielóide (MyD88) (AKIRA; TAKEDA, 2004; KAWAI; AKIRA, 2006; MOLTENI; GEMMA; ROSSETTI, 2016).

Quando ativada, a via de sinalização dependente de MyD88 ocorre principalmente na membrana plasmática e envolve a participação de duas proteínas adaptadoras: MyD88 e MAL, uma proteína adaptadora semelhante a MyD88 (**Figura 4**) (MOLTENI; GEMMA; ROSSETTI, 2016). A interação entre essas moléculas estimula o recrutamento de proteínas da família de cinases associadas ao receptor IL-1 (IRAK), formando assim um complexo conhecido como *Myddosome*. IRAK1 associa-se com a proteína Fator 6 associado ao receptor do TNF (TRAF6) ativando a cinase 1 ativadora do fator transformador de crescimento β (TAK1). TAK1, então, ativa duas diferentes vias que levam a estimulação de NFκB e de proteínas cinases ativadas por mitógenos (MAPKs). Uma vez ativada a via de sinalização do NFκB, este fator de transcrição é translocado para o núcleo, onde induz a expressão de genes relacionados a síntese de proteínas pró-inflamatórias (AKIRA; TAKEDA, 2004; KAWAI; AKIRA, 2006; KAWASAKI; KAWAI, 2014; MOLTENI; GEMMA; ROSSETTI, 2016; PÅLSSON-MCDERMOTT; O'NEILL, 2004).

As MAPK são proteínas cinases responsáveis por integrar sinais oriundos do meio extracelular com respostas intracelulares por meio da fosforilação de outras proteínas cinases e de fatores de transcrição nuclear (SUN; NAN, 2016). O sistema de sinalização destas proteínas estabelece uma via sequencial de ativação composta por três tipos de MAPK, sendo elas: a MAPKKK que, quando ativada, fosforila e ativa uma segunda cinase, a MAPKK que, por sua vez, promove a ativação da MAPK que corresponde a última cinase da cascata responsável pela fosforilação do substrato (LU; XU, 2006). As MAPKs pertencem a uma família de

serina/treonina cinases que podem ser agrupadas em três subfamílias: cinases reguladas por sinais extracelulares (ERK - ERK1 e ERK2), cinases c-Jun N-terminal (JNK - JNK1, JNK2 e JNK3) e p38 MAPKs (α, β, δ, e γ) (LU; XU, 2006). Estas proteínas levam a ativação de diversos fatores de transcrição como, por exemplo, NFκB e AP-1 (KAWAI; AKIRA, 2010) que juntos estimulam a expressão de genes que codificam a síntese de moléculas essenciais para o desenvolvimento da resposta inflamatória como, as citocinas TNF-α e IL-1, quimiocinas e proteínas de adesão (ABBAS ABUK K.; LICHTMAN ANDREW H. H.; PILLAI SHIV, 2015).

Na sinalização independente de MyD88, também conhecida como TRIF-dependente, duas outras moléculas adaptadoras participam da sinalização: TRIF (domínio TIR contendo adaptador indutor de IFN-β) e TRAM (molécula adaptadora relacionada a TRIF) (AKIRA; TAKEDA, 2004). TRIF é capaz de ativar tanto TRAF6 quanto TRAF3 (fator 3 associado ao receptor do TNF) (**Figura 4**). A interação com a molécula TRAF6 causa a ativação do complexo TAK1 e, portanto, a estimulação de NFκB e MAPKs. Acredita-se que a ativação de NFκB e MAPKs pela via independente de MyD88 esteja relacionada com uma fase tardia da resposta induzida pelo LPS (PÅLSSON-MCDERMOTT; O'NEILL, 2004). Já a ativação de TRAF3 leva ao recrutamento do fator de transcrição IRF3 que induz a expressão do interferon tipo I (IFN) (TSENG et al., 2010).

1.3.2 Prostaglandina E_2

O papel das PGs, particularmente da PGE_2, como mediador final da resposta febril está bem estabelecido e documentado na literatura (IVANOV; ROMANOVSKY, 2004; PECCHI et al., 2009). Este mediador inflamatório é sintetizado por macrófagos ativados, geralmente em um processo dependente de três passos sequenciais. Primeiramente o ácido araquidônico é liberado dos fosfolipídeos da membrana celular, onde encontra-se esterificado, pela ação da

enzima fosfolipase A2 citosólica α (cPLA2-α). Uma vez liberado, o ácido araquidônico é convertido no metabólito intermediário altamente instável, PGG_2, pela ação das enzimas cicloxigenases 1 e 2 (COX1 e COX2), a PGG_2 sofre um processo de peroxidação sendo rapidamente transformado em PGH_2. Por fim, a PGH_2 é isomerizada em PGE_2 pela ação das prostaglandinas E sintases (PGES). COX-2 e PGE sintase microssomal 1 (mPGES-1) são as principais isoformas induzidas durante processos inflamatórios, tendo sido demonstrado também o aumento da sua co-expressão em macrófagos durante a febre induzida por LPS demonstrando, portanto, o papel essencial dessas enzimas na produção de PGE_2 (IVANOV; ROMANOVSKY, 2004; YAMAGATA et al., 2001).

As prostaglandinas do tipo E exercem seus efeitos pela ligação a um grupo de receptores específicos acoplados a proteína G, denominados receptores EP. Até o momento, foram identificados quatro subtipos de receptores EP (1-4) (COLEMAN; SMITH; NARUMIYA, 1994). Os receptores EP3, encontrados em neurônios da AH/POA (NAKAMURA et al., 1999, 2000), vem sendo apontados como os responsáveis por mediar o desenvolvimento da febre em resposta a PGE_2. Análises conduzidas por Ushikubi e colaboradores demonstraram, por meio da utilização de camundongos nocaute para os quatro subtipos de receptores EP, que apenas os camundongos nocaute para EP3 não desenvolveram febre em resposta a administração de PGE_2, IL-1β ou LPS (USHIKUBI et al., 1998). Estas evidências sugerem que a PGE_2 e o receptor EP3 são essenciais para o desenvolvimento da resposta febril.

De maneira específica, isoformas do receptor EP3 foram identificadas em diferentes espécies, incluindo camundongos, ratos e humanos (NARUMIYA; SUGIMOTO; USHIKUBI, 1999; SUGIMOTO; NARUMIYA, 2007). Estas isoformas são derivadas do processo de *splicing* alternativo da extremidade carboxi-terminal da molécula de RNA (HATAE; SUGIMOTO; ICHIKAWA, 2002; KOTANI et al., 1995; SCHMID et al., 1995; VASILACHE; ANDERSSON; NILSBERTH, 2007). Apesar de possuírem propriedades de ligação a PGE_2

semelhantes, estas isoformas apresentam diferenças significativas quanto as propriedades de transdução de sinal, podendo, por exemplo, estar acopladas a diferentes proteínas G (NAMBA et al., 1993). A principal via de sinalização do receptor EP3 envolve a inibição da enzima adenilil ciclase (AC) e a estimulação da via do IP_3/Ca^{2+} através da ativação de uma proteína G inibitória (Gi), ocasionando, consequentemente, a diminuição nos níveis intracelulares de AMPc (adenosina 3', 5' - monofosfato cíclico) e aumento nos níveis de cálcio. Entretanto, outras isoformas do receptor EP3 podem induzir estimulação da AC por meio do acoplamento a uma proteína G estimulatória (Gs) (SUGIMOTO; NARUMIYA, 2007).

1.4 Termogênese no Tecido Adiposo Marrom

Animais homeotérmicos possuem mecanismos efetores responsáveis por controlar a geração, conservação e dissipação de calor endógeno, de forma a manter a temperatura corporal relativamente estável, condição denominada homeostasia. Dentre os principais mecanismos termorregulatórios podemos citar: a vasoconstrição e vasodilatação que controlam a perda de calor para o ambiente, a termogênese do tecido adiposo marrom (BAT de *brown adipose tissue*), a termogênese por tremor (*shivering*) realizada nos músculos esqueléticos, a perda de calor por meio da sudorese (que ocorre principalmente em humanos), além de alterações comportamentais que aumentam ou evitam a transferência de calor para o ambiente (HASDAY; THOMPSON; SINGH, 2014).

O tecido adiposo marrom pertence a uma classe especial de tecido adiposo. É um órgão encontrado em todos os mamíferos sendo responsável, dentre outras funções, pela termogênese, ou seja, pela produção de calor nos organismos. A termogênese é uma função metabólica específica deste tecido, contribuindo para regulação da temperatura corporal, para manutenção da temperatura durante a exposição ao frio e para elevação da temperatura durante o

desenvolvimento da resposta febril (CANNON; NEDERGAARD, 2004; MORRISON; MADDEN; TUPONE, 2014; TUPONE; MADDEN; MORRISON, 2014).

Morfologicamente o BAT apresenta grandes diferenças em comparação ao tecido adiposo branco (WAT). No citoplasma dos adipócitos marrons, são encontradas numerosas gotículas lipídicas e principalmente grande quantidade de mitocôndrias, responsáveis pela coloração diferenciada do BAT. Este tecido é ainda inervado por fibras eferentes do sistema nervoso simpático, que transmitem as informações centrais para controle da termogênese, além de ser altamente vascularizado, permitindo assim a dissipação do calor produzido (CANNON; NEDERGAARD, 2004; CONTRERAS et al., 2015; OELKRUG; POLYMEROPOULOS; JASTROCH, 2015). O tecido adiposo branco, por outro lado, apresenta adipócitos geralmente esféricos contendo uma única e volumosa gota de lipídeo e poucas mitocôndrias no citoplasma, sendo responsável principalmente pelo armazenamento do excesso de energia na forma de triglicerídeos, que podem ser liberados na circulação como ácidos graxos livres em momentos de alta demanda energética (CONTRERAS et al., 2015; OELKRUG; POLYMEROPOULOS; JASTROCH, 2015).

A sinalização desencadeada na AH/POA leva a ativação de circuitos centrais simpáticos que induzem a liberação de noradrenalina. Este neurotransmissor ativa os receptores adrenérgicos presentes nos adipócitos do BAT, desencadeando o processo de termogênese neste tecido (**Figura 5**) (CANNON; NEDERGAARD, 2004; OELKRUG; POLYMEROPOULOS; JASTROCH, 2015).

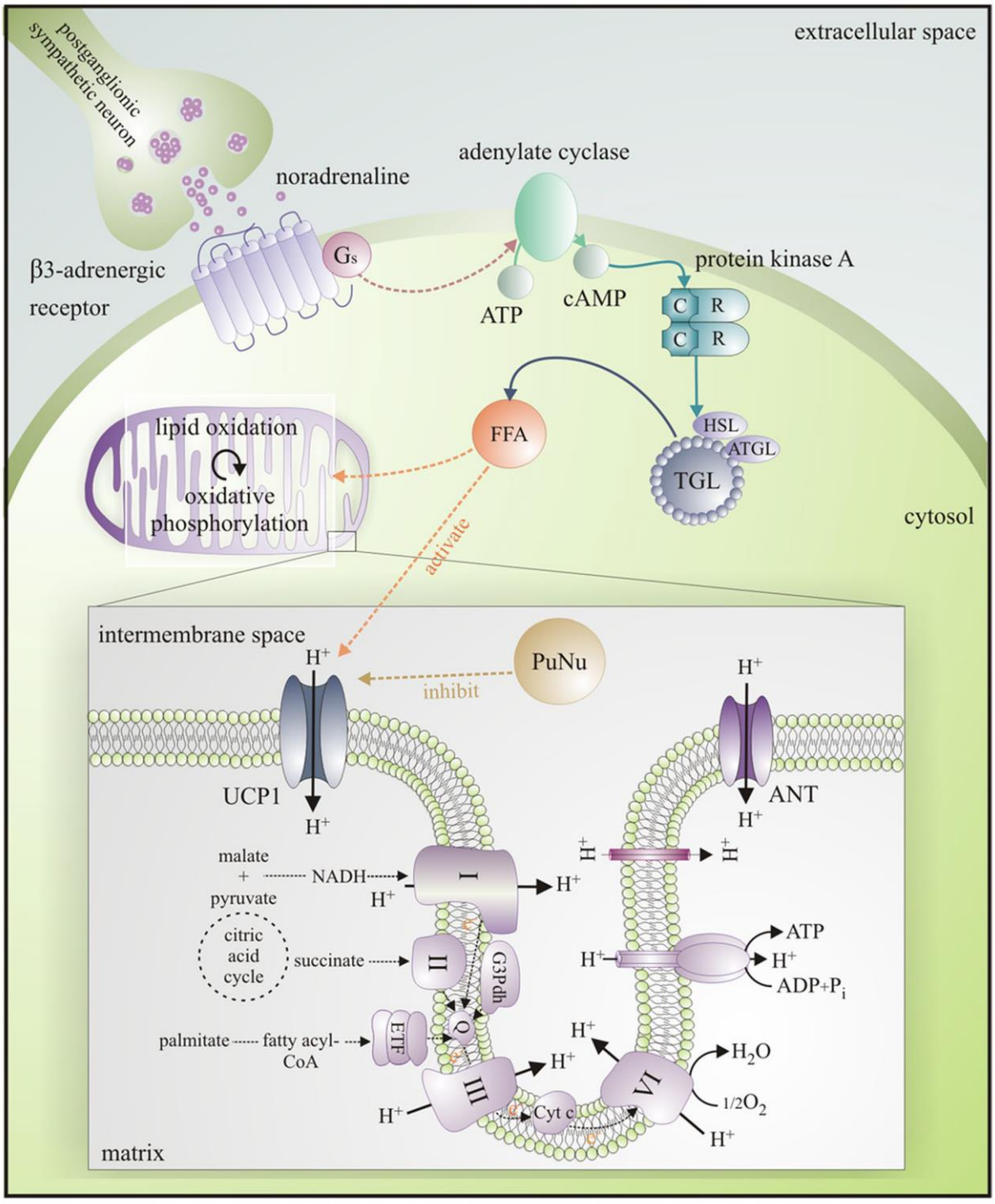

Figura 5: Termogênese no Tecido Adiposo Marrom: Receptores β_3-adrenérgicos (β_3-AR); proteína cinase A (PKA); lipase de triglicerídeos do tecido adiposo (ATGL); lipase hormônio-sensível (HSL – isoforma ativa pHSL); triglicerídeos (TGL); ácidos graxos livres (FFAs); proteína desacopladora 1 (UCP1); nucleotídeos de purina (PuNu). Extraído de: (OELKRUG; POLYMEROPOULOS; JASTROCH, 2015).

Os adipócitos maduros do BAT expressam três tipos de receptores adrenérgicos (β; α_1 e α_2). A noradrenalina possui a capacidade de se ligar a todos eles levando a ativação de

diferentes vias de sinalização. Considerando a sinalização envolvida na termogênese, acredita-se que a noradrenalina ative receptores do tipo β_3-adrenérgicos, cuja sinalização é mediada por uma proteína Gs. Esta proteína Gs ativa a enzima AC, aumentando os níveis de AMPc que por sua vez induz a ativação da PKA. A ativação da PKA contribui também para o aumento da lipólise através da estimulação de enzimas envolvidas neste processo (ATGL, pHSL), elevando os níveis de ácidos graxos livres (**Figura 5**). O aumento da concentração de ácidos graxos na circulação pode ativar diretamente a proteína desacopladora 1 (UCP1), contribuindo com a termogênese (CANNON; NEDERGAARD, 2004; CONTRERAS et al., 2015). Nós adipócitos marrons, acredita-se que a ativação de PKA aumente a expressão da UCP1 por meio da ativação da via da p38 MAPK (CANNON; NEDERGAARD, 2004; CAO et al., 2001).

A termogênese do BAT é altamente dependente da ação de proteínas desacopladoras (UCPs). Estas proteínas fazem parte de uma família de proteínas integrais de membrana que atuam como um canal de prótons, localizadas na membrana mitocondrial interna. Em mamíferos, cinco UCPs homólogas, expressas em diferentes tecidos, foram descritas: UCP1, UCP2, UCP3, UCP4 e UCP5, também chamada BMCP (*Brain Mitochondrial Carrier Protein*) (KRAUSS; ZHANG; LOWELL, 2005). A UCP1, também chamada de termogenina, é encontrada somente no tecido adiposo marrom (BOUILLAUD et al., 1985). A presença desta proteína na membrana interna das mitocôndrias do BAT confere a este tecido a capacidade única de gerar calor através do desacoplamento da cadeia transportadora de elétrons do processo de produção de ATP (CANNON; NEDERGAARD, 2004).

A oxidação de substratos energéticos em organismos com metabolismo aeróbico conserva parte da energia gerada como potencial redutor transportado pelas coenzimas reduzidas, NADH e $FADH_2$, que entregam seus equivalentes redutores para os complexos proteicos da cadeia de transporte de elétrons mitocondrial (**Figuras 5 e 6**) (KRAUSS; ZHANG; LOWELL, 2005). O gradiente de prótons, formado pelo movimento dos elétrons através dos

complexos, fornece a energia necessária para síntese de ATP. As proteínas desacopladoras fornecem uma via alternativa para os prótons retornarem a matriz mitocondrial, através de um desacoplamento parcial entre a cadeia de transporte de elétrons e a fosforilação oxidativa. Assim, parte da energia proveniente da oxidação de substratos é dissipada na forma de calor, contribuindo para a manutenção da temperatura corporal (**Figura 6**) (CONTRERAS et al., 2015; KRAUSS; ZHANG; LOWELL, 2005).

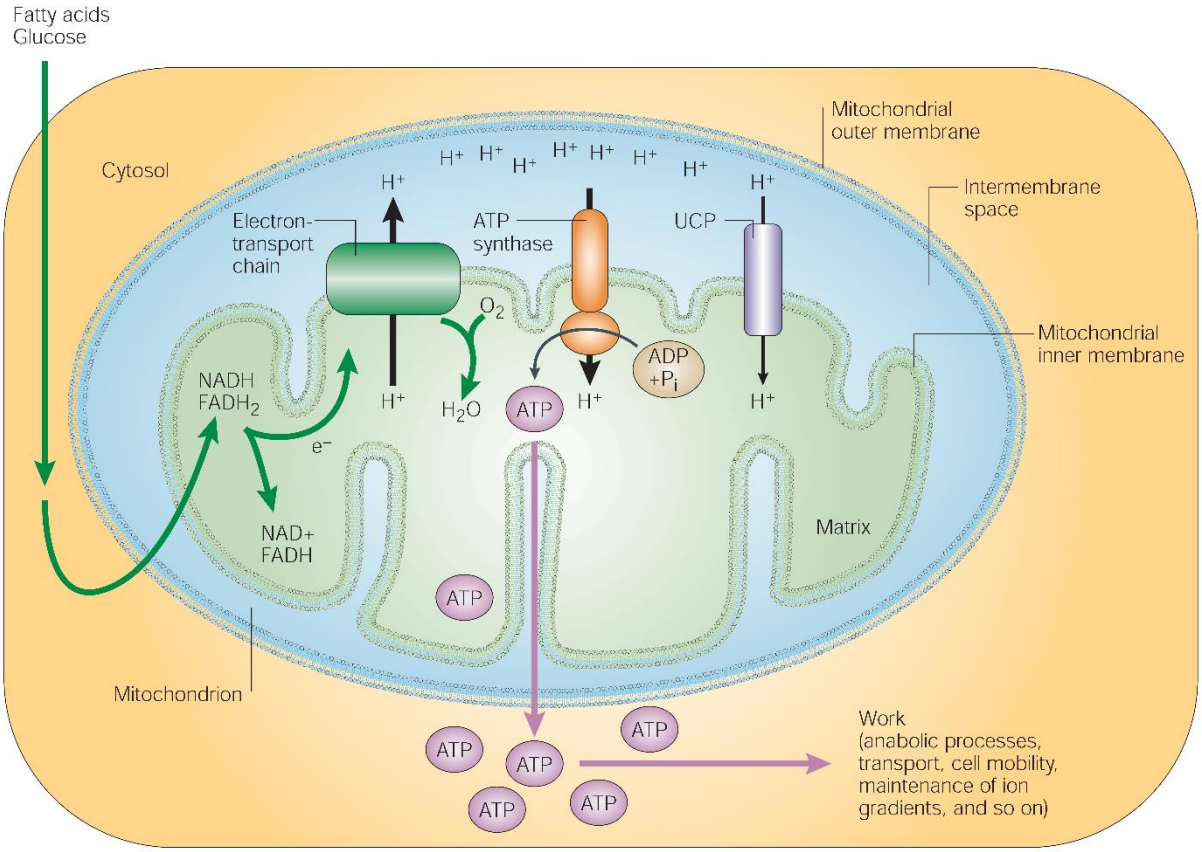

Figura 6: Oxidação do substrato e fosforilação oxidativa em células de mamíferos. Extraído de (KRAUSS; ZHANG; LOWELL, 2005).

Em adipócitos isolados de camundongos nocaute para UCP1 (Ucp1$^{-/-}$), nenhuma resposta termogênica se desenvolve em decorrência da estimulação noradrenérgica (MATTHIAS et al., 2000), demonstrando assim, a forte relação da UCP1 com o processo da termogênese.

1.5 Efeitos da Febre Sobre o Hospedeiro

Apesar de a febre ser considerada um componente da resposta de fase aguda, sua persistência evolucionária em diversos grupos de animais, a despeito do seu elevado custo metabólico, sugere que o aumento da temperatura corporal durante o desenvolvimento da febre, está associado ao aumento das taxas de sobrevivência e resolução de infecções (BARACOS; WHITMORE; GALE, 1987; HASDAY; FAIRCHILD; SHANHOLTZ, 2000; HASDAY; THOMPSON; SINGH, 2014; KLUGER, 1991; KLUGER et al., 1996; SINGH; HASDAY, 2013). Em animais endotérmicos, assim como em humanos, o aumento de 1°C na temperatura corporal requer um aumento de aproximadamente 10 a 12,5 % na atividade metabólica, evidenciando a grande quantidade de energia necessária para manter a temperatura corporal elevada (KLUGER, 1979; MANTHOUS et al., 1995).

Vários componentes da resposta imune inata e adaptativa são potencializados pela resposta febril, como: o aumento na motilidade de neutrófilos e monócitos, na fagocitose, na produção de radicais livres por fagócitos, na atividade citotóxica de células T, na produção de anticorpos e no efeito bactericida de agentes antimicrobianos (EVANS; REPASKY; FISHER, 2015; HARDEN et al., 2015; ROTH; BLATTEIS, 2014). Além destas alterações no sistema imunológico, acredita-se que a febre induza o aumento na expressão de proteínas de choque térmico (HSPs de *heat-shock proteins*), uma classe de proteínas essenciais para sobrevivência celular durante o estresse (KREGEL, 2002; RYAN; LEVY, 2003). Estas proteínas podem atuar prevenindo a desnaturação proteica ou marcando proteínas desnaturadas para posterior degradação (HASDAY; THOMPSON; SINGH, 2014; KREGEL, 2002).

Apesar de todas estas alterações celulares que contribuem para uma resolução eficiente das infecções, a febre não é considerada universalmente benéfica. Febres de difícil controle são associadas a piores prognósticos em pacientes que apresentam febres altas de origem não

infecciosa ou quando desenvolvem o quadro de sepse (HARDEN et al., 2015; LAUNEY et al., 2011). Dentre os efeitos prejudiciais da febre, podemos citar o desenvolvimento de isquemia nos tecidos em decorrência do gasto metabólico necessário para manter a resposta febril extrapolar a capacidade cardiopulmonar do hospedeiro. O aumento da temperatura corporal pode ainda reduzir progressivamente a afinidade entre o oxigênio molecular e a hemoglobina, resultando em hipóxia. Somado a estes fatores, os efeitos colaterais decorrentes da potencialização da resposta imunológica também contribui para o aumento do dano tecidual (HASDAY; FAIRCHILD; SHANHOLTZ, 2000).

Existem duas estratégias principais para o controle da febre: (1) terapia farmacológica, com a utilização de antipiréticos, que incluem anti-inflamatórios não esteroidais (AINEs) (ibuprofeno, aspirina, indometacina), metamizol (dipirona) e acetaminofeno (paracetamol); e (2) terapia física, através de mecanismos de resfriamento (HARDEN et al., 2015). De maneira geral, independentemente do tratamento escolhido, seja ele farmacológico ou físico, ele sempre irá comprometer o curso natural da resposta imune. Suprimindo a febre por resfriamento físico atenua-se também a ação de vários componentes da imunidade inata. O uso de antipiréticos, por sua vez, é capaz de reduzir ou mesmo eliminar a síntese de diversos mediadores endógenos que podem ser requeridos para defesa do hospedeiro (ARONOFF; NEILSON, 2001; HASDAY; THOMPSON; SINGH, 2014). Em diversos modelos animais, o controle da febre por agentes antipiréticos está associado ao aumento no índice de mortalidade durante infecções bacterianas (BERNHEIM; KLUGER, 1976; KLUGER et al., 1996; KUROSAWA et al., 1987; VAUGHN; VEALE; COOPER, 1980). Em humanos, o uso de antipiréticos prolonga a recuperação e o tempo de infecção (HARDEN et al., 2015). Soma-se a isso o fato de que alguns medicamentos podem potencialmente ocasionar toxicidade, seja ela direta ou indireta, como no caso do acetaminofeno, cujo metabólito principal (N-acetil-p-benzoquinonaimina) é altamente hepatotóxico (ARONOFF; NEILSON, 2001; HARDEN et al., 2015). Durante estágios iniciais

de doenças severas o uso de AINEs ou acetaminofeno podem induzir uma liberação excessiva de TNF por inibir a produção de PGE_2, que por sua vez, regula a produção de TNF por um mecanismo de *feedback* negativo, induzindo choque e dano tecidual (HARDEN et al., 2015). Apesar de os mecanismos de ação dos medicamentos antipiréticos serem, em geral, bem estudados, as indicações para uma correta aplicação clínica desses fármacos ainda não estão bem estabelecidas. O momento ideal/correto de administração ou não do antipirético em relação ao curso da doença pode ser uma variável crítica para determinar o prognóstico do paciente (ARONOFF; NEILSON, 2001; HARDEN et al., 2015).

Com base no exposto acima, a realização desse trabalho justifica-se pelo fato de que apesar de a febre ser uma condição clínica relativamente comum, os mecanismos moleculares envolvidos em sua gênese e manutenção ainda não estão totalmente esclarecidos. A avaliação da função mitocondrial e as análises proteômicas por LC-MS/MS podem revelar alvos moleculares relevantes e/ou essenciais para este processo e que poderão ser úteis para o melhor entendimento dos mecanismos envolvidos, bem como para o desenvolvimento de terapias farmacológicas mais específicas e apropriadas, que sejam capazes de controlar a resposta febril com menor incidência de efeitos indesejáveis.

2. Objetivos

2.1 Objetivo Geral

O objetivo da presente tese foi investigar vias de sinalização e alterações proteômicas e bioquímicas envolvidas no desenvolvimento da resposta febril induzida pelos estímulos de LPS e PGE_2 em ratos.

2.2 Objetivos Específicos

A. Investigar alterações nas principais vias do metabolismo energético e de processos inflamatórios, por meio da análise proteômica quantitativa em sistema LC-MS/MS, de forma a melhor compreender a resposta febril induzida pelos estímulos de LPS e PGE_2 no hipotálamo de ratos.

B. Avaliar efeitos da resposta febril induzida por LPS sobre a função mitocondrial em hipotálamo e tecido adiposo marrom, através da mensuração das atividades dos complexos I-III, II e IV da cadeia respiratória mitocondrial e das medidas de potencial de membrana mitocondrial.

C. Investigar a participação das proteínas cinases PKA e PKC e vias de sinalização relacionadas a elas na resposta febril induzida por LPS e PGE_2 em ratos, utilizando inibidores farmacológicos específicos.

3. Capítulo 1

Manuscrito: Label-free quantitative proteomics of rat hypothalamus under fever induced by LPS and PGE_2 – Aceito com *minor revision* pelo periódico *Journal of Proteomics*

Label-free quantitative proteomics of rat hypothalamus under fever induced by LPS and PGE_2

Marina Firmino[a], Simone N. Weis[a], Jaques M. F. Souza[a], Bruna R. B. Gomes[a], Alan R. Mól[a], Márcia R. Mortari[b], Gloria E. P. Souza[c], Guilherme C. Coca[d], Thomas C. R. Williams[d], Wagner Fontes[a], Carlos André O. Ricart[a], Marcelo V. de Sousa[a*] and Fabiane H. Veiga-Souza[a,e*]

[a]Laboratory of Protein Chemistry and Biochemistry, Department of Cell Biology, Institute of Biology, University of Brasilia, Brasília, DF 70910-900, Brazil

[b]Laboratory of Neuropharmacology, Department of Physiological Sciences, Institute of Biological Sciences, University of Brasilia, Brasília, DF 70910-900, Brazil

[c]Laboratory of Pharmacology, School of Pharmaceutical Sciences of Ribeirão Preto, University of São Paulo, Ribeirão Preto, SP 14040-903, Brazil

[d]Laboratory of Plant Biochemistry, Department of Botany, University of Brasilia, Brasília, DF 70910-900, Brazil

[e]School of Ceilandia, University of Brasilia, Brasília, DF 72220-275, Brazil

*****Corresponding authors:

Marcelo Valle de Sousa, Proteomics Center, Laboratory of Protein Chemistry and Biochemistry, Department of Cell Biology, Institute of Biology, University of Brasília, 70910-900, Brasília, DF, Brazil.

Email: mvsousa@unb.br

Fabiane H. Veiga de Souza, School of Ceilandia, University of Brasilia, Centro Metropolitano, Conjunto A, Lote 01, 72220-275, Brasília, DF, Brazil.

Email: fhveiga@unb.br

Abstract

Fever is a brain-mediated increase in body temperature mainly during inflammatory or infectious challenges. Although there is considerable data regarding the inflammation pathways involved in fever, metabolic alterations necessary to orchestrate the complex inflammatory response are not totally understood. We performed proteomic analysis of rat hypothalamus using label-free LC–MS/MS in a model of fever induced by lipopolysaccharide (LPS) or prostaglandin E_2 (PGE_2). In total, 7,021 proteins were identified. As far as we know, this is the largest rat hypothalamus proteome dataset available to date. Pathway analysis showed proteins from both stimuli associated with inflammatory and metabolic pathways. Considering metabolic pathways, rats exposed to LPS or PGE_2 presented lower relative abundance of proteins involved in glycolysis, pentose phosphate pathway and tricarboxylic acid cycle. Mitochondrial function may also be altered by both stimuli because significant downregulation of several proteins was found, mainly in complexes I and IV. LPS was able to induce downregulation of important proteins in the enzymatic antioxidant system, thereby contributing to oxidative stress. The results offered comprehensive information about fever responses and helped to reveal new insights into proteins potentially involved in inflammatory signaling and metabolic changes in the hypothalamus during systemic LPS and central PGE_2 administration.

Keywords: fever; lipopolysaccharide; prostaglandin E_2; hypothalamus; metabolism; proteome.

Significance

The evolutionary persistence of fever, despite the elevated cost for maintenance of this response, suggests that elevation in core temperature may represent an interesting strategy for survival. Fever response is achieved through the integrated behavioral, physiological, immunological and biochemical processes that determine the balance between heat generation and elimination. The development of such complex response arouses interest in studying how the cell metabolism responds or even contributes to promote fever. Our results offered comprehensive information about fever responses, including metabolic and inflammatory pathways, providing new insights into candidate proteins potentially involved in inflammatory signaling and metabolic changes in the hypothalamus during fever induced by systemic LPS and central PGE_2 perturbation.

Highlights:

1) LPS and PGE_2 stimuli changed the abundance of several proteins involved in inflammatory and metabolic pathways.
2) Carbohydrate metabolism was downregulated by LPS and PGE_2 exposure.
3) LPS increased enzymes involved in lipid turnover, which favors inflammation due to arachidonic acid release.
4) Mitochondrial function was altered by both stimuli, with significant downregulation of proteins, mainly in complexes I and IV.
5) LPS induced downregulation of proteins from enzymatic antioxidant system, thereby contributing to oxidative stress.

1. Introduction

Fever is a complex physiological response developed against inflammatory or infectious insults [1–3]. Several evidences indicates that the controlled increase in body temperature, characteristic of febrile response, is associated with improvement in immunity and, consequently, increase of survival and resolution of infections [3,4]. However fever is not always beneficial as uncontrolled fever is associated with worse prognostics in patient that present sepsis, high fever of non-infectious origin or in a neuronal injury situation [4–6].

The global analgesics market, including antipyretics, is expected to earn US$ 26.4 billion by 2022 as forecast by Allied Market Research. The forecast for the market compound annual growth rate (CAGR) is of 7.1 % during 2015-2022. The pharmaceutical arsenal for control of febrile response includes nonsteroidal anti-inflammatory/antipyretic drugs (NSAIDs, such as ibuprofen, aspirin and indomethacin), acetaminophen (paracetamol) and metamizol (dipyrone) [2]. Aspirin is one of the most used medications globally, with over 44,000 tons (50 to 120 billion pills) consumed per year [7,8]. To its turn, paracetamol is the most widely employed medication for pain and fever in both the United States and Europe [9] The principal action of these drugs rests in their ability to inhibit cyclooxygenase (COX) activity, and to interrupt the synthesis of inflammatory prostaglandins [2]. Besides, COX-independent mechanisms such as reduction in proinflammatory mediators and increase in anti-inflammatory signaling were also attributed to NSAIDs action [10]. For dipyrone or paracetamol, there is a possibility for other central mediators involvement in addition to PGE_2 [2,11]. Although the complex action mechanism of antipyretics are well investigated in general, the indications for their correct clinical applications for a better prognosis are less clear [10]. The comprehension of the proteins and metabolic pathways involved in mechanisms of fever production is fundamental to understand this complex response, and may consequently facilitate the

development of new, more specific drugs by biotechnological and pharmaceutical research groups and companies.

Systemic administration of lipopolysaccharide (LPS) is widely used in experimental models to induce fever, since it reproduces what naturally occurs during infectious and inflammatory processes [2,12]. LPS binding to the toll-like receptor (TLR) member TLR4 , presents in cells from both peripheral and central nervous system [13–15], triggers an intracellular cascade of events, from activation of transcription factors up to production and release of pro-inflammatory mediators, such as cytokines, chemokines and prostaglandins. Such molecules work together in a cascade of interacting mediators that coordinate the response for fever development [1,16–18].

Stimulation of macrophages by LPS induces a rapid transcription (0.5 to 2.0 h) of several genes related to inflammation [13]. This response is regulated by transcription factors that are constitutively expressed by many cell types, activated post-translationally by TLR signaling, such as nuclear factor-κB (NFκB), IFN-regulator factors (IRFs), activator protein 1(AP-1) and cAMP-responsive-element-binding protein 1 (CREB1) [13,19,20]. In the brain, NFκB and the signal transducer and activator of transcription-3 (STAT3) are the first inflammatory transcription factors induced by systemic challenge with LPS (1 to 2 h) [21–25]. These transcription factors are involved in the regulation of cyclooxygenase-2 (COX-2) and microsomal prostaglandin E synthase-1 (mPGES-1) [21,24,26], both responsible for the production of prostaglandin E_2 (PGE_2), a metabolite of arachidonic acid (AA) [2,27,28] and the main mediator of fever induced by LPS [29–31].

It is widely accepted that the central mechanism of fever induction is triggered by the action of PGE_2 on EP3 receptors (EP3R) expressed on neurons in preoptic area of the anterior hypothalamus, the brain structure responsible for controlling thermoregulatory mechanisms in normal and febrile response [30,32–34]. Multiple splice variants of EP3R allow the coupling to

several G proteins, triggering different signaling pathways that, in turn, lead to the activation of peripheral mechanisms such as cutaneous vasoconstriction and brown adipose tissue thermogenesis to ultimately increase body temperature [35–38]. Despite this, the knowledge about the exact downstream signaling activated by PGE_2/EP3R interaction is not completely elucidated. It was recently demonstrated that febrile response to peripheral inflammation induced by LPS is dependent on local synthesis of PGE_2 in its target hypothalamic neurons and not on the overall PGE_2 production in the brain [29].

Although there is a considerable amount of data regarding the inflammatory pathway involved in febrile response, the exact mechanisms of downstream PGE_2 production for the stimulation of innate and adaptive immune responses are not totally understood. Since there is an overlap between systemic physiology and neuronal circuitry in the febrile response, there is growing interest in studying how the cell metabolism responds to and interacts with the inflammatory process. Therefore, the analysis of whole proteome changes in hypothalamus after LPS or PGE_2 exposure may provide advanced and comprehensive answers to these questions. In this study, we compared inflammatory and metabolic changes during fever induced by a peripheral, LPS, and a central, PGE_2, pyrogenic stimuli. Using combined mass spectrometry-based proteomic analysis with label-free quantification, it was possible to identify proteins, many of them not previously described in the present experimental setting, as well as signaling pathways associated with febrile response.

2. Methods

2.1 Animals

Animals were obtained from the Animal House of the Institute of Biological Sciences, University of Brasilia. Experiments were conducted using male Wistar rats (180 ± 20 g body

weight), housed in a constant temperature room (24 ± 1 °C) and 50 % humidity on an 12:12 h light/dark cycle (lights on at 7 am), with free access to food and water. Each animal was used only once. The study was approved by the Animal Research Ethics Committee of the University of Brasília (Protocol. nr. 30652/2014). Moreover, the care and use of the animals were in full compliance with the Guide for the Care and Use of Laboratory Animals of the Brazilian National Council for the Control of Animal Experimentation (CONCEA) and the Guide for the Care and Use of Laboratory Animals of the Institute for Laboratory Animal Research [39].

2.2 Intracerebral cannula implantation

For intracerebroventricular (i.c.v.) injections, a 22-gauge stainless steel guide cannula (0.7 mm OD, 10 mm in length) was stereotaxically (Insight Equipments®, Ribeirão Preto, Brazil) implanted into the right lateral ventricle under ketamine (60 $mg.kg^{-1}$) and xylazine (10 $mg.kg^{-1}$) anesthesia under aseptic conditions. The stereotaxic coordinates were 1.6 mm lateral to the midline, 1.5 mm posterior to bregma and 2.5 mm below the brain surface, with the incisor bar lowered by 2.5 mm below the horizontal zero [40]. Cannulas were fixed to the skull with screws and dental acrylic. All animals received oxytetracycline hydrochloride (400 $mg.kg^{-1}$ intramuscularly) and dexamethasone (1 $mg.kg^{-1}$ intramuscularly) after surgery and were kept at rest for one week prior to the experiments.

2.3 Core temperature measurement

Body core temperature was measured in conscious unrestrained rats using data loggers (Subcue, Calgary, Canada) surgically implanted intra–abdominally at the time of the i.c.v. cannulation. Experimental measurements were conducted at the thermoneutral zone for rats [41], in a temperature-controlled room (28 ± 1 °C). Temperature was continuously monitored and recorded at 10 or 15 min intervals from 2 h before any injection until 1.5 h or 6 h after the

injection of the pyrogenic stimuli. For proteomic and metabolite analysis of hypothalamus, samples were collected 30 min after PGE_2 injection and 2.5 h after LPS injection. The time point of 2.5 h was chosen based on the early phase of LPS-induced fever whereas the time point of 30 min represents the peak of PGE_2 induced fever. The increase in core temperatures of animals at the time of collection related to basal values was expressed as ΔT (°C).

2.4 Fever induction by LPS and PGE_2

Independent groups of rats received intravenous (i.v.) injections of LPS (5 $\mu g.kg^{-1}$ in sterile saline solution) derived from *Escherichia coli*, serotype O111:B4 (Sigma-Aldrich, St. Louis, USA) or i.c.v. injections of PGE_2 (100 ng in 2 µL 0.5 % ethanol in saline – (Sigma-Aldrich, St. Louis, USA)). Control animals received i.v. injection of sterile saline or i.c.v injection of vehicle (0.5 % ethanol in saline), and their body temperature was monitored for 6 h or 1.5 h respectively. The doses of PGE_2 and LPS were chosen based on previous studies [42,43]. All injections were done at approximately 9 am. and the recordings performed during the light-on period. The second set of experiments was done to collect samples for proteomic and metabolite analysis. Rats received LPS, PGE_2 or respective vehicles as described before. At defined times for each stimulus, animals were killed by decapitation and their brains removed immediately. The entire hypothalamus was dissected from the brain using the following limits: the anterior border of the optic chiasm, the anterior border of the mammillary bodies, and the lateral hypothalamic sulci, with a depth of 2 mm. The total dissection time elapsed from decapitation was less than 2 min, and the hypothalami were immediately frozen at -80 °C until processing.

2.5 Sample preparation for proteomic analysis

Freshly thawed hypothalamus samples (n = 5, each group) were individually homogenized in 250 µL of lysis buffer (0.02 M TEAB; 0.1 M DTT; 4 % SDS, pH 8.5) using micro pestles in eppendorf microtubes. To limit potential protein degradation by protease and phosphatase activities, the buffer was supplemented with the protease and phosphatase inhibitor cocktails cOmplete™ and PhosStop™, respectively (Roche Diagnostics, Mannheim, Germany). Samples were warmed at 80 °C for 10 min and sonicated (3 cycles of 15 s) in an ultrasonic processor (Markson, Model GE 50 T 20 kHz). Homogenates were centrifuged at 18,000 × g for 20 min at 4 °C, supernatants were collected for the proteomic analysis and the debris was discarded. Protein concentration was determined using a Qubit® protein assay kit (Thermo Fisher Scientific, Maryland, USA). Aliquots containing 200 µg of protein were submitted to proteolysis with trypsin via a filter-aided sample preparation, as described elsewhere [44]. After the enzymatic digestion, peptides samples were submitted to a desalting step performed on C18-reverse phase micro-columns, using self-prepared StageTips [45]. The peptides were resuspended in 0.1 % formic acid in water, and the concentration was determined using Qubit® protein assay.

2.6 Mass spectrometry

LC–MS/MS analyses were performed on a Dionex Ultimate 3000 RSLCnano UPLC system coupled to an Orbitrap Elite™ (Thermo Scientific; San Jose, USA) mass spectrometer. The chromatography system was equipped with an in-house packed 2 cm × 100 µm i.d. pre-column (ReprosilPur C18, 5 µm, 120 Å, Dr. Maich GmbH, Ammerbuch, Germany) and 35 cm × 75 µm i.d analytical column (ReprosilPur C18, 3 µm, 120 Å, Dr. Maich GmbH, Ammerbuch, Germany). Briefly, 2 µg of peptides were automatically loaded into the trap column at a flow rate of 3 $\mu L.min^{-1}$ in 98 % buffer A (0.1 % formic acid in water) and 2 % buffer B (0.1 % formic acid in acetonitrile). After 10 min, the peptides were eluted and separated at 250 $nL.min^{-1}$ flow

rate on the analytical column using a 170 min gradient from 5 to 45 % buffer B, followed by a gradient from 45 to 85 % buffer B over 10 min, where it was held for 10 min, and then to 2 % buffer B over 5 min, followed by column re-equilibration for 18 min. Acquisition by the mass spectrometer was performed in data dependent acquisition (DDA) mode. The DDA cycle consisted of a full scan in FTMS comprising a 400-1800 m/z range under a resolution of 120,000 full width at half-maximum at m/z 400. The 15 most abundant ions with intensity of at least 1000 counts were selected and fragmented by collision induced dissociation (CID). The fragmentation was performed with a collision energy of 35 %, automatic gain control (AGC) of 1×10^6 and acquired in the ion trap analyzer with a 2 m/z isolation width and AGC 1×10^4. Dynamic exclusion was set to 90 s. Ions with charge state of +1 or undetermined were excluded.

2.7 Label-free quantification and protein identification

Label-free quantitative proteomic analyses were carried out using 5 biological and 3 analytical replicates from the LPS, saline (LPS control), PGE_2 and vehicle (PGE_2 control) groups. Quantification was performed using the Progenesis QI proteomics software (version 1.0; Non-Linear Dynamics, Newcastle upon Tyne, UK). The spectra were aligned, and MS1 events were quantified based on extracted ion chromatogram peak areas and compared among LC-MS/MS runs according to the experimental design for replicates and conditions. For peptide identification, MS/MS spectra with p value < 0.05 (ANOVA) were exported as Mascot generic files (.mgf) and searched with PEAKS Studio 7.0 (Bioinformatics Solutions Inc., Ontario, Canada) using the Uniprot Rat protein database (released on 03/17/2016, 35.144 sequences). Parameters used were 10 ppm peptide mass tolerance, 0.6 Da fragment mass tolerance and two missed cleavages allowed. Methionine oxidations and acetylation of protein N-termini were specified as variable modifications, while carbamidomethylation of cysteine was specified as a fixed modification. To assess the false-positive identification rate, the databases used was

reversed on-the-fly during the database queries and appended to the original database. Protein identification FDR was set to 0.1 %. Identifications were re-imported into Progenesis QI, for protein quantification. Only proteins quantified with a minimum of one unique peptide were considered for further analyses. Conflicting peptides were automatically detected and manually validated according to the protein score, peptide score and abundance profile. Peptides still in conflict after manual validation were excluded from protein quantification. PCA analysis was performed at both peptide and protein level to evaluate whether the grouping among replicates was more evident than the grouping of conditions, as well as to detect the eventual presence of outliers. Three technical replicates were measured for every sample preparation to verify robust experimental reproducibility.

2.8 Metabolite profiling

Frozen hypothalami (7-8 biological and 2 analytical replicates) were used for metabolic profiling analysis. About 5 mg of tissue was homogenized in 1.4 mL of methanol containing 60 µL of ribitol (0.2 mg mL^{-1} – (Sigma-Aldrich, St. Louis, USA)) as an internal reference. Samples were vortexed and incubated with occasional shaking at 70 °C for 10 min, centrifuged at 10,000 × g for 10 min, and the supernatant was transferred to a new tube. Cold ultrapure water and chloroform (2:1) was added and the extract was vortexed and centrifuged at 2,200 × g for 10 min. Aliquots from the upper aqueous phase were transferred to new tubes and vacuum dried. Derivatization was performed with 40 µL of 20 mg/mL methoxyamine hydrochloride (Sigma-Aldrich, St. Louis, USA) in pyridine (Merck, New York, USA) for 2 h with agitation at 37 °C. *N*-Methyl-*N*-(trimethylsilyl)trifluoroacetamide (MSTFA) was added, and samples were incubated at 37 °C for 30 min. Immediately after derivatization, samples were analyzed using gas chromatography–mass spectrometry (GC–MS). The separation was performed using an Agilent 7890A GC equipped with a 30 m HP5-MS column (Agilent, Santa Clara, USA), and

analytes were detected using an Agilent 5975 quadrupole mass spectrometer (Agilent, Santa Clara, USA) [46]. Samples (1 μL) were injected in split mode (10:1) at 230 °C using helium as carrier gas at a continuous flow of 0.6 mL min^{-1}. The GC oven temperature was initially maintained at 70 °C for 5 min and then increased at a rate of 7 °C min^{-1} to 350 °C, before reduction to 320 ^{o}C and maintenance at this final temperature for 5 min. The chromatograms were aligned using the MetAlign software [47]. Peak identification was performed using the NIST MSSEARCH software and the NIST mass spectral library. Peak intensities were corrected for variations in the response of the internal standard and the exact mass of tissue extracted.

2.9 Pathway analysis

The proteins that presented differences in abundance between stimulated and control groups were submitted to pathway enrichment analysis by using KOBAS 3.0 Bioinformatics tool (http://kobas.cbi.pku.edu.cn/home.do) [48]. The annotated output file of total hypothalamic proteins previously identified was used as background. This tool can identify statistically enriched related pathways for a set of proteins using pathway knowledge from multiple commonly used databases [48,49]. The hypergeometric test / Fisher exact test was used for the enrichment analysis, and the method of Benjamin and Hochberg [50] was used for correction of false discovery rates (FDR) with small term cutoff of 5. Differentially abundant proteins were subsequently annotated in the KEGG pathway database (http://www.genome.jp/kegg/pathway.html). The analysis was performed using the freely available BlastKOALA (http://www.kegg.jp/blastkoala/) sequence similarity tool. The annotated proteins obtained from the KEGG database were categorized based on their functional roles.

2.10 Statistical analysis

All data in this work are represented as the mean ± standard error of the mean. The unpaired two-tailed Student's *t* test was used to determine *p* values for all assays considering only two conditions. Significance levels for all measures were set at $p < 0.05$. *Statistical Package for the Social Sciences* software (SPSS, SPSS Inc. Chicago, IL, USA) version 23.0 was used for the statistical analyses. The differential protein abundance was analyzed using a modified Student's *t*-test from the Limma package available for the R programming environment (Goeminne et al., 2015, ; Kammers et al., 2015; Ritchie et al., 2015, please also see *www.r-project.org*), followed by multiple testing corrections using the Benjamini-Hochberg [50] procedure for false discovery rate. A *q*-value <0.05 was considered statistically significant.

3. Results

The initial goal was to confirm the time course of changes in body temperature following LPS or PGE_2 administration and to establish the collection time of the hypothalamus for proteomic analysis. The intravenous injection of 5 $\mu g.kg^{-1}$ LPS produced a biphasic fever with first (38.6 ºC) and second (38.8 ºC) peaks occurring at 2.5 and 4.5 h, respectively **(Figure 1 A)**. The central injection of PGE_2 (100 ng) caused a short-lived monophasic response, peaked at 30 min (37.8 °C) **(Figure 1B)**. Hypothalami were then collected at 2.5 h (150 min) after LPS administration and 30 min after PGE_2 administration, when both stimuli had induced significant increase in core body temperature (LPS: $\Delta T = 1.48 \pm 0.07$ °C, $p < 0.0001$ and PGE_2: $\Delta T = 1.38 \pm 0.09$ °C, $p < 0.0001$) **(Figure 1C and 1D)**.

To investigate the effects of LPS and PGE_2 on hypothalamus proteomes, the rat hypothalamus samples were submitted to tryptic digested and the resultant peptides were analyzed by MS/MS on a nano-LC system coupled to an Orbitrap mass spectrometer. To

identify fever-related proteins, a label-free quantification method was applied. The generated MS/MS data were analyzed using Peaks program to identify peptides and proteins. A total of 60 LC-MS/MS chromatograms showed the results of the global proteome profiling. From the experimental sets, we identified we identified 131,555 peptides, leading to 7,021 proteins with a protein-level FDR < 0.01 **(Supplementary Table 1)**. As far as we know, this is the largest rat hypothalamus proteome data set available (PASS01183 deposit PeptideAtlas repository).

Volcano plots illustrate the log_2-fold change and adjusted *p*-value of all proteins in LPS (**Figure 2A**) and PGE_2 (**Figure 2B**) compared with their respective controls, quantified using the Progenesis software. Venn diagrams were constructed to identify common and specific differential abundant proteins related to febrile responses (**Figures 2C and 2D**). Analysis between each stimulus and control condition led to 1,388 and 895 varying proteins for LPS and PGE_2, respectively **(Supplementary Table 2)**. Proteins were classified as presenting increased (648 - LPS group and 326 – PGE_2 group) or decreased (740 – LPS group and 569 - PGE_2 group) relative abundance **(Figure 2C and 2D)**. Among them, there were 186 proteins overlapped between groups, in which 53 had increased and 133 decreased relative abundance.

KOBAS pathway analysis of differentially abundant proteins indicated that metabolism was the most significantly enriched term (corrected *p*-value = 0.04) in the LPS group. The main terms enriched in PGE_2 group were metabolism (corrected *p*-value = 0.004), mitogen-activated protein kinases (MAPKs) signaling (corrected *p*-value = 0.02), pentose phosphate pathway (corrected *p*-value = 0.03) and cytokine signaling (corrected *p*-value = 0.03) (data not shown). Since most of the enriched pathways were related to metabolism and inflammation, the BlastKOALA software was used to carry out pathway annotation of the differentially abundant proteins. To permit a deeper interpretation of the cascade of events underlying LPS and PGE_2 during fever responses, the discussion below was centered mainly on metabolic and inflammatory pathways altered by these stimuli.

3.1 Inflammatory Pathways

Proteins related to inflammation signaling are presented in **Table 1**. As expected, systemic exposure to LPS impacted the inflammation-related proteome (67 proteins) more markedly than central injection of PGE_2 (32 proteins). Globally, inflammation-related proteins from both stimuli included those associated with MAPKs NFκB, ARA, adenylate cyclase (cAMP) and calcium signaling (**Table 1**). Assuming the classical signaling pathway in which LPS binds to TLR4, data from the LPS group demonstrated increased levels of MAPK pathway protein mitogen-activated protein kinase kinase 6 (MKK6), JIP3 protein and the stress-activated protein kinase JNK3. In the PGE_2 group, MAP2K4 delta and MAP 8-interacting protein 3 were increased compared to control. Cell division control protein 42 homolog (Cdc42/Rac) was more abundant in both LPS and PGE_2 groups than their respective controls. On the other hand, mitogen-activated protein kinase kinase 1-interacting protein 1 (MP1) in the LPS group and extracellular signal-regulated kinase 1 (ERK1) in both LPS and PGE_2 groups were found to be less abundant than controls **(Table 1)**.

In NFκB signaling, the upregulation of ELKS/Rab6-interacting/CAST family member 1 (ELKS), casein kinase II (CKII) and the decrease of TNF receptor-associated factor 3 (TRAF3) was identified in the LPS group. In the PGE_2 group, only TRAF3 was found to be upregulated **(Table 1)**.

Regarding arachidonic acid metabolism, CYP2J16, a family 2 cytochrome P450, was found upregulated in the LPS group, whereas carbonyl reductase 1 (CBR1) was increased in the PGE_2 group. A high level of prostaglandin E synthase 3-like 1 (Ptges3|1) was observed in both groups **(Table 1)**.

TLR-independent signaling pathways can also contribute to the development of inflammatory responses induced by LPS, including those involving cAMP and calcium signaling. In agreement with this, in the LPS group increased levels of cAMP-dependent protein

kinase catalytic subunit beta (PKA C-beta), pituitary adenylate cyclase-activating polypeptide type I receptor (PACAP) and adenylate cyclase 9 were found whilst rap guanine nucleotide exchange factor 4 were decreased. In contrast, PGE_2 acts by binding to the EP3 receptor in the APO, ultimately activating a pathway that may involve cAMP [54]. In the PGE_2 group, there was an upregulation of cAMP-dependent protein kinase catalytic subunit (PKA), guanine nucleotide-binding protein G(s) subunit alpha (Gs), calcium/calmodulin-dependent protein kinase type II subunit beta (CaMK-II) and adenylate cyclase type 5 **(Table 1)**.

In the calcium signaling pathway, LPS caused an increase in abundance of two isoforms of phosphoinositide phospholipase C beta, Plcb4 and Plcb3, and a decrease in Plcg1 isoform. Sodium/calcium exchanger 1 levels were higher in both groups LPS and PGE_2, and voltage-dependent anion-selective channel protein 3 (VDAC-3) was decreased in both groups. Several isoforms of protein kinase C (PKC) were upregulated in LPS group, including two beta type PKCs and one gamma type PKC. In the PGE_2 group, only one protein specie of PKC beta type was found to be increased **(Table 1)**.

3.2 Metabolic Pathways

Interestingly, various proteins related to energy metabolism had their abundance changed by both LPS (71 proteins) and PGE_2 (57 proteins) groups when compared to their respective controls **(Table 2)**.

Regarding carbohydrate metabolism, most of the proteins involved in glycolysis were downregulated in both groups. Despite this, in the LPS group, hexokinase was presented at higher concentrations. In the PGE_2 group, glucose-6-phosphate isomerase, phosphoglycerate kinase, enolase and pyruvate kinase were increased. In response to both stimuli, levels of the rate-limiting enzyme of glycolytic pathway phosphofructokinase decreased **(Table 2)**. Most

proteins involved in the pentose phosphate pathway were downregulated in the LPS group, whereas in the PGE_2 group, three proteins were upregulated **(Table 2)**.

Similar to the changes observed in the glycolytic and pentose phosphate pathways, administration of LPS and PGE_2 stimuli induced a reduction in the abundance of tricarboxylic acid (TCA) cycle enzymes, with the exception of citrate synthase and succinyl-CoA synthetase, which increased in both groups **(Table 2)**.

Considering amino acid metabolism, in the LPS group, 47 proteins were downregulated and 15 upregulated; in the PGE_2 group, 38 proteins were downregulated and 10 upregulated (data not shown). Degradation of valine, leucine and isoleucine was the most altered pathway in both stimuli **(Table 2)**.

In relation to fatty acid (FA) biosynthesis, LPS caused an increase in long-chain-fatty-acid--CoA ligase 1 (ACSL1) and acetyl-CoA carboxylase 1 levels, and a decrease in fatty acid synthase. In the PGE_2 group, fatty acid synthase and long-chain-fatty-acid-CoA ligase 6 were decreased **(Table 2)**. On the other hand, considering proteins related to degradation of fatty acid, a large number of proteins were decreased in both LPS and PGE_2 groups **(Table 2)**.

In glycerophospholipid metabolism, most of the proteins were upregulated in the LPS group **(Table 2)**. Among them, notable ones were the glycerophospholipid turnover membrane-bound O-acyltransferase domain-containing protein 2 (MBOAT2), 1-acylglycerol-3-phosphate O-acyltransferase 4 (AGPAT4), glycerol-3-phosphate dehydrogenase and diacylglycerol kinase gamma and beta. Interestingly, in the LPS group, the abundance of proteins related to synthesis of ARA-containing glycerophospholipids increased, including ethanolamine-phosphate cytidylyltransferase, phosphatidate cytidylyltransferase 2 and phosphatidylinositol synthase. In the PGE_2 group, most proteins involved with ARA synthesis were downregulated **(Table 2)**.

Quantitative proteome analysis also revealed alterations in mitochondrial proteins **(Table 3)**. According to KEGG annotation, 48 mitochondrial proteins were found significantly altered in the LPS group compared to 28 in PGE_2 group **(Table 3)**. Concerning mitochondrial carriers, LPS upregulated the oxoglutarate carrier (SLC25A11), whereas PGE_2 increased the citrate carrier and the aspartate/glutamate carrier (SLC25A12). Mitochondrial pyruvate carrier 1 (MPC1) increased in both groups. The four largest mitochondrial membrane protein complexes of the respiratory chain as well as the Fo-F1 ATP synthase complex (complex V) had their levels altered by both stimuli. LPS and PGE_2 caused significant downregulation, mainly in complexes I and IV. Only LPS was able to downregulate proteins related to complexes II and III. Considering complex V, there was almost equal distribution between down and upregulated proteins in both LPS and PGE_2 groups **(Table 3)**.

Disturbance in the mitochondrial function may lead to increase of ROS. Besides, we observed that levels of antioxidant enzymes of hypothalamic cells were found to be downregulated, more severely in the LPS group **(Figure 3)**. Still related to mitochondrion, concerning proteins related to apoptosis, alterations were observed only in the LPS group with proapoptotic proteins (BCL2-like 13, apoptosis regulator BAX, FAS-associated death domain protein and apoptosis-inducing factor 1 (mitochondrial)) downregulated and antiapoptotic proteins (Bcl-2-like protein 1 and Bcl-2-interacting death suppressor) upregulated **(Table 3)**.

3.3 Amino and Organic Acids

To investigate levels of amino and organic acids in the LPS, PGE_2 and control groups, the relative intensities of ions from different metabolites were compared **(Figure 4)**. Bars represent the ion intensity divided by the mass of each sample, normalized in function of control values. When compared to the control group, a decrease in the level of one metabolite (glycine)

was observed in the LPS group, whilst in the PGE_2 group, no significant change was observed **(Figure 4)**.

4. Discussion

In this study, high resolution mass spectrometry-based quantitative proteomics was used to identify proteins and signaling pathways associated with febrile responses induced by LPS and PGE_2 in rats. With 7,021 proteins identified, this is the largest rat hypothalamus proteome data set available to our knowledge. A total of 1,388 and 895 differentially abundant proteins were found in LPS and PGE_2 groups respectively. Such a high number of differentially abundant proteins is a pattern observed in different studies using LPS since it induces systemic inflammation capable of changing several cellular pathways [55,56].

Although both stimuli are experimentally used to produce fever, they are widely different from each other. LPS is an exogenous pyrogen used as a pathogenic agent administrated systemically, producing a complex and aggressive inflammatory response that leads to fever [1,17]. Initially, LPS stimulates distinct signaling pathways to induce pro-inflammatory cytokines and other inflammatory mediators that can directly and indirectly produce fever through PGE_2 downstream [1,17]. PGE_2, an endogenous pyrogen, is synthesized peripherally or centrally [57,58] being considered the ultimate mediator of the febrile response.

4.1 Inflammatory Pathways

Is it well characterized that binding of LPS to TLR4 receptor leads to the recruitment of adaptor proteins that induce activation of two distinct intracellular signaling pathways: the myeloid differentiation primary response protein 88 (MyD88) dependent pathway and the MyD88-independent pathway (also known as TRIF-dependent) [19,59].

In the MyD88 dependent pathway, TLR engagement induces formation of the protein complex called myddosome, which initiates a signal transduction cascade that culminates in the activation of NFκB and MAPK to regulate the expression of cytokines, chemokines and type I interferon, which ultimately protect the organism from microbial infection [60,61]. The classic MAPK family consists of three subfamilies: extracellular signal-regulated kinase (ERK; ERK1 and ERK2), c-Jun N-terminal kinase (JNK; JNK1, JNK2 and JNK3) and p38 MAPK (α, β, δ, and γ) [62]. The MAPK signaling is a three-tiered cascade: MAPK, MAP kinase kinase (MKK or MAP2K) and MAP kinase/ERK kinase (MEK) kinase or MAP kinase kinase kinase (MEKK or MAP3K) [62]. A number of studies have shown that the activation of ERK1/2 can play multiple roles in the regulation of neuronal function, and are also involved in neuroinflammation and cell death [63–65]. In the present study, differential abundance of several MAPKs family members was observed in response to LPS and PGE_2 administration in relation to the control. The levels of ERK1 were decreased in both groups. In the LPS group, MP-1, an ERK1-related protein able to selectively induce the activation of ERK-1, was downregulated. The reduction in ERK1 abundance may suggest the activation of mechanisms that prevent neural cell death.

In mammalian cells, p38 isoforms and JNK are strongly activated by environmental stresses and inflammatory cytokines [66]. In the LPS group, the MKK6 and Cdc42 had increased abundance. MKK6 is a MAPKK able to activate all p38 isoforms, and Cdc42, a small GTPase responsible for stimulating MKK6, is known to be increased after LPS stimulation in macrophages [67]. Upregulation of JNK3 and JIP3 was also observed in LPS group. JNKs, in particular the neuronal isoform JNK3, have been recognized as important for cytokine production in LPS-stimulated microglia [68]. JIP3, a scaffold protein, can modulate and facilitate JNK activation *in vivo* [69]. Some authors have argued that scaffold proteins may be responsible for the specific regulation of JNK function, and are therefore very important in

some pathological conditions [70]. Cdc42 was also elevated in PGE_2 group. In addition, other proteins increased in the PGE_2 group were MKK4, a MAPKK responsible for JNK activation, and MAP 8-interacting protein 3, a JIP3 isoform. The activation of those proteins related to p38 and JNK pathways in LPS and PGE_2 groups reinforces the hypothesis of activation of these signaling pathways in hypothalamic cells during febrile response.

As mentioned above, TLR4 stimulation by LPS binding can activate TRIF-dependent pathways. Data from the literature demonstrate that tumor necrosis factor receptor-associated factor 3 (TRAF3) can differently interact with both MyD88 and TRIF, regulating the production of interferon (IFN) or proinflammatory cytokines [71]. Within the MyD88 complex, TRAF3 is degraded, causing transforming growth factor β-activated kinase 1 (TAK1) activation, which in turn activates MAPKs and NFκB [60]. Supporting this idea, binding of LPS to TLR4 is known to stimulate ubiquitination and degradation of TRAF3 in CNS-resident macrophages [72]. The low levels of TRAF3 in the LPS group that we detected are consistent with previous findings, which suggested that degradative TRAF3 ubiquitination during MyD88-dependent TLR signaling is essential for activation of MAPKs and inflammatory cytokine production [72].

Differently to what was observed for LPS, we detected TRAF3 upregulation in the PGE_2 group, which may support the activation of the TRIF-pathway and IFN production. The NFκB family play an important role in immunological responses, regulating the expression of proinflammatory cytokines and chemokines, such as COX-2, IL-1β and TNF-α [73,74]. It has been demonstrated that degradation of TRAF3 is sufficient for triggering NFκB signaling [75,76] through the combined action of NFκB-inducing kinase (NIK) and the inhibitor of NFκB kinase α (IKKα). Under normal conditions, TRAF3 induces NIK ubiquitination and degradation. When NIK levels are stabilized, as a result of TRAF3 degradation, activation of NFκB takes place [77,78]. Along with low levels of TRAF3, high levels of CKII, responsible for activation of NFκB, were observed in the LPS group, suggesting the regulation of NFκB

activity [79]. In fact, in TRIF-dependent signaling, TRAF is recruited by TRIF causing the phosphorylation of interferon regulatory factor 3 (IRF3) that translocate into the nucleus to regulate transcription of type I-IFN. Interestingly, inhibition of degradation of ubiquitinated TRAF3 prevents the expression of all proinflammatory cytokines without impacting the IFN response [71].

Among various cytokines produced after the LPS challenge, TNF-α is the first to appear in the bloodstream, followed by IL-1β and IL-6 [12]. NFκB is activated approximately 15 min after LPS administration [80] and seems to be involved in the initiation of fever [81]. The maintenance of brain inflammation and fever responses, however, are mediated by nuclear STAT3-translocation which is induced after 90 min [22,25]. At 150 min, the activation of NFκB is accompanied by the induction of more TNF-α in addition to IL-1β and IL-6, the main plasma cytokines [82]. TNF-α interacts with cell surface receptors, such as TNF receptor-1 (TNF-R1) and involve several signal transduction pathways as ERK, JNK and p38 MAP kinases. These MAPK signaling pathways induce the activation of NFκB, a secondary response which increases the expression of multiple inflammatory cytokines. As MAPK function both upstream and downstream of TNF-α signaling [83,84] it is possible that the MAPKs that were altered in the present study, may be involved in both LPS and TNF-α signaling.

Cytosolic PGE synthase (cPGES) were found in higher levels in both stimuli – LPS and PGE_2. This enzyme is constitutively expressed and can be functionally coupled to COX-1 to promote fast PGE_2 production. Higher levels of cPGES suggest the involvement of constitutive COX1/cPGES pathway in fever responses. cPGES can also be regulated by phosphorylation through CKII, increasing PGE_2 production [85,86]. The stimulation of CKII activity by H_2O_2 indicates that ROS may indirectly increase the activity of cPGES through CKII [87]. Based on this, we speculate that constitutive cPGES may contribute to PGE_2 generation during the early phase of fever. Evidence supporting this hypothesis is the elevated expression of cPGES in an

experimental LPS-induced inflammation in rodent brain, with no significant changes in other organs [88]. Once formed, PGE_2 can be converted to prostaglandin F2-alpha ($PGF_{2\alpha}$), another fever-related prostaglandin [89,90]. In the PGE_2 group, a tenfold increase was identified for carbonyl reductase 1 (CBR1), the NADPH-dependent reductase responsible for the conversion of PGE_2 in $PGF_{2\alpha}$, suggesting a draining of excess hypothalamic PGE_2, probably due to local PGE_2 administration. In line with this, it was demonstrated that CBR1 had anti-inflammatory properties *in vivo* and *in vitro* through inhibition of NFκB and MAPK activation [91].

We found higher levels of cytochrome P450 family 2 (CYP2) after LPS stimulation. There is growing evidence for a thermoregulatory role of non-canonical proteins involved in fever response. CYP2 is a protein responsible for the production of epoxyeicosatrienoic acid (EET) compounds, which are primary products of ARA metabolism. Intracerebroventricular administration of EETs inhibits fever induced by LPS and IL-1β in mice [92,93]. In this way, inhibitors of cytochrome P450 can augment fever in rats and mice, indicating that metabolites of this enzyme may be good candidates for endogenous antipyretic compounds [94,95]. The results might represent a possible mechanism of temperature self-regulation.

PGE_2 is believed to exert its effects by activation of G proteins through binding to EP3 receptor [1,3,96], the main subtype receptor involved in the development of febrile response [34,97]. This process can modulate intracellular levels of cAMP in addition to enhancing calcium levels. Alternatively, there can be increase of just intracellular calcium levels. Important changes in cAMP and calcium pathways were caused by both stimuli, providing evidence for the role of these pathways in fever induction. In fact, high levels of PGE_2 in the hypothalamus induce the production of cAMP and activation of thermosensitive neurons that in turn activate brown adipose tissue, resulting in thermogenesis [17]. An upregulation of different isoforms of adenylate cyclase and PKA subunits was identified in both LPS and PGE_2 groups. In experimental models of pain and inflammation, it was demonstrated that PKA, a

kinase coupled to cAMP signaling, participates in the inflammatory hypernociception developed in response to the administration of PGE_2 [98,99], which was prevented by cAMP and PKA inhibitors in a dose-dependent manner [100].

In relation to calcium signaling, both stimuli led to alterations in the abundance of proteins related to this pathway, though this was more marked in the LPS group. Neurons, astrocytes and microglial cells respond to LPS, TNF-α, PGE_2 and also IL-1β by increasing intracellular calcium levels [101–103]. Calcium is required for cytosolic phospholipase A2 (cPLA2) activation, which is responsible for ARA release from phospholipids [104]. Along with diacylglycerol (DAG), calcium can activate PKC, a kinase identified as responding to both stimuli, and detected in more than one protein specie in the LPS group. It is known that PKC inhibitors reduce LPS-stimulated cytokine secretion by macrophages and LPS-induced fever [105–107]. In fact, several PKC isoforms can be associated to the TLR or close components of the receptor complex participating in downstream activation of MAPK and NFκB [108]. As mentioned, in this study PKC relative abundance increased, while the known substrate of PKC (Prksh) was found to be downregulated in both stimuli, suggesting the participation of this kinase in the fever induced by LPS and PGE_2. As PKC is a ubiquitous enzyme, taking part in a great number and variety of cell signals, more studies are necessary to indicate the exact involvement of PKC in fever responses.

4.2 Energy Metabolism

Glucose is the main source of energy for the mammalian brain. Pyruvate formed through glycolysis enters the mitochondrial TCA cycle, where it is oxidatively decarboxylated to form acetyl-CoA, which is then completely oxidized to CO_2. Part of the energy released during cellular respiration is converted into heat and contributes to maintaining body temperature at

37 °C [109]. Our proteomic results showed that most proteins associated with metabolism were reduced in both LPS and PGE_2 groups.

Most glycolytic proteins were downregulated in the LPS group. However, hexokinase I levels increased. Under normal physiological conditions, excessive glucose-6-phosphate produced by hexokinase activity could be redirected to the pentose phosphate pathway to generate NADPH and pentoses that make up DNA and RNA. This metabolic shift may not occur in this instance, since several proteins from the pentose phosphate pathway were downregulated. At the same time, other phosphorylated glucose utilizing pathways, such as gluconeogenesis, were downregulated, rendering the high hexokinase levels an intriguing question. It is known that plant hexokinase is a moonlighting protein, a single protein that can exert multiple physiological functions that are not due to gene fusions, multiple RNA splice variants or proteolytic fragments [110–112]. There is evidence that glycolytic inhibitors and metabolic conditions affecting hexokinase function and localization can induce inflammasome activation in mammalian cells [113]. The increased hexokinase I levels observed here may be related to a possible attempt to control the inflammatory response, possibly as a moonlighting protein having a secondary, unpredicted function. This proposition needs to be further explored in future experiments.

In agreement with the effects on glycolytic enzymes, the concentrations of proteins participating in the TCA cycle were also disturbed in the LPS group. Although most of the proteins had their abundance diminished, a surprising increase in both citrate synthase and succinyl-CoA ligase was observed. These alterations seem to be accompanied by a decrease in mitochondrial respiration, since several protein subunits of the five complexes that constitute the oxidative phosphorylation machinery were reduced.

In the PGE_2 group, although an increase in important enzymes of the glycolytic pathway were identified, several other essential glycolysis enzymes were downregulated followed by

similar changes for TCA cycle enzymes and mitochondrial protein complexes as observed in the LPS group.

We then summarized protein changes for LPS and PGE_2 groups in **Figure 5**. Important changes in TCA cycle proteins were observed in both stimuli. In the LPS group, half of the proteins were upregulated and the other half were downregulated, whereas only citrate synthase were upregulated in the PGE_2 group. Notably, the abundance of mitochondrial carriers, such as the mitochondrial pyruvate carrier 1 (MPC1), augmented in both LPS and PGE_2 groups. Considering the results from both LPS and PGE_2 groups, pyruvate formed by glycolysis can be transported to the mitochondrial matrix through mitochondrial pyruvate carrier 1 (MPC1), where it can either be converted into oxaloacetate by pyruvate carboxylase or into acetyl-CoA by pyruvate dehydrogenase (PDH). Recent studies have revealed a relationship between MPC expression and activity and changes in cellular metabolism. Vacanti et al.[114] demonstrated that transcriptional or pharmacological inhibition of MPC1 in skeletal muscle myoblasts causes reliance on substrates for energy and biosynthetic metabolism shifted from glucose to amino acid and fatty acid oxidation. Mice deficient in MPC1 are embryonically lethal at E12-E14 stages of development. In addition, mutant embryos presented lesions in the pons region of the brain stem, and the metabolome of the telencephalic brain showed significant anomalies, including lactate accumulation and an imbalance in the levels of several neurotransmitters [115].

Also, the solute carrier family 25 member 12, also known as aspartate/glutamate carrier 1 (AGC1), and the mitochondrial tricarboxylate transport protein, also known as mitochondrial citrate carrier (CIC), were upregulated upon the PGE_2 treatment. Considering the possibility that intermediates are not being completely oxidized in the cycle, some of them such as citrate and succinate may be withdrawn and diverted to the cytosol. Citrate, coming from the upregulated citrate synthase in both groups, could be exported to the cytoplasm by the specific

mitochondrial citrate carrier (CIC). Citrate works as an allosteric activator of acetyl-CoA carboxylase, increased in the LPS group, favoring the production of fatty acids that can give rise to phospholipids and, consequently, ARA. In macrophages treated with LPS, both silencing of CIC expression by siRNA and inhibiting CIC by the inhibitor BTA (benzene-1,2,3-tricarboxylate) impaired the production of ROS, NO and PGs [116].

In the PGE_2 group, it is possible that part of the oxaloacetate within the mitochondrial matrix to be converted into aspartate by mitochondrial aspartate aminotransferase and transported to cytosol by the AGC1. AGC1 catalyzes the calcium-dependent exchange of cytoplasmic glutamate with mitochondrial aspartate across the mitochondrial inner membrane [117]. Once in the cytosol, oxaloacetate is regenerated by cytosolic aspartate aminotransferase and then reduced to malate through malate dehydrogenase. Malate is the substrate for malic enzyme, which produces NADPH and pyruvate. Pyruvate transported to the mitochondrial matrix through MPC1 is probably being converted into oxaloacetate by pyruvate carboxylase, which was increased in PGE_2 group. Oxaloacetate produced by this alternative cycle supports the continued citrate production.

Succinate may contribute to the inflammatory process by binding to succinate receptor 1 (SUCNR1), which increases intracellular release of ARA and induces the production of PGE_2 and calcium-dependent NO [118]. In macrophages stimulated by LPS, accumulation of succinate stabilizes hypoxia-inducible factor-1α (HIF-α), leading to the induction of a range of target genes, such as proinflammatory cytokine IL-1β, exacerbating inflammation [119]. Under LPS treatment, succinyl-COA synthetase (also known as succinyl-CoA ligase) was upregulated, while succinate dehydrogenase (SDH) was downregulated.

The proteomic data indicate that some metabolites could have altered abundance during fever. To provide more insight into how LPS and PGE_2 affect hypothalamic metabolism, we undertook comparative organic metabolite analysis. It is known that the TCA cycle is not only

a central process in energy metabolism, but also a cycle whose metabolites can be important in signaling pathways, mainly in pathological circumstances [118,120]. However, we did not find any changes in the abundance of TCA metabolites, such as citrate, succinate, fumarate and malate. For example, despite the changes observed in enzyme abundance involved in citrate and succinate synthesis/degradation, the levels of such metabolites remained the same at the time point selected for analysis. If any metabolite is diverted from the cycle, it must be replaced by anaplerotic reactions to ensure its continued function [121]. Thus, metabolites are expended and replenished in a dynamic equilibrium, which makes it difficult to detect changes in their levels. In macrophages, such changes could only be visualized after 4 up to 24 hours after LPS stimulation [119]. Besides, the oxidation of the branched-chain amino acids yielding succinyl-CoA and acetyl-CoA for the TCA cycle supports the concept of citrate and succinate production by the only two highly abundant proteins increased, while glycolysis and the cycle itself seem inhibited.

Conversely, the metabolite analysis revealed decreased glycine levels in the LPS group in comparison to the control group. Glycine is a nonessential amino acid that in the central nervous system plays a role as inhibitory neurotransmitter, thereby regulating several functions as behavior and food intake [122]. Also relevant is that degradation of glycine in mammals occur via three pathways, one of which regenerates pyruvate [121,123]. Such pyruvate regeneration can explain how carbon can be fed into the TCA cycle even in a scenario of downregulation of glycolysis.

Dysfunction of mitochondrial oxidative phosphorylation can favor the escape of electrons, increasing ROS production during pathological conditions [37,124]. In this study, several important antioxidant proteins were reduced upon LPS treatment. We recently demonstrated an increase in ROS formation in the hypothalamus, brown adipose tissue and liver of the rats during an LPS-induced fever (Gomes et al, 2018). These data reinforce the

hypothesis of intensification of oxidative stress during the inflammatory process. In agreement, previous studies assessing neuroinflammation and mitochondrial dysfunction after a systemic LPS injection found a depletion of endogenous antioxidant capacities in brain regions [125]. In other models using LPS, mitochondrial oxidative stress, electron chain dysfunction and decreased antioxidant activity were also observed [126]. Considering the great number of downregulated subunits of mitochondrial electron transport chain complexes , the observed metabolic alterations and the reduction of antioxidant capacity, there is a possible attempt of cell survival during febrile response since proapoptotic proteins were found downregulated concomitantly to the upregulation of antiapoptotic proteins (**Table 3**), suggesting a mechanism to prevent cell death.

4.3 Lipid Metabolism

The increased abundance of acetyl-CoA carboxylase 1 in LPS group was accompanied by an overall reduction of proteins involved in fatty acid (FA) degradation in both groups. FAs are known to have important roles in inflammation [127]. Glycerophospholipids can be produced after LPS stimulation through increased lipolysis and impaired lipid catabolism [128]. Therefore, the development of mechanisms to increase FA biosynthesis and to reduce FA degradation may contribute to the inflammatory response.

Under physiological conditions, ARA is found in the *sn-2* position of glycerophospholipids, particularly choline glycerophospholipids (PCs), ethanolamine glycerophospholipids (PEs) and phosphatidylinositol (PI) [129]. During the inflammatory process, cytokines and growth factors modulate the generation of ARA by PLA2 isozymes that cleave phospholipids in the *sn-2* position, producing free ARA and the corresponding lysophospholipid [130,131]. However, only a minor fraction of the free ARA released is converted into eicosanoids, while the remainder is effectively reincorporated into phospholipids

by reacylation [132]. Therefore, the production of free ARA is a highly regulated process that represents a balance between two competing reactions: phospholipid hydrolysis and reacylation [129,133]. Reacylation is carried out in two steps. Activation of the carboxyl group of the fatty acid by thioesterification with CoA, catalyzed by acyl-CoA synthetases, is the first step for ARA incorporation. The next step consists of the esterification of ARA into the *sn-2* position of glycerophospholipids mediated by lysophospholipid acyltransferases [132]. Two families of lysophospholipid acyltransferase enzymes have been recognized, the MBOAT family and the AGPAT family [134,135]. In the LPS group, the upregulation of ACSL1, MBOAT2 and AGPAT4 might indicate a possible reincorporation of free ARA, important for the replenishment of intracellular ARA exhausted during the inflammatory response [133].

Glycerophospholipids are integral components of neural membranes that possess important biological roles, including acting as a reservoir for the generation of second messengers and their precursors [136–139], in apoptosis [140,141], as a membrane anchor [142,143] and as a stimulus for RNA synthesis [144]. They are synthesized from glycerol-3-phosphate in a *de novo* pathway, producing phosphatidic acid (PA) and DAG or cytidine diphosphate-DAG. In the LPS group, a significant increase in diacylglycerol kinase gamma and beta types was found. Diacylglycerol kinases, using ATP as the phosphate donor, catalyze the conversion of DAG to PA [145]. In addition to its functions as an allosteric activator of PKC, DAG occupies a central position in the synthesis of PC and PE [146]. PA in turn is an important metabolite of phospholipid biosynthesis, and it has been suggested as a second messenger in inflammatory responses [147,148]. It also acts as a mediator that specifically stimulates the production of pro-inflammatory cytokines (TNF-α; IL-1β and IL-6), NO and PGE_2 in macrophages, facilitating the initiation of host inflammation [147]. These observations are consistent with this study, which shows that LPS administration increased the abundance of proteins related to the synthesis of ARA-containing glycerophospholipids: ethanolamine-

phosphate cytidylyltransferase (Pcyt2) in PE biosynthesis and both phosphatidatecytidylyltransferase 2 (Cds2) and phosphatidylinositol synthase in PI biosynthesis.

5. Conclusions

In general terms, based on proteome abundance, hypothalami of rats exposed to LPS or PGE_2 presented a decrease in some metabolic pathways, such as glycolysis, pentose phosphate pathway, TCA cycle and mitochondrial electron transport chain complexes. Despite the general reduction, the abundance of some important proteins increased, suggesting that both local and systemic stimuli modulate metabolism to converge on the synthesis of important metabolites such as citrate and succinate. They may then emerge as important signal metabolites in inflammation, despite the unchanged levels of these metabolites at the times selected for analysis, maybe due to the efficiency of anaplerotic interventions in the TCA cycle. Along with NFκB, these metabolites can stimulate the production of inflammatory mediators, such as PGE_2, as a mechanism of feedback, which contributes to the maintenance of the inflammatory and febrile response. In addition, in the LPS group, changes in the lipid metabolism favor the production of ARA, leading to formation of eicosanoids. The present results corroborate the literature, emphasizing that signals triggered by the immune system in response to external stimuli are highly correlated to dynamic changes in cellular metabolism [149]. A stimulus does not activate the immune system without interfering in cell physiology; the understanding of this fact represents an important breakthrough in the study of disease development and has allowed the discovery of new targets for controlling fever-related inflammation in the attempt to reestablish homeostasis. It is important to emphasize that the approach of the present study considered only proteome and metabolite abundance to evaluate the metabolism of the whole hypothalamus. Nevertheless, this analysis provided comprehensive information about fever

responses, and helped to reveal new insights into candidate proteins potentially involved in inflammatory signaling and metabolic changes in the brain during systemic LPS and central PGE_2 administration.

Acknowledgments

We would like to thank Nuno Domingues for technical support and Susan Casement for English language review of the manuscript. Funding was provided by grant 483191/2013-2 from the Brazilian National Council for Scientific and Technological Development (CNPq) and grants 0439/11 and 0694/13 from Financiadora de Estudos e Projetos (FINEP) to M.V.S.; grant 193.000.648/2015 from the Federal District Research Support Foundation (FAPDF), and CNPq to F.H.V.S.; grant (01-2006) from FINEP (CT-INFRA) to T.C.R.W. M.F. is recipient of a scholarship from CNPq (146256/2013-1), and S.N.W. is recipient of a fellowship from the Coordination for the Improvement of Higher Education Personnel (CAPES) (PNPD20132991).

Conflicts of Interest

The authors reports no conflict of interest.

References

[1] J. Roth, C.M. Blatteis, Mechanisms of fever production and lysis: lessons from experimental LPS fever., Compr. Physiol. 4 (2014) 1563–604. doi:10.1002/cphy.c130033.

[2] A.R. Zampronio, D.M. Soares, G.E.P. Souza, Central mediators involved in the febrile response: effects of antipyretic drugs, Temperature. 2 (2015) 506–521. doi:10.1080/23328940.2015.1102802.

[3] S.S. Evans, E.A. Repasky, D.T. Fisher, Fever and the thermal regulation of immunity:

the immune system feels the heat, Nat. Rev. Immunol. 15 (2015) 335–349. doi:10.1038/nri3843.

[4] L.M. Harden, S. Kent, Q.J. Pittman, J. Roth, Fever and sickness behavior: Friend or foe?, Brain. Behav. Immun. 50 (2015) 322–333. doi:10.1016/j.bbi.2015.07.012.

[5] Y. Launey, N. Nesseler, Y. Mallédant, P. Seguin, Clinical review: fever in septic ICU patients--friend or foe?, Crit. Care. 15 (2011) 222. doi:10.1186/cc10097.

[6] B. Lee, D. Inui, G. Suh, J. Kim, J. Kwon, J. Park, K. Tada, K. Tanaka, K. Ietsugu, K. Uehara, K. Dote, K. Tajimi, K. Morita, K. Matsuo, K. Hoshino, K. Hosokawa, K. Lee, K. Lee, M. Takatori, M. Nishimura, M. Sanui, M. Ito, M. Egi, N. Honda, N. Okayama, N. Shime, R. Tsuruta, S. Nogami, S.-H. Yoon, S. Fujitani, S. Koh, S. Takeda, S. Saito, S. Hong, T. Yamamoto, T. Yokoyama, T. Yamaguchi, T. Nishiyama, T. Igarashi, Y. Kakihana, Y. Koh, Fever and Antipyretic in Critically ill patients Evaluation (FACE) Study Group, Association of body temperature and antipyretic treatments with mortality of critically ill patients with and without sepsis: multi-centered prospective observational study, Crit. Care. 16 (2012) R33. doi:10.1186/cc11211.

[7] A. Jones, Chemistry : an introduction for medical and health sciences, J. Wiley, 2005. https://books.google.com.br/books/about/Chemistry_An_Introduction_for_Medical_an.html?id=ubE0ILq_aDQC&redir_esc=y (accessed April 10, 2018).

[8] T.D. Warner, J.A. Mitchell, Cyclooxygenase-3 (COX-3): Filling in the gaps toward a COX continuum?, Proc. Natl. Acad. Sci. 99 (2002) 13371–13373. doi:10.1073/pnas.222543099.

[9] R. Aghababian, Essentials of emergency medicine, 2 nd editi, Jones and Bartlett Publishers, 2011.

[10] D.M. Aronoff, E.G. Neilson, Antipyretics: mechanisms of action and clinical use in fever suppression., Am. J. Med. 111 (2001) 304–15.

http://www.ncbi.nlm.nih.gov/pubmed/11566461 (accessed March 28, 2018).

[11] D. do C. Malvar, F.A. Aguiar, A. de L.L. Vaz, D.C.R. Assis, M.C.C. de Melo, V.A.P. Jabor, E. Kalapothakis, S.H. Ferreira, G.C. Clososki, G.E.P. de Souza, Dipyrone metabolite 4-MAA induces hypothermia and inhibits PGE_2 -dependent and -independent fever while 4-AA only blocks PGE_2 -dependent fever, Br. J. Pharmacol. 171 (2014) 3666–3679. doi:10.1111/bph.12717.

[12] J. Roth, G.E. De Souza, Fever induction pathways: evidence from responses to systemic or local cytokine formation., Brazilian J. Med. Biol. Res. = Rev. Bras. Pesqui. Medicas e Biol. 34 (2001) 301–14. doi:10.1590/S0100-879X2001000300003.

[13] R. Medzhitov, T. Horng, Transcriptional control of the inflammatory response., Nat. Rev. Immunol. 9 (2009) 692–703. doi:10.1038/nri2634.

[14] M.M. Buchanan, M. Hutchinson, L.R. Watkins, H. Yin, Toll-like receptor 4 in CNS pathologies, J. Neurochem. (2010) no-no. doi:10.1111/j.1471-4159.2010.06736.x.

[15] T. Kielian, Toll-like receptors in central nervous system glial inflammation and homeostasis., J. Neurosci. Res. 83 (2006) 711–30. doi:10.1002/jnr.20767.

[16] B. Conti, I. Tabarean, C. Andrei, T. Bartfai, Cytokines and fever., Front. Biosci. 9 (2004) 1433–49. doi:10.1111/j.1749-6632.1998.tb09600.x.

[17] C.A. Dinarello, Infection, fever, and exogenous and endogenous pyrogens: some concepts have changed., J. Endotoxin Res. 10 (2004) 201–22. doi:10.1179/096805104225006129.

[18] C.M. Blatteis, A personal recollection: 60 years in thermoregulation., Temp. (Austin, Tex.). 3 (2016) 1–7. doi:10.1080/23328940.2016.1148524.

[19] M. Molteni, S. Gemma, C. Rossetti, The Role of Toll-Like Receptor 4 in Infectious and Noninfectious Inflammation, Mediators Inflamm. 2016 (2016) 1–9. doi:10.1155/2016/6978936.

[20] M. Rahimifard, F. Maqbool, S. Moeini-Nodeh, K. Niaz, M. Abdollahi, N. Braidy, S.M. Nabavi, S.F. Nabavi, Targeting the TLR4 signaling pathway by polyphenols: A novel therapeutic strategy for neuroinflammation., Ageing Res. Rev. 36 (2017) 11–19. doi:10.1016/j.arr.2017.02.004.

[21] J. Damm, L.M. Harden, R. Gerstberger, J. Roth, C. Rummel, The putative JAK-STAT inhibitor AG490 exacerbates LPS-fever, reduces sickness behavior, and alters the expression of pro- and anti-inflammatory genes in the rat brain, Neuropharmacology. 71 (2013) 98–111. doi:10.1016/j.neuropharm.2013.03.014.

[22] L. Gautron, P. Lafon, M. Chaigniau, G. Tramu, S. Layé, Spatiotemporal analysis of signal transducer and activator of transcription 3 activation in rat brain astrocytes and pituitary following peripheral immune challenge., Neuroscience. 112 (2002) 717–29. http://www.ncbi.nlm.nih.gov/pubmed/12074913 (accessed October 8, 2017).

[23] N. Laflamme, S. Lacroix, S. Rivest, An essential role of interleukin-1beta in mediating NF-kappaB activity and COX-2 transcription in cells of the blood-brain barrier in response to a systemic and localized inflammation but not during endotoxemia., J. Neurosci. 19 (1999) 10923–30. file:///Unknown/An Essential Role of Interleukin-1 in Mediating NF- B Activity and COX-2 Transcription in Cells of - 0.pdf.

[24] C. Rummel, C. Sachot, S. Poole, G.N. Luheshi, Circulating interleukin-6 induces fever through a STAT3-linked activation of COX-2 in the brain, Am. J. Physiol. Integr. Comp. Physiol. 291 (2006) R1316–R1326. doi:10.1152/ajpregu.00301.2006.

[25] C. Rummel, Inflammatory transcription factors as activation markers and functional readouts in immune-to-brain communication, Brain. Behav. Immun. 54 (2016) 1–14. doi:10.1016/j.bbi.2015.09.003.

[26] C. Rummel, K. Matsumura, G.N. Luheshi, Circulating IL-6 contributes to peripheral LPS-induced mPGES-1 expression in the rat brain, Brain Res. Bull. 86 (2011) 319–325.

doi:10.1016/j.brainresbull.2011.09.006.

[27] S. Li, Y. Wang, K. Matsumura, L.. Ballou, S.. Morham, C.. Blatteis, The febrile response to lipopolysaccharide is blocked in cyclooxygenase-2−/−, but not in cyclooxygenase-1−/− mice, Brain Res. 825 (1999) 86–94. doi:10.1016/S0006-8993(99)01225-1.

[28] A.I. Ivanov, A.A. Romanovsky, Prostaglandin E2 as a mediator of fever: synthesis and catabolism., Front. Biosci. 9 (2004) 1977–93. doi:10.2741/1383.

[29] A. Eskilsson, T. Matsuwaki, K. Shionoya, E. Mirrasekhian, J. Zajdel, M. Schwaninger, D. Engblom, A. Blomqvist, Immune-Induced Fever Is Dependent on Local But Not Generalized Prostaglandin E2 Synthesis in the Brain., J. Neurosci. 37 (2017) 5035–5044. doi:10.1523/JNEUROSCI.3846-16.2017.

[30] C.B. Saper, A.A. Romanovsky, T.E. Scammell, Neural circuitry engaged by prostaglandins during the sickness syndrome, Nat. Neurosci. 15 (2012) 1088–1095. doi:10.1038/nn.3159.

[31] D.B. Wilhelms, M. Kirilov, E. Mirrasekhian, A. Eskilsson, U.Ö. Kugelberg, C. Klar, D.A. Ridder, H.R. Herschman, M. Schwaninger, A. Blomqvist, D. Engblom, Deletion of prostaglandin E2 synthesizing enzymes in brain endothelial cells attenuates inflammatory fever., J. Neurosci. 34 (2014) 11684–90. doi:10.1523/JNEUROSCI.1838-14.2014.

[32] M. Lazarus, K. Yoshida, R. Coppari, C.E. Bass, T. Mochizuki, B.B. Lowell, C.B. Saper, EP3 prostaglandin receptors in the median preoptic nucleus are critical for fever responses, Nat. Neurosci. 10 (2007) 1131–1133. doi:10.1038/nn1949.

[33] K. Nakamura, Central circuitries for body temperature regulation and fever, AJP Regul. Integr. Comp. Physiol. 301 (2011) R1207–R1228. doi:10.1152/ajpregu.00109.2011.

[34] F. Ushikubi, E. Segi, Y. Sugimoto, T. Murata, T. Matsuoka, T. Kobayashi, H. Hizaki, K. Tuboi, M. Katsuyama, A. Ichikawa, T. Tanaka, N. Yoshida, S. Narumiya, Impaired

febrile response in mice lacking the prostaglandin E receptor subtype EP3., Nature. 395 (1998) 281–4. doi:10.1038/26233.

[35] A.M. Vasilache, J. Andersson, C. Nilsberth, Expression of PGE2 EP3 receptor subtypes in the mouse preoptic region, Neurosci. Lett. 423 (2007) 179–183. doi:10.1016/j.neulet.2007.06.048.

[36] A. Schmid, K.H. Thierauch, W.D. Schleuning, H. Dinter, Splice variants of the human EP3 receptor for prostaglandin E2., Eur. J. Biochem. 228 (1995) 23–30. http://www.ncbi.nlm.nih.gov/pubmed/7883006 (accessed February 20, 2018).

[37] P.S. Brookes, Y. Yoon, J.L. Robotham, M.W. Anders, S.-S. Sheu, Calcium, ATP, and ROS: a mitochondrial love-hate triangle., Am. J. Physiol. Cell Physiol. 287 (2004) C817-33. doi:10.1152/ajpcell.00139.2004.

[38] M. Kotani, I. Tanaka, Y. Ogawa, T. Usui, K. Mori, A. Ichikawa, S. Narumiya, T. Yoshimi, K. Nakao, Molecular cloning and expression of multiple isoforms of human prostaglandin E receptor EP3 subtype generated by alternative messenger RNA splicing: multiple second messenger systems and tissue-specific distributions., Mol. Pharmacol. 48 (1995) 869–79. http://www.ncbi.nlm.nih.gov/pubmed/7476918 (accessed February 20, 2018).

[39] E. Edition, Guide, 2011. doi:10.1163/1573-3912_islam_DUM_3825.

[40] G. Paxinos, C. Watson, The rat brain in stereotaxic coordinates, Elsevier, 2007.

[41] C.J. Gordon, Thermal biology of the laboratory rat., Physiol. Behav. 47 (1990) 963–91. doi:10.1016/0031-9384(90)90025-Y.

[42] E. Satinoff, E. Peloso, C.R. Plata–Salamn, Prostaglandin E2-Induced Fever in Young and Old Long–Evans Rats, Physiol. Behav. 67 (1999) 149–152. doi:10.1016/S0031-9384(99)00029-3.

[43] D.M. Soares, R. Cristofoletti, M.C.C. Melo, C.J. Lindsey, F.H. Veiga-Souza, A.S.C.

Fabricio, G.E.P. Souza, Cyclooxygenase-independent mechanism of ibuprofen-induced antipyresis: the role of central vasopressin V1 receptors, Fundam. Clin. Pharmacol. 25 (2011) 670–681. doi:10.1111/j.1472-8206.2010.00894.x.

[44] J.R. Wiśniewski, A. Zougman, N. Nagaraj, M. Mann, Universal sample preparation method for proteome analysis, Nat. Methods. 6 (2009) 359–362. doi:10.1038/nmeth.1322.

[45] J. Rappsilber, M. Mann, Y. Ishihama, Protocol for micro-purification, enrichment, pre-fractionation and storage of peptides for proteomics using StageTips., Nat. Protoc. 2 (2007) 1896–1906. doi:10.1038/nprot.2007.261.

[46] J. Lisec, N. Schauer, J. Kopka, L. Willmitzer, A.R. Fernie, Gas chromatography mass spectrometry–based metabolite profiling in plants, Nat. Protoc. 1 (2006) 387–396. doi:10.1038/nprot.2006.59.

[47] A. Lommen, MetAlign: Interface-Driven, Versatile Metabolomics Tool for Hyphenated Full-Scan Mass Spectrometry Data Preprocessing, Anal. Chem. 81 (2009) 3079–3086. doi:10.1021/ac900036d.

[48] C. Xie, X. Mao, J. Huang, Y. Ding, J. Wu, S. Dong, L. Kong, G. Gao, C.-Y. Li, L. Wei, KOBAS 2.0: a web server for annotation and identification of enriched pathways and diseases, Nucleic Acids Res. 39 (2011) W316–W322. doi:10.1093/nar/gkr483.

[49] J. Wu, X. Mao, T. Cai, J. Luo, L. Wei, KOBAS server: a web-based platform for automated annotation and pathway identification., Nucleic Acids Res. 34 (2006) W720-4. doi:10.1093/nar/gkl167.

[50] Y. Benjamini, Y. Hochberg, Controlling the False Discovery Rate: A Practical and Powerful Approach to Multiple Testing, J. R. Stat. Soc. Ser. B. 57 (1995) 289–300. doi:10.2307/2346101.

[51] M.E. Ritchie, B. Phipson, D. Wu, Y. Hu, C.W. Law, W. Shi, G.K. Smyth, limma powers

differential expression analyses for RNA-sequencing and microarray studies, Nucleic Acids Res. 43 (2015) e47–e47. doi:10.1093/nar/gkv007.

[52] K. Kammers, R.N. Cole, C. Tiengwe, I. Ruczinski, Detecting significant changes in protein abundance, EuPA Open Proteomics. 7 (2015) 11–19. doi:10.1016/j.euprot.2015.02.002.

[53] L.J.E. Goeminne, A. Argentini, L. Martens, L. Clement, Summarization vs Peptide-Based Models in Label-Free Quantitative Proteomics: Performance, Pitfalls, and Data Analysis Guidelines, J. Proteome Res. 14 (2015) 2457–2465. doi:10.1021/pr501223t.

[54] S. Mohan, A.S. Ahmad, A. V. Glushakov, C. Chambers, S. Doré, Putative role of prostaglandin receptor in intracerebral hemorrhage., Front. Neurol. 3 (2012) 145. doi:10.3389/fneur.2012.00145.

[55] M.M. Müller, R. Lehmann, T.E. Klassert, S. Reifenstein, T. Conrad, C. Moore, A. Kuhn, A. Behnert, R. Guthke, D. Driesch, H. Slevogt, Global analysis of glycoproteins identifies markers of endotoxin tolerant monocytes and GPR84 as a modulator of TNFα expression., Sci. Rep. 7 (2017) 838. doi:10.1038/s41598-017-00828-y.

[56] A. Manousopoulou, Y. Koutmani, S. Karaliota, C.H. Woelk, E.S. Manolakos, K. Karalis, S.D. Garbis, Hypothalamus proteomics from mouse models with obesity and anorexia reveals therapeutic targets of appetite regulation., Nutr. Diabetes. 6 (2016) e204. doi:10.1038/nutd.2016.10.

[57] C. Cao, K. Matsumura, K. Yamagata, Y. Watanabe, Induction by lipopolysaccharide of cyclooxygenase-2 mRNA in rat brain; its possible role in the febrile response., Brain Res. 697 (1995) 187–96. doi:10.1016/0006-8993(95)00839-I.

[58] J. Davidson, H.T. Abul, A.S. Milton, D. Rotondo, Cytokines and cytokine inducers stimulate prostaglandin E2 entry into the brain., Pflugers Arch. 442 (2001) 526–33. doi:10.1007/s004240100572.

[59] A.F. McGettrick, L.A.J. O'Neill, Regulators of TLR4 Signaling by Endotoxins, in: Subcell. Biochem., 2010: pp. 153–171. doi:10.1007/978-90-481-9078-2_7.

[60] T. Kawasaki, T. Kawai, Toll-like receptor signaling pathways., Front. Immunol. 5 (2014) 461. doi:10.3389/fimmu.2014.00461.

[61] N.J. Gay, M. Gangloff, L.A.J. O'Neill, What the Myddosome structure tells us about the initiation of innate immunity., Trends Immunol. 32 (2011) 104–9. doi:10.1016/j.it.2010.12.005.

[62] Z. Lu, S. Xu, ERK1/2 MAP kinases in cell survival and apoptosis, IUBMB Life. 58 (2006) 621–631. doi:10.1080/15216540600957438.

[63] J. Sun, G. Nan, The extracellular signal-regulated kinase 1/2 pathway in neurological diseases: A potential therapeutic target (Review)., Int. J. Mol. Med. 39 (2017) 1338–1346. doi:10.3892/ijmm.2017.2962.

[64] S. Subramaniam, K. Unsicker, ERK and cell death: ERK1/2 in neuronal death., FEBS J. 277 (2010) 22–9. doi:10.1111/j.1742-4658.2009.07367.x.

[65] C. Peyssonnaux, A. Eychène, The Raf/MEK/ERK pathway: new concepts of activation, Biol. Cell. 93 (2001) 53–62. doi:10.1016/S0248-4900(01)01125-X.

[66] P.P. Roux, J. Blenis, ERK and p38 MAPK-activated protein kinases: a family of protein kinases with diverse biological functions., Microbiol. Mol. Biol. Rev. 68 (2004) 320–44. doi:10.1128/MMBR.68.2.320-344.2004.

[67] L. Kong, B.-X. Ge, MyD88-independent activation of a novel actin-Cdc42/Rac pathway is required for Toll-like receptor-stimulated phagocytosis., Cell Res. 18 (2008) 745–55. doi:10.1038/cr.2008.65.

[68] M. Uesugi, K. Nakajima, Y. Tohyama, S. Kohsaka, T. Kurihara, Nonparticipation of nuclear factor kappa B (NFkappaB) in the signaling cascade of c-Jun N-terminal kinase (JNK)- and p38 mitogen-activated protein kinase (p38MAPK)-dependent tumor necrosis

factor alpha (TNFalpha) induction in lipopolysaccharide (LPS)-stim, Brain Res. 1073–1074 (2006) 48–59. doi:10.1016/j.brainres.2005.12.043.

[69] N. Kelkar, S. Gupta, M. Dickens, R.J. Davis, Interaction of a mitogen-activated protein kinase signaling module with the neuronal protein JIP3., Mol. Cell. Biol. 20 (2000) 1030–43. doi:10.1128/MCB.20.3.1030-1043.2000.Updated.

[70] X. Antoniou, M. Falconi, D. Di Marino, T. Borsello, JNK3 as a therapeutic target for neurodegenerative diseases., J. Alzheimers. Dis. 24 (2011) 633–42. doi:10.3233/JAD-2011-091567.

[71] P. Tseng, A. Matsuzawa, W. Zhang, T. Mino, D.A.A. Vignali, M. Karin, Different modes of ubiquitination of the adaptor TRAF3 selectively activate the expression of type I interferons and proinflammatory cytokines., Nat. Immunol. 11 (2010) 70–5. doi:10.1038/ni.1819.

[72] Y. Xiao, J. Jin, M. Chang, J.-H. Chang, H. Hu, X. Zhou, G.C. Brittain, C. Stansberg, Ø. Torkildsen, X. Wang, R. Brink, X. Cheng, S.-C. Sun, Peli1 promotes microglia-mediated CNS inflammation by regulating Traf3 degradation, Nat. Med. 19 (2013) 595–602. doi:10.1038/nm.3111.

[73] L. Tornatore, A.K. Thotakura, J. Bennett, M. Moretti, G. Franzoso, The nuclear factor kappa B signaling pathway: integrating metabolism with inflammation, Trends Cell Biol. 22 (2012) 557–566. doi:10.1016/j.tcb.2012.08.001.

[74] Q. Zhang, M.J. Lenardo, D. Baltimore, 30 Years of NF-κB: A Blossoming of Relevance to Human Pathobiology, Cell. 168 (2017) 37–57. doi:10.1016/j.cell.2016.12.012.

[75] M.S. Hayden, S. Ghosh, Shared Principles in NF-κB Signaling, Cell. 132 (2008) 344–362. doi:10.1016/j.cell.2008.01.020.

[76] S.-C. Sun, Non-canonical NF-κB signaling pathway., Cell Res. 21 (2011) 71–85. doi:10.1038/cr.2010.177.

[77] S.-C. Sun, The noncanonical NF-κB pathway, Immunol. Rev. 246 (2012) 125–140. doi:10.1111/j.1600-065X.2011.01088.x.

[78] G. Liao, M. Zhang, E.W. Harhaj, S.C. Sun, Regulation of the NF-κB-inducing kinase by tumor necrosis factor receptor-associated factor 3-induced degradation, J. Biol. Chem. 279 (2004) 26243–26250. doi:10.1074/jbc.M403286200.

[79] D. Wang, S.D. Westerheide, J.L. Hanson, A.S. Baldwin, Tumor Necrosis Factor α-induced Phosphorylation of RelA/p65 on Ser 529 Is Controlled by Casein Kinase II, J. Biol. Chem. 275 (2000) 32592–32597. doi:10.1074/jbc.M001358200.

[80] P. Parnet, F. Pousset, S. Laye, NF kappa B activation in mouse pituitary: comparison of response to interleukin-1 beta and lipopolysaccharide., J. Neuroendocrinol. 15 (2003) 304–14. http://www.ncbi.nlm.nih.gov/pubmed/12588520 (accessed October 8, 2017).

[81] J.-J. Lee, W.-T. Huang, D.-Z. Shao, J.-F. Liao, M.-T. Lin, Blocking NF-kappaB activation may be an effective strategy in the fever therapy., Jpn. J. Physiol. 53 (2003) 367–75. http://www.ncbi.nlm.nih.gov/pubmed/14975183 (accessed October 8, 2017).

[82] L. Janský, S. Vybíral, D. Pospísilová, J. Roth, J. Dornand, E. Zeisberger, J. Kamínková, Production of systemic and hypothalamic cytokines during the early phase of endotoxin fever., Neuroendocrinology. 62 (1995) 55–61. http://www.ncbi.nlm.nih.gov/pubmed/7566439 (accessed October 5, 2017).

[83] G. Chen, TNF-R1 Signaling: A Beautiful Pathway, Science (80-.). 296 (2002) 1634–1635. doi:10.1126/science.1071924.

[84] G. Sabio, R.J. Davis, TNF and MAP kinase signalling pathways, Semin. Immunol. 26 (2014) 237–245. doi:10.1016/j.smim.2014.02.009.

[85] S. Hara, D. Kamei, Y. Sasaki, A. Tanemoto, Y. Nakatani, M. Murakami, Prostaglandin E synthases: Understanding their pathophysiological roles through mouse genetic models., Biochimie. 92 (2010) 651–9. doi:10.1016/j.biochi.2010.02.007.

[86] T. Kobayashi, Y. Nakatani, T. Tanioka, M. Tsujimoto, S. Nakajo, K. Nakaya, M. Murakami, I. Kudo, Regulation of cytosolic prostaglandin E synthase by phosphorylation., Biochem. J. 381 (2004) 59–69. doi:10.1042/BJ20040118.

[87] S. Schoonbroodt, V. Ferreira, M. Best-Belpomme, J.R. Boelaert, S. Legrand-Poels, M. Korner, J. Piette, Crucial role of the amino-terminal tyrosine residue 42 and the carboxyl-terminal PEST domain of I kappa B alpha in NF-kappa B activation by an oxidative stress., J. Immunol. 164 (2000) 4292–300. doi:10.4049/jimmunol.164.8.4292.

[88] T. Tanioka, Y. Nakatani, N. Semmyo, M. Murakami, I. Kudo, Molecular identification of cytosolic prostaglandin E2 synthase that is functionally coupled with cyclooxygenase-1 in immediate prostaglandin E2 biosynthesis., J. Biol. Chem. 275 (2000) 32775–82. doi:10.1074/jbc.M003504200.

[89] N.J. Rothwell, Eicosanoids, thermogenesis and thermoregulation., Prostaglandins. Leukot. Essent. Fatty Acids. 46 (1992) 1–7. doi:10.1016/0952-3278(92)90051-J.

[90] V. Fraifeld, J. Kaplanski, Brain eicosanoids and LPS fever: species and age differences., Prog. Brain Res. 115 (1998) 141–57. doi:https://doi.org/10.1016/S0079-6123(08)62034-8.

[91] Y.N. Kim, D.W. Kim, H.S. Jo, M.J. Shin, E.H. Ahn, E.J. Ryu, J.I. Yong, H.J. Cha, S.J. Kim, H.J. Yeo, J.K. Youn, J.H. Hwang, J.-H. Jeong, D.-S. Kim, S.-W. Cho, J. Park, W.S. Eum, S.Y. Choi, Tat-CBR1 inhibits inflammatory responses through the suppressions of NF-κB and MAPK activation in macrophages and TPA-induced ear edema in mice., Toxicol. Appl. Pharmacol. 286 (2015) 124–34. doi:10.1016/j.taap.2015.03.020.

[92] W. Kozak, V. Fraifeld, Non-prostaglandin eicosanoids in fever and anapyrexia., Front. Biosci. 9 (2004) 3339–55. doi:1486 [pii].

[93] T. Nakashima, Y. Yoshida, S. Miyata, T. Kiyohara, Hypothalamic 11,12-epoxyeicosatrienoic acid attenuates fever induced by central interleukin-1beta in the rat.,

Neurosci. Lett. 310 (2001) 141–4. doi:10.1016/S0304-3940(01)02115-2.

[94] W. Kozak, I. Archuleta, K.P. Mayfield, A. Kozak, K. Rudolph, M.J. Kluger, Inhibitors of alternative pathways of arachidonate metabolism differentially affect fever in mice., Am. J. Physiol. 275 (1998) R1031-40. http://www.ncbi.nlm.nih.gov/pubmed/9756531 (accessed August 28, 2017).

[95] T. Nakashima, Y. Harada, S. Miyata, T. Kiyohara, Inhibitors of cytochrome P-450 augment fever induced by interleukin-1 beta., Am. J. Physiol. 271 (1996) R1274-9. http://www.ncbi.nlm.nih.gov/pubmed/8945964 (accessed August 28, 2017).

[96] S. Narumiya, Y. Sugimoto, F. Ushikubi, Prostanoid receptors: structures, properties, and functions., Physiol. Rev. 79 (1999) 1193–226. http://www.ncbi.nlm.nih.gov/pubmed/10508233.

[97] K. Nakamura, T. Kaneko, Y. Yamashita, H. Hasegawa, H. Katoh, A. Ichikawa, M. Negishi, Immunocytochemical localization of prostaglandin EP3 receptor in the rat hypothalamus, Neurosci. Lett. 260 (1999) 117–120. doi:10.1016/S0304-3940(98)00962-8.

[98] K.O. Aley, J.D. Levine, Role of protein kinase A in the maintenance of inflammatory pain., J. Neurosci. 19 (1999) 2181–6. http://www.ncbi.nlm.nih.gov/pubmed/10066271 (accessed August 28, 2017).

[99] A.B. Malmberg, E.P. Brandon, R.L. Idzerda, H. Liu, G.S. McKnight, A.I. Basbaum, Diminished inflammation and nociceptive pain with preservation of neuropathic pain in mice with a targeted mutation of the type I regulatory subunit of cAMP-dependent protein kinase., J. Neurosci. 17 (1997) 7462–7470. http://www.ncbi.nlm.nih.gov/pubmed/9295392 (accessed August 28, 2017).

[100] D. Sachs, C. Villarreal, F. Cunha, C. Parada, S. Ferreira, The role of PKA and PKCepsilon pathways in prostaglandin E2-mediated hypernociception., Br. J.

Pharmacol. 156 (2009) 826–34. doi:10.1111/j.1476-5381.2008.00093.x.

[101] D. Ott, J. Murgott, S. Rafalzik, F. Wuchert, B. Schmalenbeck, J. Roth, R. Gerstberger, Neurons and glial cells of the rat organum vasculosum laminae terminalis directly respond to lipopolysaccharide and pyrogenic cytokines., Brain Res. 1363 (2010) 93–106. doi:10.1016/j.brainres.2010.09.083.

[102] B. Simm, D. Ott, E. Pollatzek, J. Murgott, R. Gerstberger, C. Rummel, J. Roth, Effects of prostaglandin E2 on cells cultured from the rat organum vasculosum laminae terminalis and median preoptic nucleus, Neuroscience. 313 (2016) 23–35. doi:10.1016/j.neuroscience.2015.11.034.

[103] M. Palmi, A. Meini, Role of the nitric oxide/cyclic GMP/Ca2+ signaling pathway in the pyrogenic effect of interleukin-1beta., Mol. Neurobiol. 25 (2002) 133–147. doi:10.1385/MN:25:2:133.

[104] J.E. Burke, E.A. Dennis, Phospholipase A2 structure/function, mechanism, and signaling., J. Lipid Res. 50 Suppl (2009) S237-42. doi:10.1194/jlr.R800033-JLR200.

[105] M.A. West, T. LeMieur, L. Clair, J. Bellingham, J.L. Rodriguez, Protein kinase C regulates macrophage tumor necrosis factor secretion: Direct protein kinase C activation restores tumor necrosis factor production in endotoxin tolerance, Surgery. 122 (1997) 204–212. doi:10.1016/S0039-6060(97)90010-6.

[106] V. Fronhofer, M.R. Lennartz, D.J. Loegering, Role of PKC isoforms in the Fc(gamma)R-mediated inhibition of LPS-stimulated IL-12 secretion by macrophages., J. Leukoc. Biol. 79 (2006) 408–15. doi:10.1189/jlb.0805438.

[107] W. Kozak, J.J. Klir, C.A. Conn, M.J. Kluger, Attenuation of lipopolysaccharide fever in rats by protein kinase C inhibitors., Am. J. Physiol. 273 (1997) R873-9. http://www.ncbi.nlm.nih.gov/pubmed/9321862 (accessed August 28, 2017).

[108] D.J. Loegering, M.R. Lennartz, Protein Kinase C and Toll-Like Receptor Signaling,

Enzyme Res. 2011 (2011) 1–7. doi:10.4061/2011/537821.

[109] S. Mrozek, F. Vardon, T. Geeraerts, Brain temperature: physiology and pathophysiology after brain injury., Anesthesiol. Res. Pract. 2012 (2012) 989487. doi:10.1155/2012/989487.

[110] C.J. Jeffery, An introduction to protein moonlighting: Table 1, Biochem. Soc. Trans. 42 (2014) 1679–1683. doi:10.1042/BST20140226.

[111] C. Gancedo, C.-L. Flores, J.M. Gancedo, The Expanding Landscape of Moonlighting Proteins in Yeasts., Microbiol. Mol. Biol. Rev. 80 (2016) 765–77. doi:10.1128/MMBR.00012-16.

[112] L. Wang, Q. Dong, Q. Zhu, N. Tang, S. Jia, C. Xi, H. Zhao, S. Han, Y. Wang, Conformational Characteristics of Rice Hexokinase OsHXK7 as a Moonlighting Protein involved in Sugar Signalling and Metabolism, Protein J. 36 (2017) 249–256. doi:10.1007/s10930-017-9718-x.

[113] A.J. Wolf, C.N. Reyes, W. Liang, C. Becker, K. Shimada, M.L. Wheeler, H.C. Cho, N.I. Popescu, K.M. Coggeshall, M. Arditi, D.M. Underhill, Hexokinase Is an Innate Immune Receptor for the Detection of Bacterial Peptidoglycan., Cell. 166 (2016) 624–36. doi:10.1016/j.cell.2016.05.076.

[114] N.M. Vacanti, A.S. Divakaruni, C.R. Green, S.J. Parker, R.R. Henry, T.P. Ciaraldi, A.N. Murphy, C.M. Metallo, Regulation of substrate utilization by the mitochondrial pyruvate carrier., Mol. Cell. 56 (2014) 425–35. doi:10.1016/j.molcel.2014.09.024.

[115] B. Vanderperre, S. Herzig, P. Krznar, M. Hörl, Z. Ammar, S. Montessuit, S. Pierredon, N. Zamboni, J.-C. Martinou, Embryonic Lethality of Mitochondrial Pyruvate Carrier 1 Deficient Mouse Can Be Rescued by a Ketogenic Diet, PLOS Genet. 12 (2016) e1006056. doi:10.1371/journal.pgen.1006056.

[116] V. Infantino, P. Convertini, L. Cucci, M.A. Panaro, M.A. Di Noia, R. Calvello, F.

Palmieri, V. Iacobazzi, The mitochondrial citrate carrier: a new player in inflammation., Biochem. J. 438 (2011) 433–6. doi:10.1042/BJ20111275.

[117] L. Palmieri, B. Pardo, F.M. Lasorsa, A. del Arco, K. Kobayashi, M. Iijima, M.J. Runswick, J.E. Walker, T. Saheki, J. Satrústegui, F. Palmieri, Citrin and aralar1 are Ca(2+)-stimulated aspartate/glutamate transporters in mitochondria., EMBO J. 20 (2001) 5060–9. doi:10.1093/emboj/20.18.5060.

[118] E. Mills, L.A.J. O'Neill, Succinate: a metabolic signal in inflammation., Trends Cell Biol. 24 (2014) 313–20. doi:10.1016/j.tcb.2013.11.008.

[119] G.M. Tannahill, A.M. Curtis, J. Adamik, E.M. Palsson-McDermott, A.F. McGettrick, G. Goel, C. Frezza, N.J. Bernard, B. Kelly, N.H. Foley, L. Zheng, A. Gardet, Z. Tong, S.S. Jany, S.C. Corr, M. Haneklaus, B.E. Caffrey, K. Pierce, S. Walmsley, F.C. Beasley, E. Cummins, V. Nizet, M. Whyte, C.T. Taylor, H. Lin, S.L. Masters, E. Gottlieb, V.P. Kelly, C. Clish, P.E. Auron, R.J. Xavier, L.A.J. O'Neill, Succinate is an inflammatory signal that induces IL-1β through HIF-1α, Nature. 496 (2013) 238–242. doi:10.1038/nature11986.

[120] V. Iacobazzi, V. Infantino, Citrate – new functions for an old metabolite, Biol. Chem. 395 (2014) 387–399. doi:10.1515/hsz-2013-0271.

[121] O.E. Owen, S.C. Kalhan, R.W. Hanson, The Key Role of Anaplerosis and Cataplerosis for Citric Acid Cycle Function, J. Biol. Chem. 277 (2002) 30409–30412. doi:10.1074/jbc.R200006200.

[122] S. Rajendra, J.W. Lynch, P.R. Schofield, The glycine receptor., Pharmacol. Ther. 73 (1997) 121–46. http://www.ncbi.nlm.nih.gov/pubmed/9131721 (accessed November 23, 2017).

[123] M.A. Razak, P.S. Begum, B. Viswanath, S. Rajagopal, Multifarious Beneficial Effect of Nonessential Amino Acid, Glycine: A Review., Oxid. Med. Cell. Longev. 2017 (2017)

1716701. doi:10.1155/2017/1716701.

[124] H.Y. Chung, M. Cesari, S. Anton, E. Marzetti, S. Giovannini, A.Y. Seo, C. Carter, B.P. Yu, C. Leeuwenburgh, Molecular inflammation: Underpinnings of aging and age-related diseases, Ageing Res. Rev. 8 (2009) 18–30. doi:10.1016/j.arr.2008.07.002.

[125] H. Noh, J. Jeon, H. Seo, Systemic injection of LPS induces region-specific neuroinflammation and mitochondrial dysfunction in normal mouse brain., Neurochem. Int. 69 (2014) 35–40. doi:10.1016/j.neuint.2014.02.008.

[126] Y. Song, G.J. Pinniger, A.J. Bakker, T.J.M. Moss, P.B. Noble, C.A. Berry, J.J. Pillow, Lipopolysaccharide-induced weakness in the preterm diaphragm is associated with mitochondrial electron transport chain dysfunction and oxidative stress., PLoS One. 8 (2013) e73457. doi:10.1371/journal.pone.0073457.

[127] J.A. van Diepen, J.F.P. Berbée, L.M. Havekes, P.C.N. Rensen, Interactions between inflammation and lipid metabolism: relevance for efficacy of anti-inflammatory drugs in the treatment of atherosclerosis., Atherosclerosis. 228 (2013) 306–15. doi:10.1016/j.atherosclerosis.2013.02.028.

[128] W. Khovidhunkit, M.-S. Kim, R.A. Memon, J.K. Shigenaga, A.H. Moser, K.R. Feingold, C. Grunfeld, Thematic review series: The Pathogenesis of Atherosclerosis. Effects of infection and inflammation on lipid and lipoprotein metabolism mechanisms and consequences to the host, J. Lipid Res. 45 (2004) 1169–1196. doi:10.1194/jlr.R300019-JLR200.

[129] G. Pérez-Chacón, A.M. Astudillo, D. Balgoma, M.A. Balboa, J. Balsinde, Control of free arachidonic acid levels by phospholipases A2 and lysophospholipid acyltransferases., Biochim. Biophys. Acta. 1791 (2009) 1103–13. doi:10.1016/j.bbalip.2009.08.007.

[130] N.G. Bazan, Synaptic lipid signaling, J. Lipid Res. 44 (2003) 2221–2233.

doi:10.1194/jlr.R300013-JLR200.

[131] A.A. Farooqui, L.A. Horrocks, Brain phospholipases A2: a perspective on the history, Prostaglandins, Leukot. Essent. Fat. Acids. 71 (2004) 161–169. doi:10.1016/j.plefa.2004.03.004.

[132] A.M. Astudillo, D. Balgoma, M.A. Balboa, J. Balsinde, Dynamics of arachidonic acid mobilization by inflammatory cells., Biochim. Biophys. Acta. 1821 (2012) 249–56. doi:10.1016/j.bbalip.2011.11.006.

[133] F.H. Chilton, A.N. Fonteh, M.E. Surette, M. Triggiani, J.D. Winkler, Control of arachidonate levels within inflammatory cells, Biochim. Biophys. Acta - Lipids Lipid Metab. 1299 (1996) 1–15. doi:10.1016/0005-2760(95)00169-7.

[134] H. Shindou, T. Shimizu, Acyl-CoA:Lysophospholipid Acyltransferases, J. Biol. Chem. 284 (2009) 1–5. doi:10.1074/jbc.R800046200.

[135] H. Shindou, D. Hishikawa, T. Harayama, K. Yuki, T. Shimizu, Recent progress on acyl CoA: lysophospholipid acyltransferase research., J. Lipid Res. 50 Suppl (2009) S46-51. doi:10.1194/jlr.R800035-JLR200.

[136] E.A. Dennis, S.G. Rhee, M.M. Billah, Y.A. Hannun, Role of phospholipase in generating lipid second messengers in signal transduction, FASEB J. 5 (1991) 2068–2077. http://www.ncbi.nlm.nih.gov/pubmed/1901288 (accessed August 29, 2017).

[137] J.H. Exton, Phosphatidylcholine breakdown and signal transduction, Biochim. Biophys. Acta - Lipids Lipid Metab. 1212 (1994) 26–42. doi:10.1016/0005-2760(94)90186-4.

[138] A.A. Farooqui, H.-C. Yang, T.A. Rosenberger, L.A. Horrocks, Phospholipase A2 and Its Role in Brain Tissue, J. Neurochem. 69 (2002) 889–901. doi:10.1046/j.1471-4159.1997.69030889.x.

[139] A.A. Farooqui, W.Y. Ong, L.A. Horrocks, T. Farooqui, Brain Cytosolic Phospholipase A2: Localization, Role, and Involvement in Neurological Diseases, Neurosci. 6 (2000)

169–180. doi:10.1177/107385840000600308.

[140] V.A. Fadok, D.R. Voelker, P.A. Campbell, J.J. Cohen, D.L. Bratton, P.M. Henson, Exposure of phosphatidylserine on the surface of apoptotic lymphocytes triggers specific recognition and removal by macrophages., J. Immunol. 148 (1992) 2207–16. http://www.ncbi.nlm.nih.gov/pubmed/1545126 (accessed August 29, 2017).

[141] R. De Simone, M.A. Ajmone-Cat, P. Tirassa, L. Minghetti, Apoptotic PC12 cells exposing phosphatidylserine promote the production of anti-inflammatory and neuroprotective molecules by microglial cells., J. Neuropathol. Exp. Neurol. 62 (2003) 208–16. doi:10.1093/jnen/62.2.208.

[142] M.G. Low, The glycosyl-phosphatidylinositol anchor of membrane proteins, BBA - Rev. Biomembr. 988 (1989) 427–454. doi:10.1016/0304-4157(89)90014-2.

[143] P.. Englund, The structure and biosynthesis of glycosyl phosphatidylinositol protein anchors, Annu Rev Biochem. 62 (1993) 121–138. doi:10.1017/CBO9781107415324.004.

[144] A.M. Martelli, S. Capitani, L.M. Neri, The generation of lipid signaling molecules in the nucleus, Prog. Lipid Res. 38 (1999) 273–308. doi:10.1016/S0163-7827(99)00009-0.

[145] T. Harayama, M. Eto, H. Shindou, Y. Kita, E. Otsubo, D. Hishikawa, S. Ishii, K. Sakimura, M. Mishina, T. Shimizu, Lysophospholipid Acyltransferases Mediate Phosphatidylcholine Diversification to Achieve the Physical Properties Required In Vivo, Cell Metab. 20 (2014) 295–305. doi:10.1016/j.cmet.2014.05.019.

[146] M.K. Topham, S.M. Prescott, Mammalian Diacylglycerol Kinases, a Family of Lipid Kinases with Signaling Functions, J. Biol. Chem. 274 (1999) 11447–11450. doi:10.1074/jbc.274.17.11447.

[147] H.-K. Lim, Y.-A. Choi, W. Park, T. Lee, S.H. Ryu, S.-Y. Kim, J.-R. Kim, J.-H. Kim, S.-H. Baek, Phosphatidic acid regulates systemic inflammatory responses by modulating

the Akt-mammalian target of rapamycin-p70 S6 kinase 1 pathway., J. Biol. Chem. 278 (2003) 45117–27. doi:10.1074/jbc.M303789200.

[148] D.E. Agwu, L.C. McPhail, S. Sozzani, D.A. Bass, C.E. McCall, Phosphatidic acid as a second messenger in human polymorphonuclear leukocytes. Effects on activation of NADPH oxidase., J. Clin. Invest. 88 (1991) 531–539. doi:10.1172/JCI115336.

[149] M.D. Buck, R.T. Sowell, S.M. Kaech, E.L. Pearce, Metabolic Instruction of Immunity, Cell. 169 (2017) 570–586. doi:10.1016/j.cell.2017.04.004.

Captions:

Table 1. Protein Annotation according to Inflammatory Pathways

Pathway annotation analysis was performed using software BlastKOALA sequence similarity tool, based on the KEGG database. Data are represented as the full protein name of each differently expressed protein in LPS/SAL and PGE_2/VEH group, respectively. *Acc. No.* means accession number, provided by the UniProt rat protein database (03/17/2016, 35.144 sequences). *FC* indicates fold change of each differently expressed protein in each comparison pair LPS/SAL or PGE_2/VEH. *q* value < 0.05 was considered to be significant when compared to the corresponding control group. Abbreviations: polypeptide (polyp.); subunit (sub.)

Table 2. Protein Annotation according to Metabolic Pathways

Pathway annotation analysis was performed using software BlastKOALA sequence similarity tool, based on the KEGG database. Data are represented as the full protein name of each differentially abundant protein in LPS/SAL and PGE_2/VEH group, respectively. *Acc. No.* means accession number, provided by the UniProt rat protein database (03/17/2016, 35.144 sequences). *FC* indicates fold change of each differentially abundant protein in each

comparison pair LPS/SAL or PGE_2/VEH. *q* value < 0.05 was considered to be significant when compared to the corresponding control group. Abbreviations: dehydrogenase (dehyd.); mitochondrial (mito.); cytosolic (cyto.); subunit (sub.).

Table 3. Protein Annotation according to mitochondrial proteins

Pathway annotation analysis was performed using software BlastKOALA sequence similarity tool, based on the KEGG database. Data are represented as the full protein name of each differentially abundant protein in LPS/SAL and PGE_2/VEH group, respectively. *Acc. No.* means accession number, provided by the UniProt rat protein database (03/17/2016, 35.144 sequences). *FC* indicates fold change of each differentially abundant protein in each comparison pair LPS/SAL or PGE_2/VEH. *q* value < 0.05 was considered to be significant when compared to the corresponding control group. Abbreviations: dehydrogenase (dehyd.); mitochondrial (mito.); subcomplex (subc.).

Figure 1. Time course of changes in body temperature following LPS or PGE_2 injection. (A) Response induced by i.v. injection of LPS (5 µg/kg) or saline (0.9%) in the body temperature of rats. (B) Response induced by i.c.v. injection of PGE_2 (100 ng/rat) or vehicle (0.5% ethanol in saline). Values are represented as the mean ± S.E.M of the body temperature (°C) of 5-6 animals. Panels C and D contain the profile of the febrile response at selected times for collection of hypothalami. Values represent mean ± S.E.M. of body temperature as ΔT (in °C) of 5 animals per group. *p < 0.05 or ***p < 0.001 compared with the saline or vehicle groups.

Figure 2. Profile of differentially expressed proteins. Panel A and B represent volcano plot of significant differentially abundant proteins. Data were plotted as a function of the fold change

(≤ 1) in a log_2 scale, for each protein. (A) represents data from LPS x saline group and (B) represents data from PGE_2 x vehicle group. The horizontal dashed line shows where p-value = 0.05. Panel C and D represent Venn diagram of the common proteins between LPS and PGE_2 groups. The analysis considered only statistically different proteins. (C) proteins with increased abundance (↑) in both groups. (D) proteins with decreased abundance (↓) in both groups.

Figure 3. Profile of antioxidant enzymes during fever response. Data are presented as percentage of the control. Cu-Zn-SOD (cooper-zinc superoxide dismutase), Mn-SOD (manganese superoxide dismutase), GPX (gluthatione peroxidase) and CAT (catalase). *p < 0.05 compared with the corresponding value of control group.

Figure 4. Profile of organic and amino acids metabolites during fever response. Relative abundance of (A) metabolites of the tricarboxylic acid cycle, (B) amino acids, (C) further organic acids identified. n = 7-8 animals per group. *p < 0.05 when comparing LPS with the corresponding control group.

Figure 5. Changes in relative abundance of proteins in LPS and PGE_2 groups considering TCA cycle as the center of metabolism for didactic purposes. blue arrows = proteins identified in LPS group; orange arrows = proteins identified in PGE_2 group.↑ = proteins with increased abundance; ↓ = proteins with decreased abundance.

Supplementary Table 1. Proteins Identified by PEAKS Studio 7.0.

Whole proteome from rat hypothalamus identified in all experimental groups.

Supplementary Table 2. Differentially expressed proteins.

List of all proteins differentially abundant between in LPS/SAL and PGE_2/VEH group, respectively. q value < 0.05 was considered to be significant when compared to the corresponding control group.

Table 1 – Differentially abundant proteins involved in inflammatory pathways in hypothalamus during fever induced by LPS or PGE_2.

Pathway	Abundance	LPS	Acc. No.	FC	*q* value	PGE_2	Acc. No.	FC	*q* value
MAPK	**High**	Heat shock cognate 71 kDa protein	D4A4S3	1.84	0.008	Ras GTPase-activating protein 1	P50904	2.13	0.03
		Serine/threonine-protein phosphatase	A0A0G2K7T5	1.17	0.02	Serine/threonine-protein kinase PAK 1	P35465	1.29	0.03
		Growth factor receptor-bound protein 2	P62994	1.19	0.01	Growth factor receptor-bound protein 2	P62994	1.36	0.03
		Cell division control protein 42 homolog (Cdc42)	Q8CFN2	1.49	0.009	Cell division control protein 42 homolog (Cdc42)	Q8CFN2	1.77	0.03
		Mitogen-activated protein kinase kinase 6 (MKK6)	Q925D6	1.22	0.03	Mitogen-activated protein kinase kinase 4 delta (MKK4)	S4VP54	1.40	0.03
		C-Jun-amino-terminal kinase-interacting protein 3 (JIP3)	B0VXR4	1.28	0.03	Mitogen-activated protein kinase 8-interacting protein 3	E9PSK7	3.89	0.03
		Filamin, beta	D4A8D5	1.61	0.01				
		Adapter molecule crk	Q63768	1.70	0.008				
		Stress-activated protein kinase JNK3	P49187	2.71	0.01				
		Protein phosphatase 3, regulatory subunit B, α isoform	A0A0H2UHV6	1.37	0.009				
		Ras-related protein R-Ras	D3Z8L7	1.20	0.02				
		RAS guanyl-releasing protein 3	D3ZZN2	1.98	0.01				
		Protein tyrosine phosphatase, non-receptor type 5	Q56A30	2.09	0.01				
	Low	Mitogen-activated protein kinase kinase 1-interacting protein 1 (MP1)	Q5U204	1.62	0.008	Serine/threonine-protein phosphatase	A0A0G2K7T5	1.18	0.03
		Extracellular signal-regulated kinase 1 (ERK1)	P21708	1.18	0.02	Extracellular signal-regulated kinase 1 (ERK1)	P21708	1.14	0.04
		Mitogen-activated protein kinase kinase kinase kinase 4 (Map4k4)	A0A0G2K7W4	3.38	0.007	Ribosomal protein S6 kinase	F1M7N7	1.31	0.04
		Serine/threonine-protein kinase PAK 2	Q64303	1.27	0.01	Serine/threonine-protein kinase PAK 2	Q64303	1.28	0.03
		Mitogen-activated protein kinase kinase 4 (MKK4)	F1LP57	1.47	0.02	Microtubule-associated protein	A0JN25	1.41	0.03
		Beta-arrestin-1	P29066	2.07	0.02	Adapter molecule crk	Q63768	1.30	0.03
		Protein phosphatase 1A	P20650	1.31	0.01	Protein phosphatase 1B	P35815	1.19	0.04
		Serine/threonine-protein phosphatase	Q68G16	2.85	0.009				
		Neurofibromin (Nf1)	A0A0G2JWL3	1.47	0.03				
NFκB	**High**	Casein kinase II subunit beta (CKII)	N0E631	1.21	0.04	TNF receptor-associated factor 3 (TRAF3)	D3Z9G0	1.31	0.03
		Bcl-2-like protein 1	A0A0G2JZS5	1.66	0.01				
		ELKS/Rab6-interacting/CAST family member 1	Q811U3	1.23	0.01				
	Low	TNF receptor-associated factor 3 (TRAF3)	A0A0G2K7X2	1.49	0.01				
ARA	**High**	Cytochrome P450, family 2, subfamily j, polyp.16	A0A0G2JTQ9	1.65	0.01	Carbonyl reductase [NADPH] 1 (Cbr1)	A0A096MJ24	10.03	0.03
		Prostaglandin E synthase 3-like 1	Q5PQL9	1.89	0.01	Prostaglandin E synthase 3-like 1	Q5PQL9	1.36	0.03
	Low	Carbonyl reductase [NADPH] 1 (Cbr1)	A0A096MJ24	1.28	0.03	Leukotriene A(4) hydrolase	Q499P2	1.25	0.03
		Glutathione peroxidase	Q6PDW8	1.39	0.008				
		Prostaglandin E synthase 2	D4AE56	1.39	0.03				
cAMP	**High**	Protein kinase A (PKA) catalytic subunit beta	P68182	1.68	0.008	Protein kinase A (PKA) catalytic subunit	Q05759	1.65	0.03
		Pituitary adenylate cyclase-activating polyp. type I receptor (PACAP)	P32215	1.27	0.03	Ras-related C3 botulinum toxin substrate 1 (RAC1)	Q923X0	1.64	0.03
		Gamma-aminobutyric acid type B receptor sub. 2 (GABA-B receptor 2)	O88871	1.28	0.02	Guanine nucleotide-binding protein G(s) sub. α	Q63803	1.44	0.03

		Rho-associated protein kinase 2	Q62868	1.32	0.03	Calcium/calmodulin-dependent protein kinase type II subunit β	P08413	2.07	0.03
		Serine/threonine-protein phosphatase (PP1)	A0A0G2JYS8	1.19	0.04	Afadin	F1LT10	1.62	0.03
		Ras-related protein R-Ras	D3Z8L7	1.20	0.02	Adenylate cyclase type 5	Q04400	1.63	0.03
		Related RAS viral (r-ras) oncogene homolog 2 (Rras 2)	A0A0G2K508	1.29	0.01				
		Adenylate cyclase 9	M0R5U4	1.46	0.01				
		Myosin regulatory light polypeptide 9	Q64122	1.63	0.01				
	Low	Rap guanine nucleotide exchange factor 4	F1LQ26	1.43	0.01	Ras-related protein Rap 1B	O08814	1.22	0.03
		Ras-related protein Rap-1A	P62836	1.41	0.02	Protein phosphatase 1 regulatory subunit 12A	D4ACS0	1.21	0.03
		RhoA (Fragment)	O35791	1.36	0.01				
		Adenylate cyclase-inhibiting G alpha protein (Gi)	P10824	1.86	0.008				
		Adenylate cyclase-stimulating G alpha protein (Gs)	Q63803	1.24	0.01				
		Calcium/calmodulin-dependent protein kinase type II subunit gamma	P11730	1.46	0.02				
		AMPA-selective glutamate receptor 2	P19491	1.94	0.009				
		Ras-related C3 botulinum toxin substrate 3 (Rac3)	M0R5T4	1.27	0.02				
		Adenylate cyclase 5	G3V9G1	1.32	0.03				
Calcium	**High**	ADP-ribosyl cyclase 1 (CD38H)	Q64244	1.56	0.008	Plasma membrane calcium-transporting ATPase 3	Q64568	1.35	0.03
		Sodium/calcium exchanger 1	M0R3V7	1.22	0.01	Sodium/calcium exchanger 1	R9PXX9	1.41	0.03
		Voltage-dependent N-type calcium channel sub. α-1B	Q02294	1.64	0.01	Protein kinase C beta type	A0A0G2K5Q0	1.87	0.03
		Calcium-transporting ATPase	D4A8B3	1.17	0.02				
		Phosphoinositide phospholipase C (Plcb4)	D3ZCI6	1.34	0.008				
		Phosphoinositide phospholipase C (Plcb3)	Q45QJ4	1.73	0.01				
		Calcineurin subunit B type 1	A0A0H2UHV6	1.37	0.009				
		Protein kinase C beta type	P68403	2.48	0.01				
		Protein kinase C beta type	A0A0G2K5Q0	1.77	0.009				
		Protein kinase C gamma type	P63319	1.17	0.03				
	Low	Inositol-trisphosphate 3-kinase B	P42335	1.32	0.04	Phospholipase C-gamma-1	P10686	1.53	0.03
		Phosphoinositide phospholipase C (Plcg1)	G3V845	2.91	0.01	ADP-ribosyl cyclase 1 (CD38H)	Q64244	1.37	0.03
		Voltage-dependent P/Q-type calcium channel sub. α	A0A0G2JXK1	1.89	0.02	Voltage-dependent anion-selective channel protein 1 (VDAC-1)	Q9Z2L0	1.25	0.03
		Guanine nucleotide-binding protein (Gq) sub. α	D4AE68	1.69	0.007	Voltage-dependent anion-selective channel protein 3 (VDAC-3)	Q9R1Z0	1.15	0.04
		Voltage-gated calcium channel pore forming subunit CaV1.3alpha1	Q91WX8	1.35	0.02				
		Calcium-transporting ATPase	E9PSX6	1.19	0.04				
		Nitric oxide synthase, brain	P29476	1.31	0.02				
		Voltage-dependent anion-selective channel protein 3 (VDAC-3)	Q9R1Z0	1.27	0.03				

Table 2 – Differentially abundant proteins involved in energy metabolism in hypothalamus during fever induced by LPS or PGE_2.

Pathway	Abundance	LPS	Acc. No.	FC	*q* value	PGE_2	Acc. No.	FC	*q* value
Glycolysis	**High**	Hexokinase I	M0RAQ6	1.26	0.03	Glucose-6 phosphate isomerase	Q6P6V0	1.99	0.03
						Pyruvate kinase	P11980	1.37	0.03
						Gamma-enolase	P07323	1.46	0.03
						Phosphoglycerate kinase 1	P16617	1.35	0.03
	Low	Glyceraldehyde-3-phosphate dehyd.	P04797	1.37	0.01	Glyceraldehyde-3-phosphate dehyd.	P04797	1.35	0.04
		Dihydrolipoyl dehyd. mito.	Q6P6R2	1.25	0.01	ATP-dependent 6-phosphofructokinase type B	P30835	1.58	0.03
		Pyruvate dehyd. complex component E2	P08461	1.38	0.01	Phosphoenolpyruvate carboxykinase 2, mito. (Pck2)	F1LQJ7	1.42	0.03
		ATP-dependent 6-phosphofructokinase	A0A0A0MXY5	1.95	0.01	Fructose-bisphosphate aldolase	Q6AY07	1.67	0.03
		Fructose-bisphosphate aldolase A	P05065	1.11	0.04	Phosphoglycerate mutase 1	P25113	1.55	0.03
		Beta-enolase	P15429	1.35	0.01	Phosphoglucomutase 1 (Pgm 1 protein)	A1A5L2	1.20	0.03
		Glucose-6-phosphate isomerase	Q6P6V0	1.19	0.02				
		Phosphoglucomutase 1	Q499Q4	1.27	0.02				
		ADP-dependent glucokinase (Adpgk)	Q5D001	1.38	0.02				
Tricarboxylic Acid Cycle	**High**	Citrate synthase	G3V936	1.20	0.02	Citrate synthase	Q0QEL8	1.66	0.03
		Succinyl-CoA ligase sub. β (ADP-forming SUCL)	B2RZ24	1.60	0.01	Succinate-CoA ligase, alpha sub.	A0A0H2UHE1	1.30	0.03
		DLST protein	D0VYQ0	1.25	0.02	Pyruvate carboxylase, mito.	P52873	1.36	0.03
		Aconitate hydratase	G3V6S2	1.24	0.01				
	Low	Malate dehyd., mito.	P04636	1.26	0.01	Malate dehyd., mito.	P04636	1.75	0.03
		Isocitrate dehyd. [NAD] sub.α, mito.	Q99NA5	1.49	0.009	Isocitrate dehyd. [NAD] sub., mito.	F1LNF7	1.73	0.03
		Isocitrate dehyd. [NADP] cyto.	P41562	1.38	0.02	Isocitrate dehyd. [NADP], mito.	P56574	1.56	0.03
		2-oxoglutarate dehyd. mito.	Q5XI78	1.17	0.01	2-oxoglutarate dehyd., mito.	Q5XI78	1.21	0.03
		Flavoprotein sub. of complex II mito.	Q920L2	1.34	0.009	Phosphoenolpyruvate carboxykinase 2, mito. (Pck2)	F1LQJ7	1.42	0.03
		Iron-sulfur sub. of complex II mito.	P21913	1.24	0.01	Aconitate hydratase	G3V6S2	1.36	0.03
		Succinate dehyd. complex sub. C (Sdhc)	Q641Z9	1.22	0.03	Succinyl-CoA ligase sub. β (GDP-forming SUCL)	Q5EBA9	1.27	0.03
		Dihydrolipoyl dehyd., mito.	Q6P6R2	1.25	0.01				
		Pyruvate dehyd. complex component E2	P08461	1.38	0.01				
		ATP-citrate synthase	G3V9G4	1.61	0.01				
		Fumarate hydratase, mito.	P14408	1.40	0.01				
Pentose phosphate	**High**	Ribose-phosphate pyrophosphokinase 1	P60892	1.24	0.01	6-phosphogluconate dehydrogenase, decarboxylating	A0A0G2K7Q8	1.73	0.03
						Transketolase	P50137	1.35	0.03
						Glucose-6-phosphate isomerase	Q6P6V0	1.99	0.03
	Low	Glucose-6-phosphate 1-dehyd.	P05370	1.19	0.01	Glucose-6-phosphate 1-dehyd.	P05370	1.16	0.04
		ATP-dependent 6-phosphofructokinase	A0A0A0MXY5	1.95	0.01	ATP-dependent 6-phosphofructokinase type B	P30835	1.58	0.03
		Transaldolase	Q9EQS0	1.56	0.01	Ribose-phosphate pyrophosphokinase 1	P60892	1.17	0.03
		Fructose-bisphosphate aldolase A	P05065	1.11	0.04	Fructose-bisphosphate aldolase	Q6AY07	1.67	0.03

		Phosphoglucomutase 1 (Pgm 1 protein)	Q499Q4	1.27	0.02	Phosphoglucomutase 1 (Pgm 1 protein)	A1A5L2	1.20	0.03
		Glucose-6-phosphate isomerase	Q6P6V0	1.19	0.02				
		6-phosphogluconolactonase	P85971	1.29	0.02				
Aminoacid degradation (valine, leucine and isoleucine)	**High**	Succinyl-CoA:3-ketoacid coenz. A transferase 1, mito.	B2GV06	1.66	0.009	Branched-chain-amino-acid aminotransferase, cyto.	P54690	1.76	0.03
		Propionyl-CoA carboxylase α chain, mito.	A0A0G2K401	1.32	0.02				
		Propionyl-CoA carboxylase β chain, mito.	Q68FZ8	1.50	0.02				
		3-hydroxyisobutyryl-coenzyme A hydrolase, mito.	Q5XIE6	1.61	0.008				
		AU RNA-binding methylglutaconyl-CoA hydratase	F1LU71	2.24	0.009				
		Dihydrolipoamide branched chain transacylase E2	B2GV15	1.47	0.01				
	Low	3-hydroxyisobutyrate dehyd., mito.	P29266	1.34	0.01	4-trimethylaminobutyraldehyde dehyd.	Q9JLJ3	1.20	0.03
		Aldehyde dehyd., mito.	F1LN88	1,25	0.01	Aldehyde dehyd., mito.	P11884	1.44	0.03
		Malonate-semialdehyde dehyd. [acylating]	Q02253	1.37	0.009	Malonate-semialdehyde dehyd. [acylating]	Q02253	1.40	0.03
		2-oxoisovalerate dehyd. sub. α, mito.	P11960	1.37	0.02	2-oxoisovalerate dehyd. sub.β, mito.	A0A0A0MXW1	1.21	0.03
		Branched chain keto acid dehyd. E1, β polypeptide	B0BNK6	1.17	0.02	Hydroxymethylglutaryl-CoA synthase, mito.	P22791	1.60	0.03
		Isovaleryl-CoA dehyd., mito.	P12007	1.23	0.01	Methylcrotonoyl-CoA carboxylase β chain, mito.	Q5XIT9	1.27	0.03
		Dihydrolipoyl dehyd., mito.	Q6P6R2	1.25	0.01	3-hydroxyisobutyryl-CoA hydrolase, mito.	Q5XIE6	1.29	0.03
		3-hydroxyacyl-CoA dehydrogenase type-2	O70351	1.31	0.009	Methylmalonyl CoA epimerase	D4A197	1.66	0.03
		4-aminobutyrate aminotransferase, mito.	P50554	1.27	0.01	3-ketoacyl-CoA thiolase, mito.	A0A0G2K642	1.28	0.03
		Alpha-aminoadipic semialdehyde dehyd.	Q64057	1.14	0.04	Alpha-aminoadipic semialdehyde dehyd	Q64057	1.19	0.04
						Dihydrolipoamide branched chain transacylase E2	B2GV15	1.54	0.03
Fatty acid biosynthesis	**High**	Long-chain-fatty-acid--CoA ligase 1 (ACLS1)	P18163	2.25	0.02				
		Acetyl-CoA carboxylase 1	A0A0G2K5G8	2.10	0.008				
	Low	Fatty acid synthase	P12785	1.14	0.03	Fatty acid synthase	P12785	1.23	0.03
						Long-chain-fatty-acid--CoA ligase 6	P33124	1.19	0.03
Fatty acid degradation	**High**	Long-chain-fatty-acid--CoA ligase 1 (ACLS1)	P18163	2.25	0.02	Enoyl-CoA delta isomerase 1, mito.	P23965	1.50	0.03
		Acyl-Coenzyme A dehyd., very long chain	Q5M9H2	1.28	0.008				
	Low	Short-chain specific acyl-CoA dehyd., mito.	P15651	1.88	0.01	Medium-chain specific acyl-CoA dehyd., mito.	P08503	1.25	0.03
		2-methyl branched chain acyl-CoA dehyd.	P70584	2.82	0.01	Long-chain specific acyl-CoA dehyd., mito.	P15650	1.27	0.03
		Acetyl-CoA acetyltransferase, mito.	P17764	2.18	0.01	Very long-chain specific acyl-CoA dehyd. mito.	P45953	1.29	0.03
		Trifunctional enzyme sub. β, mito.	Q60587	1.35	0.008	Long-chain-fatty-acid--CoA ligase 6	P33124	1.19	0.03
		Trifunctional enzyme sub. α, mito.	Q64428	1.44	0.008	Trifunctional enzyme sub. β, mito.	Q60587	1.38	0.03
		Enoyl-CoA delta isomerase 1, mito.	P23965	1.36	0.01	Trifunctional enzyme sub. α, mito.	Q64428	1.32	0.03
		Enoyl-CoA delta isomerase 2, mito.	Q5XIC0	1.49	0.03	3-ketoacyl-CoA thiolase, mito.	A0A0G2K642	1.28	0.03
						Enoyl-CoA hydratase, mito.	P14604	1.19	0.03
Glyceroph. metabolism	**High**	Glycerol-3-phosphate dehyd.	F1LNI0	1.78	0.02	Acyl-protein thioesterase 2	Q9QYL8	1.96	0.03
		Diacylglycerol kinase gamma	P49620	4.63	0.02				
		Diacylglycerol kinase beta	P49621	2.13	0.01				

	Ethanolamine-phosphate cytidylyltransferase	O88637	3.16	0.01				
	Phosphatidate cytidylyltransferase 2	Q91XU8	1.74	0.008				
	Phosphatidylinositol synthase	P70500	1.31	0.01				
	Membrane-bound O-acyltransferase domain-containing protein 2	Q3T1J2	1.76	0.01				
	1-acylglycerol-3-phosphate O-acyltransferase 4 (AGPAT4)	Q924S1	1.35	0.02				
Low	Glycerol-3-phosphate dehydrogenase [NAD(+)], cyto.	O35077	1.47	0.008	Glycerol-3-phosphate dehyd., mito.	P35571	1.20	0.03
	Acyl-protein thioesterase 2	Q9QYL8	1.42	0.03	Phosphatidate cytidylyltransferase	G3V8W2	1.72	0.04
					1-acyl-sn-glycerol-3-phosphate acyltransferase	Q6MG85	1.19	0.04
					Leng4 protein	B5DFK0	1.55	0.03
					Agpat3 protein	B0BNL8	1.24	0.04

Table 3 – Differentially abundant mitochondrial proteins in hypothalamus during fever induced by LPS and PGE_2.

Complex	Abundance	LPS	Acc. No.	FC	*q* value	PGE_2	Acc. No.	FC	*q* value
Complex I	**High**	NADH-ubiquinone oxidoreductase chain 4	Q06Q89	1.50	0.01	NADH-ubiquinone oxidoreductase chain 5	P11661	1.68	0.03
		NADH dehyd. [ubiquinone] Fe-S protein 3	D3ZG43	1.69	0.009	NADH dehyd. [ubiquinone] Fe-S protein 8	B0BNE6	1.41	0.03
		NADH dehyd. [ubiquinone] 1 alpha subc. subunit.5	Q63362	1.28	0.03	NADH dehyd. [ubiquinone] 1 alpha subc. subunit 9, mito.	Q5BK63	1.18	0.03
		NADH dehyd. [ubiquinone] 1 beta subc., 11	D4A7L4	1.49	0.03	NADH dehyd. [ubiquinone] 1 beta subc., 9	B2RYW3	1.21	0.04
	Low	NADH-ubiquinone oxidoreductase chain 5	A0A096XKT9	1.62	0.01	NADH-ubiquinone oxidoreductase 75 kDa subunit, mito.	Q66HF1	1.28	0.04
		NADH dehyd. [ubiquinone] Fe-S protein 7	Q5RJN0	1.61	0.01	NADH dehyd. [ubiquinone] iron-sulfur protein 6, mito.	D3ZCZ9	1.40	0.03
		NADH dehyd. [ubiquinone] 1 alpha subc. subunit 11	Q80W89	1.26	0.009	NADH dehyd. [ubiquinone] 1 alpha subc. subunit 11	Q80W89	1.65	0.03
		NADH dehyd. [ubiquinone] flavoprotein 1	Q5XIH3	1.35	0.008	NADH dehyd. [ubiquinone] 1 beta subc. subunit 8, mito.	B2RYS8	1.24	0.04
		NADH dehyd. [ubiquinone] 1 alpha subc. 10	Q6P6W6	1.22	0.01	NADH dehyd. [ubiquinone] 1 alpha subc. 10	Q6P6W6	1.31	0.04
		NADH dehyd. [ubiquinone] 1 alpha subc. subunit 9, mito.	Q5BK63	1.41	0.008	Protein LOC103694107	M0RA24	1.21	0.03
		NADH dehyd. [ubiquinone] 1 alpha subc., 8	A0A0G2JVL6	1.29	0.01				
		NADH dehyd. [ubiquinone] 1 beta subc., 2	B2RYU0	1.22	0.01				
		NADH dehyd. [ubiquinone] 1 beta subc., 5	D4A565	1.61	0.02				
		NADH dehyd. [ubiquinone] 1 beta subc., 6	D3ZZ21	1.60	0.01				
		NADH dehyd. [ubiquinone] 1 beta subc., 9	B2RYW3	6.91	0.007				
		NADH [ubiquinone] oxidoreductase subunit B10	D4A0T0	1.85	0.009				
		Acyl carrier protein	D3ZF13	1.33	0.01				
Complex II	**Low**	Succinate dehyd. complex subunit C	Q641Z9	1.22	0.03				
		Succinate dehyd. [ubiquinone] flavoprotein subunit, mito.	Q920L2	1.34	0.009				
		Succinate dehyd. [ubiquinone] iron-sulfur subunit, mito.	P21913	1.24	0.01				
Complex III	**High**					Cytocrome b-c1 complex subunit 7	B2RYS2	1.18	0.04
						Cytochrome c-1	D3ZFQ8	3.21	0.03
	Low	Cytochrome b-c1 complex subunit 8	Q7TQ16	2.19	0.009				
		Cytochrome b-c1 complex subunit 6, mito.	Q5M9I5	1.36	0.02				
		Cytochrome b-c1 complex subunit Rieske, mito.	P20788	1.22	0.01				
		Cytochrome c-1	D3ZFQ8	1.44	0.01				
Complex IV	**High**	Cytochrome c oxidase subunit 2	S5RZM8	1.51	0.009	Cytochrome c oxidase subunit 1	P05503	1.36	0.03
		Cytochrome c oxidase subunit 1	P05503	1.48	0.008				
	Low	Cytochrome c oxidase subunit 6C-2	P11951	2.01	0.009	Cytochrome c oxidase subunit 8A, mito.	P80433	1.18	0.03
		Cytochrome c oxidase subunit 6A1, mito.	P10818	1.19	0.01	Cytochrome c oxidase subunit VIIa polypeptide 2 like	B2RYT5	1.14	0.03
		Cytochrome c oxidase subunit 4 isoform 1, mito.	P10888	2.00	0.009	Cytochrome c oxidase subunit 6B1	D3ZSB0	1.17	0.03
						Cytochrome c oxidase subunit 6A1, mitochondrial	P10818	1.35	0.04
Complex V	**High**	ATP synthase subunit delta, mito.	G3V7Y3	1.49	0.008	Pyrophosphatase (inorganic) 2	D4A830	1.27	0.03

		ATP synthase subunit d, mito.	P31399	1.27	0.01	ATPase H+-transporting V1 subunit H	E9PTI1	1.58	0.04
		ATPase, H+ transporting, lysosomal 38kDa, V0 subunit d1	Q5M7T6	1.75	0.01	V-type proton ATPase subunit B, brain isoform	P62815	1.38	0.03
		ATPase, H+ transporting, V1 subunit D	Q6P503	1.91	0.009				
		V-type proton ATPase subunit F	P50408	1.70	0.01				
		ATPase, H transporting, lysosomal V1 subunit G1	B2GUV5	1.61	0.008				
	Low	Pyrophosphatase (inorganic) 2	D4A830	1.44	0.03	ATP synthase F(0) complex subunit B1, mito.	P19511	1.25	0.03
		ATP synthase-coupling factor 6, mito.	P21571	1.25	0.01	ATP synthase-coupling factor 6, mito.	P21571	1.25	0.03
		ATP synthase subunit O, mito.	Q06647	1.36	0.008	ATP synthase subunit alpha	F1LP05	1.12	0.04
		ATP synthase subunit g, mito.	Q6PDU7	2.11	0.009	ATP synthase subunit g, mito.	Q6PDU7	1.94	0.03
		V-type proton ATPase subunit C 1	Q5FVI6	1.30	0.03	V-type proton ATPase subunit C 1	Q5FVI6	1.40	0.03
		V-type proton ATPase 16 kDa proteolipid subunit	P63081	1.28	0.009				
Carriers	**High**	Mito. 2-oxoglutarate/malate carrier protein (SLC25A11)	G3V6H5	1.53	0.009	Tricarboxylate transport protein, mito. (SLC25A12)	P32089	1.60	0.03
		Mitochondrial pyruvate carrier 1 (MCP1)	P63031	1.69	0.008	Mitochondrial pyruvate carrier 1 (MCP1)	P63031	1.83	0.03
						Solute carrier family 25 member 12	A0A0G2K2J7	1.25	0.03
Pro-apoptotic proteins	**Low**	BCL2-like 13 (BID isoform)	D3ZT71	1.20	0.02				
		Apoptosis regulator BAX	Q9JKL3	1.24	0.04				
		FAS-associated death domain protein	Q8R2E7	1.51	0.02				
		Apoptosis-inducing factor 1, mito.	A0A0G2K7K2	1.36	0.009				
Anti-apoptotic proteins	**High**	Bcl-2-like protein 1	A0A0G2JZS5	1.66	0.01				
		Bcl-2-interacting death suppressor	Q156J1	1.49	0.03				

Figure 1

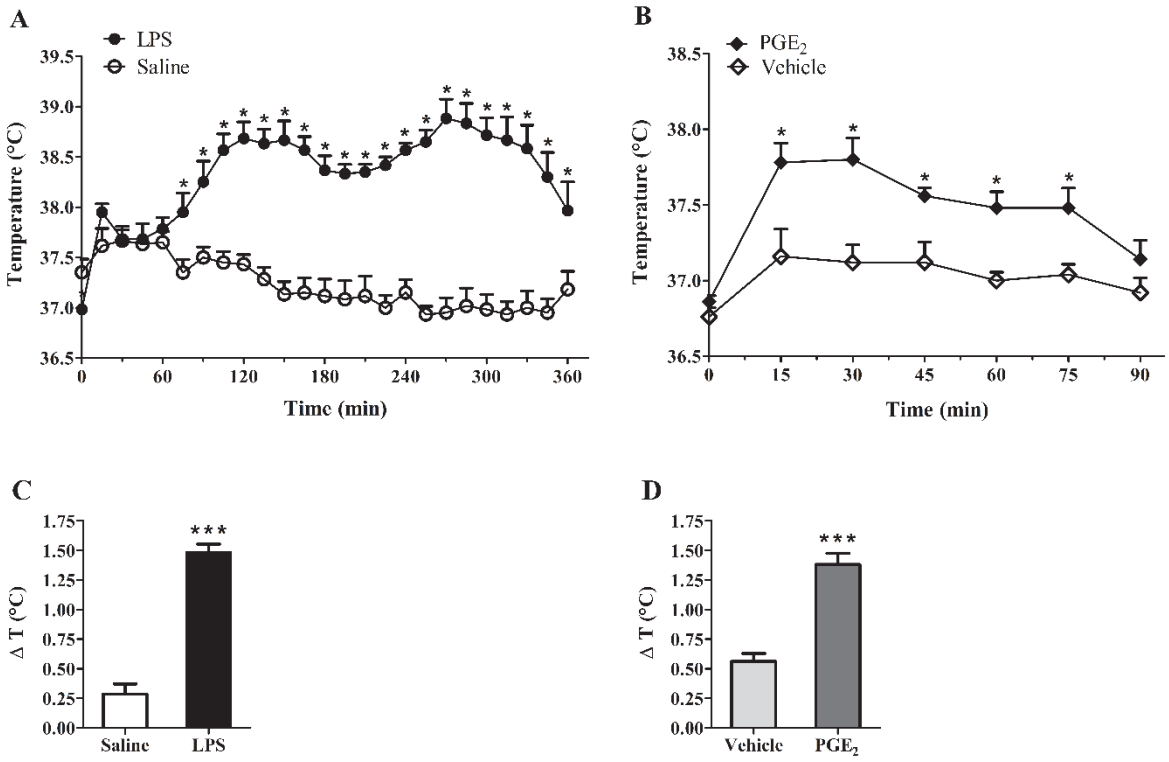

Figure 2

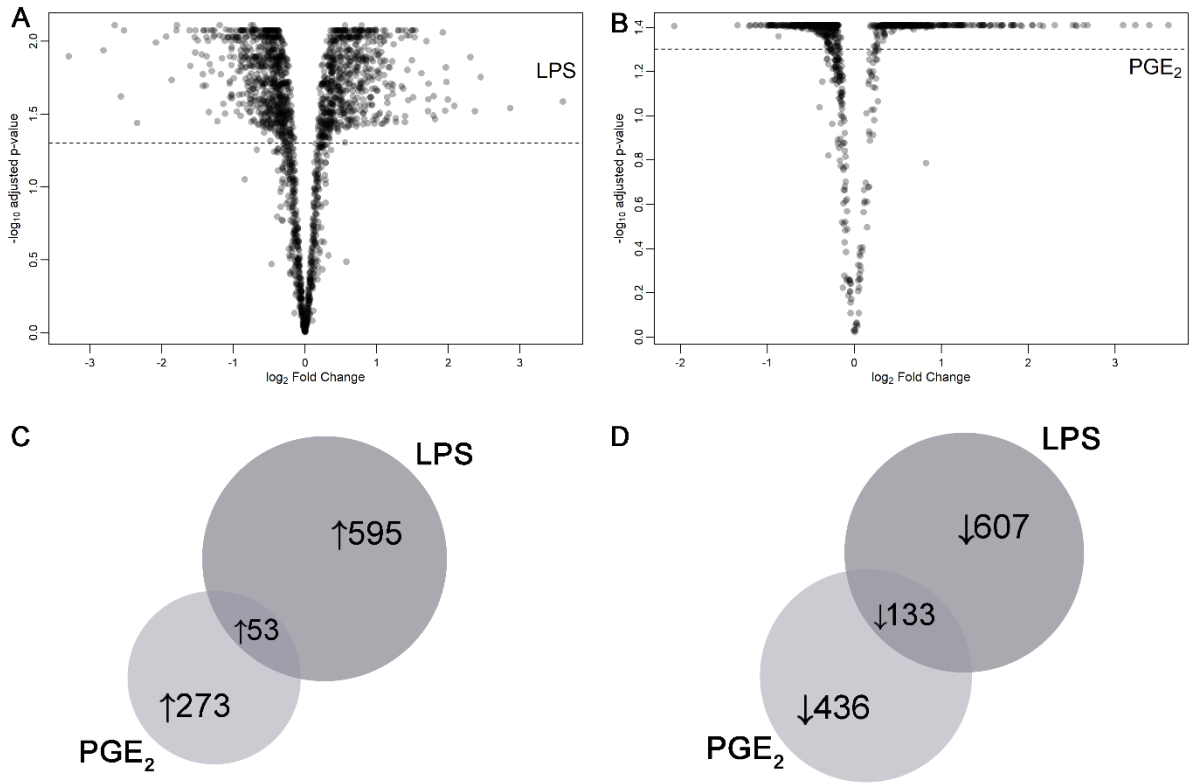

Figure 3

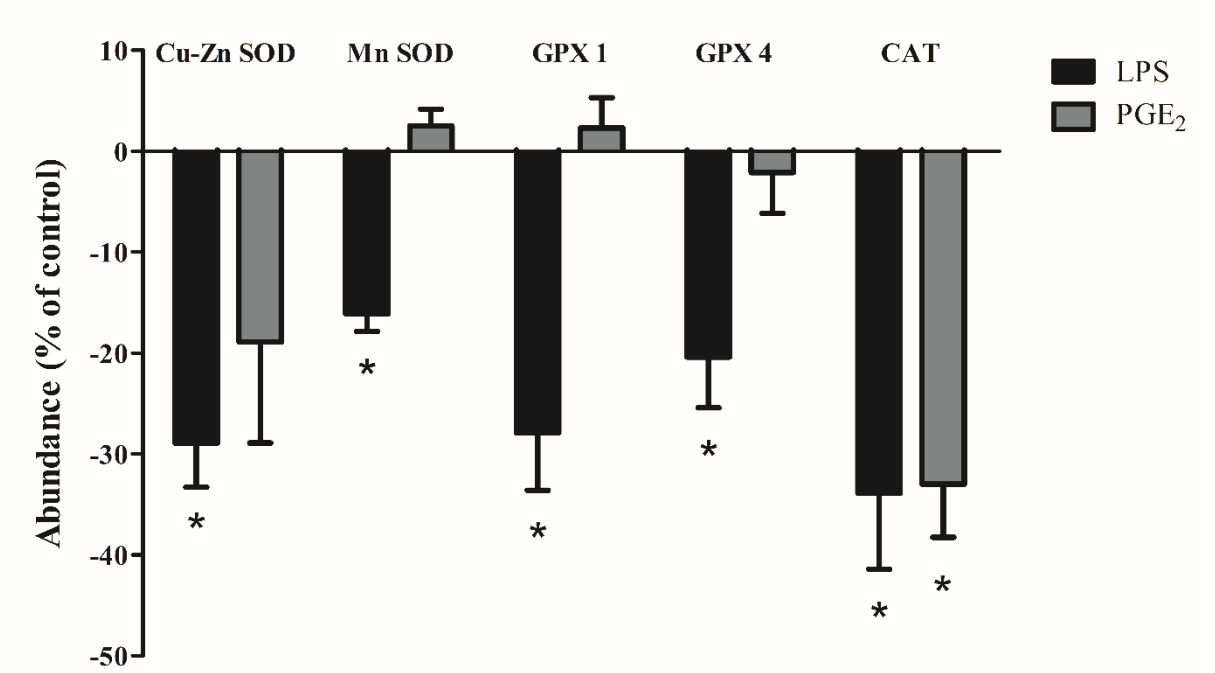
Cu-Zn SOD
Mn SOD
GPX 1
GPX 4
CAT
LPS
PGE2
Abundance (% of control)
10
0
-10
-20
-30
-40
-50
*

Figure 4

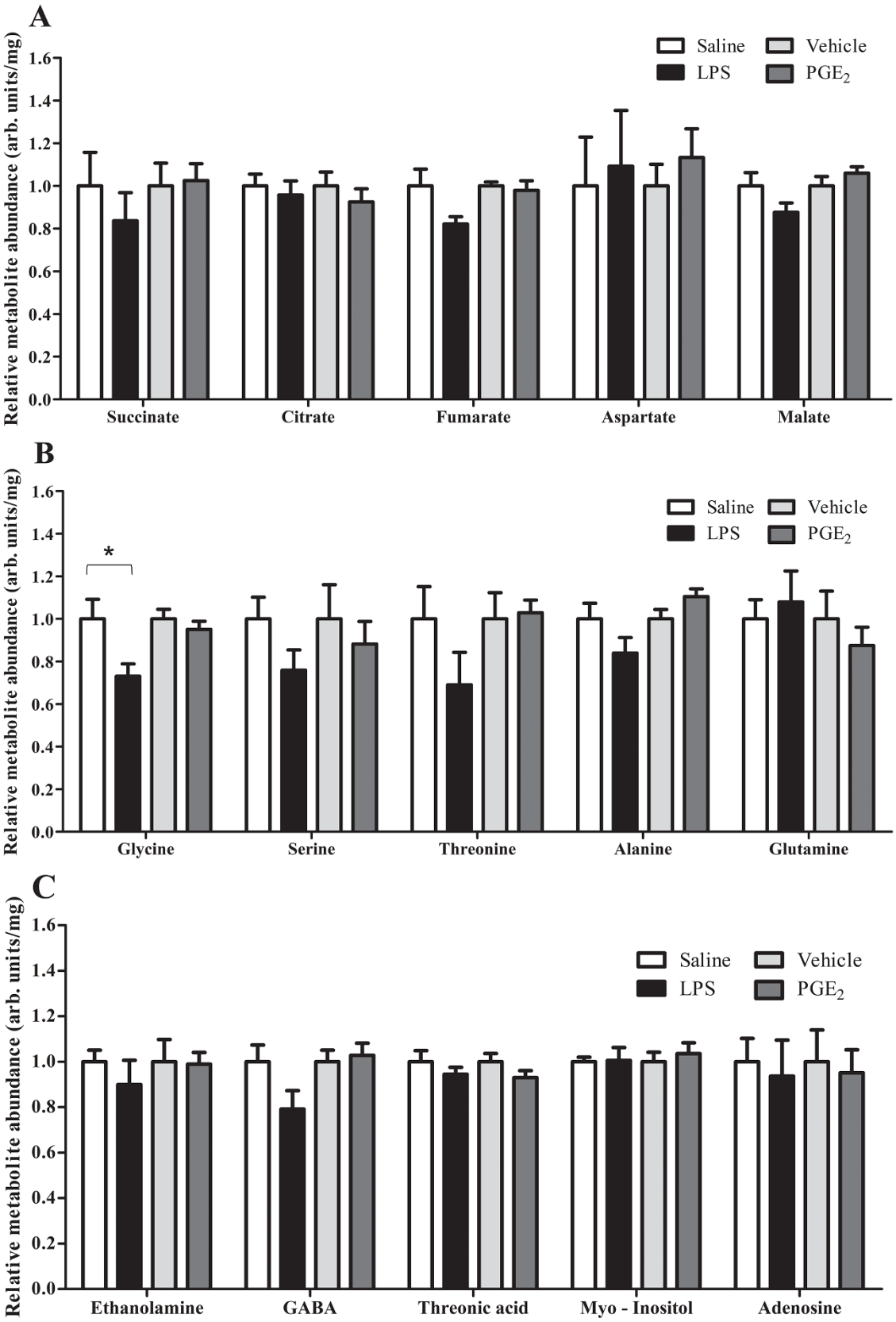
A
Relative metabolite abundance (arb. units/mg)
Saline
Vehicle
LPS
PGE2
1.6
1.4
1.2
1.0
0.8
0.6
0.4
0.2
0.0
Succinate
Citrate
Fumarate
Aspartate
Malate
B
Relative metabolite abundance (arb. units/mg)
Saline
Vehicle
LPS
PGE2
*
Glycine
Serine
Threonine
Alanine
Glutamine
C
Relative metabolite abundance (arb. units/mg)
Saline
Vehicle
LPS
PGE2
Ethanolamine
GABA
Threonic acid
Myo - Inositol
Adenosine

Figure 5

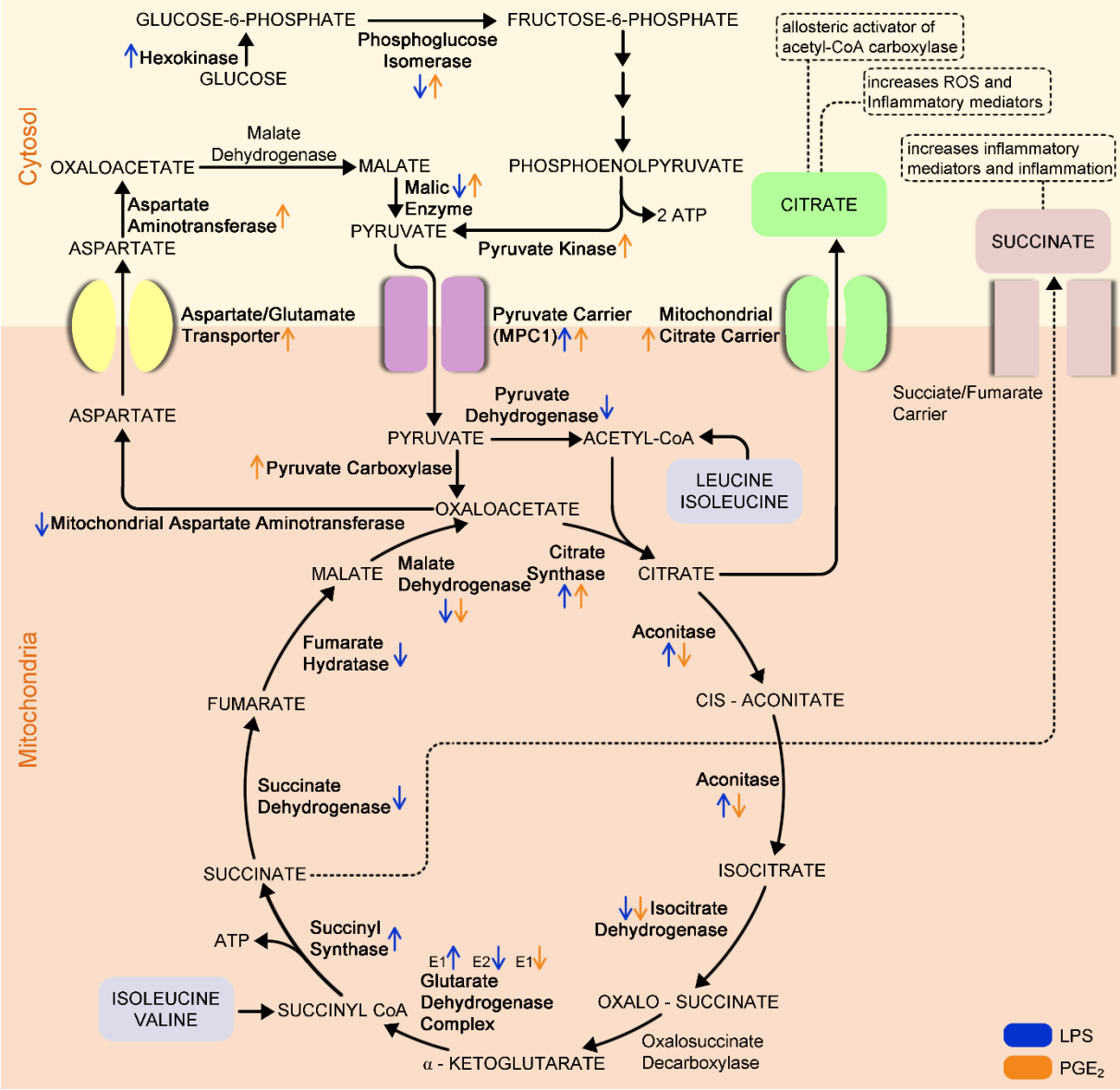
GLUCOSE-6-PHOSPHATE
FRUCTOSE-6-PHOSPHATE
Hexokinase
GLUCOSE
Phosphoglucose Isomerase
allosteric activator of acetyl-CoA carboxylase
increases ROS and Inflammatory mediators
increases inflammatory mediators and inflammation
Cytosol
Malate Dehydrogenase
OXALOACETATE
MALATE
PHOSPHOENOLPYRUVATE
Malic Enzyme
Aspartate Aminotransferase
ASPARTATE
PYRUVATE
2 ATP
Pyruvate Kinase
CITRATE
SUCCINATE
Aspartate/Glutamate Transporter
Pyruvate Carrier (MPC1)
Mitochondrial Citrate Carrier
Succiate/Fumarate Carrier
ASPARTATE
Pyruvate Dehydrogenase
PYRUVATE
ACETYL-CoA
Pyruvate Carboxylase
LEUCINE
ISOLEUCINE
Mitochondrial Aspartate Aminotransferase
OXALOACETATE
MALATE
Malate Dehydrogenase
Citrate Synthase
CITRATE
Aconitase
Mitochondria
Fumarate Hydratase
FUMARATE
CIS - ACONITATE
Succinate Dehydrogenase
Aconitase
SUCCINATE
ISOCITRATE
Isocitrate Dehydrogenase
ATP
Succinyl Synthase
E1 E2 E1
Glutarate Dehydrogenase Complex
ISOLEUCINE
VALINE
SUCCINYL CoA
OXALO - SUCCINATE
Oxalosuccinate Decarboxylase
α - KETOGLUTARATE
LPS
PGE2

Figure 6: Graphical Abstract

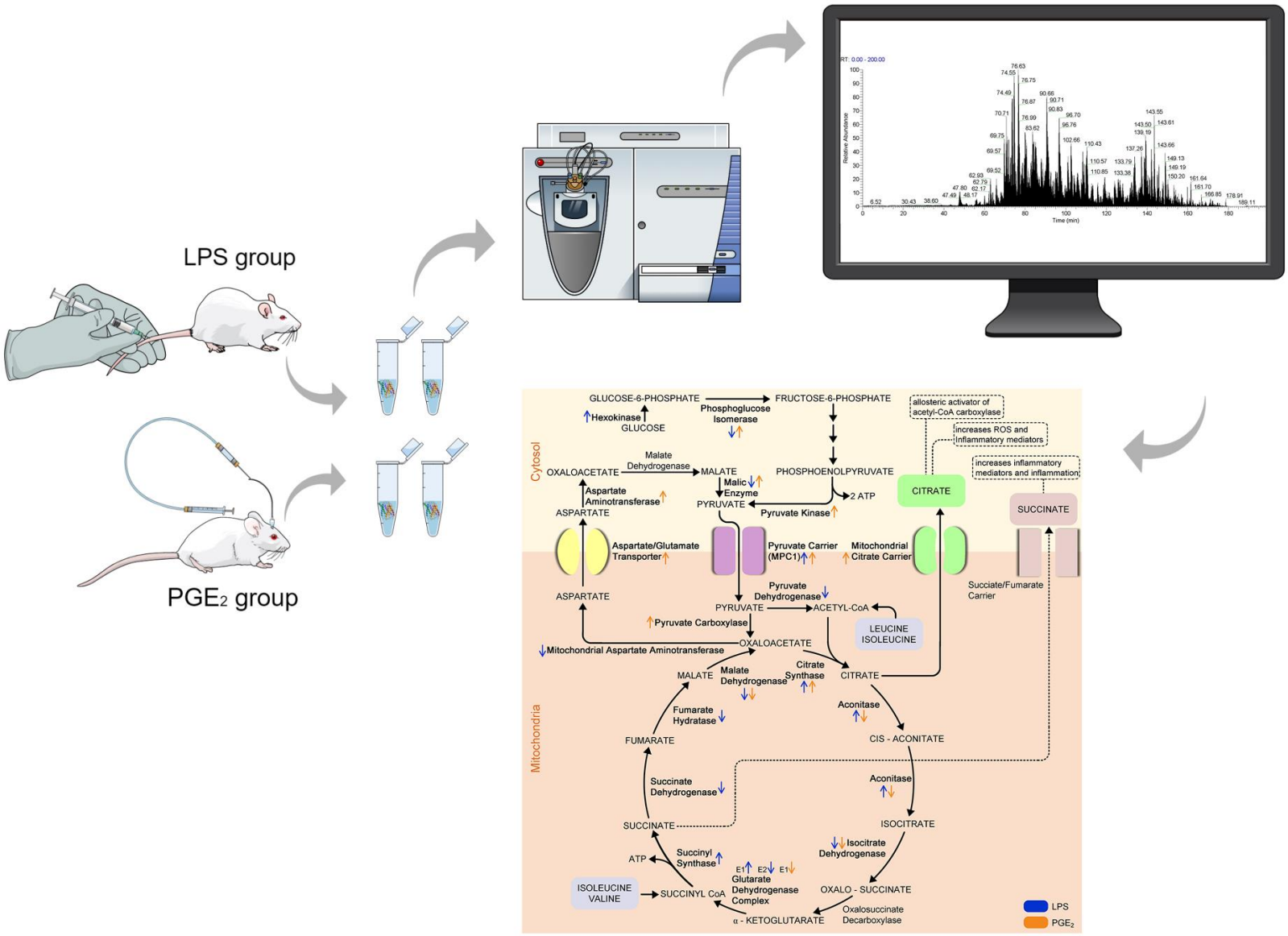

4. Capítulo 2

Manuscrito: Mitochondrial Dysfunctions Associated with Fever induced by LPS in Rat Hypothalamus and Brown Adipose Tissue - a ser submetido ao periódico *Neuroscience Letters*

Mitochondrial Dysfunctions Associated with Fever induced by LPS in Rat Hypothalamus and Brown Adipose Tissue

Marina Firmino[a], Simone N. Weis[a], Jaques M. F. Souza[a], Consuelo M. R. Lima[a], Tatiana K.S. Borges[b], Fabiane H. Veiga-Souza[a,c], Marcelo V. de Sousa[a*]

[a]Laboratory of Protein Chemistry and Biochemistry, Department of Cell Biology, Institute of Biology, University of Brasilia, Brasília, DF 70910-900, Brazil

[b]Laboratory of Cellular Immunology, Pathology, Faculty of Medicine, University of Brasilia, Brasília, DF 70910-900, Brazil

[c]School of Ceilandia, University of Brasilia, Brasília, DF 72220-275, Brazil

*****Corresponding author:

Marcelo Valle de Sousa, Proteomics Center, Laboratory of Protein Chemistry and Biochemistry, Department of Cell Biology, Institute of Biology, University of Brasília, 70910-900, Brasília, DF, Brazil.

E-mail address: mvsousa@unb.br

Abstract

Fever is a process phylogenetically preserved, which is executed by integrated physiological and neuronal circuitry. It confers a survival benefit during infection. The response is generally initiated by the production of PGE_2 within preoptic area in the anterior hypothalamus (AH/POA) in response to inflammatory mediators, released during inflammatory or infectious challenges. The signaling triggered in AH/POA induces the activation of mechanisms for heat production, such as shivering, brown adipose tissue (BAT) thermogenesis and cutaneous vasoconstriction. Since mitochondria is the organelle responsible for heat generation, we investigated mitochondrial alterations during fever induced by LPS in hypothalamus (HT) and BAT. Inhibition in electron transport chain complex I-III activity (around 30%) was observed in BAT with no impairment of mitochondrial membrane potential. On the other hand, no changes were detected in the hypothalamus neither in mitochondrial complexes activities nor in membrane potential at the time point observed. These findings suggest that LPS caused a mild inhibition in BAT mitochondrial function that may contribute for fever generation.

Keywords: fever; lipopolysaccharide, mitochondria, hypothalamus, brown adipose tissue.

1. Introduction

Fever is a phylogenetically preserved, physiological process induced by PGE_2 within preoptic area in the anterior hypothalamus (AH/POA) in response to inflammatory mediators, such as cytokines, released during infectious or inflammatory processes [1]. The AH/POA is involved in physiological and behavioral processes, including modulation in energy expenditure and food intake [2,3], reproductive cycle in female rats [4] and sexual behavior in males [5]. AH/POA is also the most important region for autonomic temperature control, being responsible for body temperature maintenance [6]. PGE_2 binds specifically to EP3 receptors on inhibitory warm-sensitive neurons in the AH/POA, and inhibits their activity. The resultant disinhibition of this thermoregulatory network causes the activation of mechanisms for heat production, such as shivering, brown adipose tissue (BAT) thermogenesis and cutaneous vasoconstriction [7–11].

In mammals BAT is a specialized thermogenic organ responsible for non-shivering thermogenesis (NST) [12]. BAT thermogenesis has been intensively studied in small laboratory rodents, which present the largest BAT depots in the interscapular and dorso-cervical regions [13]. BAT thermogenesis is such species significantly contributes to the heat production necessary to rise core body temperature during infectious fever. As in rodents, human BAT can be activated by cold exposure for maintenance of adequate core body temperature [14,15].

The large amounts of mitochondria present in BAT confer the unique capacity to this tissue to generate heat through uncoupling of oxidative respiration from ATP synthesis [12,16,17]. Under physiological conditions, cold stimulation induces the release of noradrenaline (NA) from postganglionic neurons. NA binds to β3-adrenergic receptors promoting downstream cAMP-PKA signaling, that in turn provoke the mobilization of fatty acids from adipocytes. The free fatty acids are known to be a potent activator of the uncoupling protein 1 (UCP1), also called thermogenin in BAT.

During oxidative phosphorylation, protons are pumped through the mitochondrial ATP synthase (F_oF_1-ATPase) from the mitochondrial matrix to the mitochondrial intermembrane space, generating an electrochemical gradient. The high negative membrane potential within the matrix drive protons to bypass the ATP synthase by leaking back into the matrix through proton conductance pathways embedded in the inner membrane [18–21]. In the meantime, protons can alternatively return to mitochondrial matrix through uncoupling proteins, as the UCP1, draining the energy derived from oxidized substrates as heat (Contreras et al., 2015). Such mechanism not only serves to regulate body temperature, but probably also serves to maintain NAD^+/NADH ratio to continuous substrate oxidation and to attenuate reactive oxygen species (ROS) production [22–24]. These ROS, including superoxide anion ($O_2^{\bullet -}$), hydrogen peroxide (H_2O_2) and hydroxyl radical ($^{\bullet}OH$), are generated through the four protein complexes of electron transport chain [25]. It has been demonstrated that ROS is related to the progression of inflammatory diseases [26–28], and could be associated to fever induced by LPS [29].

In light of the above considerations, the present study was designed to address the changes in mitochondrial function in both HT and BAT tissue during the first phase of LPS-induced fever.

2. Materials and methods

2.1 Animals

Adult male Wistar rats (180 ± 20 g body weight) were obtained from the Animal House of the Institute of Biological Sciences, University of Brasilia. Animals were maintained under a 12 h light/dark cycle (lights on at 7 a.m.), at constant room temperature (24 ± 1 °C) and 50 % humidity, with free access to food and water. Each animal was used only once. All procedures were previously approved by the Animal Research Ethics Committee of the University of

Brasilia (Protocol No. 30652/2014). Moreover, the care and use of the animals were in full compliance with the Guide for the Care and Use of Laboratory Animals of the Brazilian National Council for the Control of Animal Experimentation (CONCEA) and the Guide for the Care and Use of Laboratory Animals of the Institute for Laboratory Animal Research [30]. All efforts were done to minimize animal suffering as well as to reduce the number of used animals.

2.2 Core temperature measurement

Body temperature was measured in conscious unrestrained rats using data loggers (Subcue, Calgary, Canada) surgically implanted into the peritoneal cavity of the rats, under ketamine (60 $mg.kg^{-1}$) and xylazine (10 $mg.kg^{-1}$) anesthesia. All animals received oxytetracycline hydrochloride (400 $mg.kg^{-1}$ intramuscularly) and dexamethasone (1 $mg.kg^{-1}$ intramuscularly) after surgery, and were kept at rest for one week prior to the experiments. Experimental measurements were conducted at the thermoneutral zone for rats [31], in a temperature-controlled room (28 ± 1 °C). Temperature was continuously monitored and recorded at 15 min intervals from 2 h before any injection until the end of the experiments.

2.3 LPS/Saline administration

All chemicals used in this work were of proanalysis grade or better. Independent groups of rats received intravenous (i.v.) injections of LPS, derived from *Escherichia coli*, serotype O111:B4 (Sigma-Aldrich, St. Louis, USA) (5 $\mu g.kg^{-1}$ in sterile saline solution) or 0.2 mL sterile saline. The dose of LPS was chosen based on previous studies [29,32,33]. By preliminary experimental investigation, all injections were done at approximately 9 a.m. and fever was monitored for 2.5 h after LPS/saline administration [29].

2.4 Tissue preparation

Exactly 2.5 hours after the injections, the animals were sacrificed by decapitation. Brains and BATs were rapidly removed. HTs and BATs were dissected on ice. The entire hypothalamus was dissected from the brain using the following limits: the anterior border of the optic chiasm, the anterior border of the mammillary bodies, and the lateral hypothalamic sulci, with a depth of 2 mm. Interscapular BAT (IBAT) is characterized by a consistent "brown" cellular origin, located subcutaneously between the shoulders, and can be precisely identified and easily dissected.

For determination of respiratory chain complex activities, HT and BAT samples were homogenized using a Teflon-glass homogenizer (1:20 w/v) in SET buffer (250 mM sucrose, 2 mM EDTA, 10 mM Trizma base), pH 7.4. Samples were centrifuged at 1000 *xg* for 15 min, and the supernatants were immediately frozen at -80 °C until enzyme activity determination [34,35].

To investigate mitochondrial membrane potential through flow cytometry, HT and BAT samples were dissociated using PBS buffer containing 0,1 % DNase from bovine pancreas (Sigma-Aldrich, St. Louis, USA) plus 0,1 % collagenase type IV from *Clostridium histolyticum* (Sigma-Aldrich, St. Louis, USA), for HT samples [34], and 0,1 % DNase plus 2 mg/mL collagenase type II from *Clostridium histolyticum* (Sigma-Aldrich, St. Louis, USA), plus $CaCl_2$ 10 mM, for BAT samples. BAT samples were incubated in a rotational shaker (200 rpm) at 37 °C for 20 min [36, with some modifications]. The dissociated contents were then filtered into sterile 50 mL Falcon tubes (BD Biosciences, Bedford, MA, USA) through 40 µm nylon cell strainer (Cell Filter Strainer – BD Biosciences, Bedford, MA, USA), and kept on ice until mitochondrial staining.

2.5 Mitochondrial respiratory chain activity measurement

The evaluation of mitochondrial respiratory chain enzymatic activities is fundamental for investigating mitochondrial function. The activities of the ETC complexes I-III, II and IV were determined according to standard methods previously described [34,37–39]. For complex I–III (complex I + CoQ + III) activity, the reduction of cytochrome *c* from equine heart (Sigma-Aldrich, St. Louis, USA) at 550 nm was measured with and without rotenone (Sigma-Aldrich, St. Louis, USA)[38]. The reaction mixture contained 20 mM potassium phosphate buffer, pH 8.0, 2 mM KCN, 10 mM EDTA, 50 mM cytochrome *c* and 8 to 14 µg homogenate protein. The reaction was initiated by addition of 25 mM NADH and monitored at 25 °C for 3 min followed by the addition of 10 mM rotenone, measured for an additional 3 min. Complex II activity was measured through the decrease in absorbance due to the reduction of 2,6-diclorofenol-indofenol (2,6-DCIP) (Sigma-Aldrich, St. Louis, USA) at 600 nm [37]. The reaction mixture was preincubated with 28 to 54 µg protein at 30 °C for 20 min, and consisted of 40 mM potassium phosphate buffer, pH 7.4, 16 mM sodium succinate, and 8 mM DCIP. Subsequently, 4 mM sodium azide, 7 mM rotenone and 40 mM DCIP were added to the medium, and monitored for 5 min. The activity of cytochrome *c* oxidase (complex IV, COX) was determined by the method described by Rustin et al. [39], in which the decrease in absorbance due to the oxidation of previously reduced cytochrome *c* was detected at 550 nm. The reaction mixture contained 10 mM potassium phosphate buffer, pH 7.0, 0.6 mM n-dodecyl-ß-D-maltoside (Sigma-Aldrich, St. Louis, USA) and 1.5 to 3 µg homogenate protein. The reaction was initiated with addition of 0.7 mg of reduced cytochrome *c*, and complex IV activity was measured at 25 °C for 10 min. Protein concentration was determined using a Qubit® protein assay kit (Thermo Fisher Scientific, Maryland, USA). The activities of the mitochondrial respiratory chain complexes were reported as nmol/min/mg protein.

2.6 Determination of mitochondrial membrane potential

Mitochondrial function was evaluated using the MitoTracker Red dye (MTR or chloromethyl-X-rosamine) (Thermo Fisher Scientific Waltham, MA USA). MTR passively diffuse across the membrane, and can be deposited in the negatively charged mitochondrial matrix. The dissipation of the membrane potential and subsequent decrease in cell-associated fluorescence can be measure by flow cytometry [40]. MTR was dissolved in dimethylsulfoxide (DMSO) to a 1 mM stock concentration. One aliquot of each sample, previously dissociated and filtered, were stained with 100 nm MTR, for 45 min, at 37 °C, in a water bath in a dark room according to method described by [41,42] with some modifications [34]. Immediately after staining, cell suspensions were removed from the water bath and analyzed by flow cytometry.

2.7 Flow cytometry analysis

Samples stained with MTR dye were analyzed on a FACS LSR Fortessa flow cytometer (Becton Dickinson, Franklin Lakes, New Jersey). Excitation was achieved using the 640 nm laser. Gating parameters on the flow cytometer were established using a negative control sample (sample without stain) and adjusting the voltages for the forward scatter, side scatter and MitoTracker Red [recorded through APC bandpass fluorescence filter (670/14 nm)]. All samples were run on the same day under the same settings. Fluorescence emission was collected using logarithmic amplification. Briefly, data from 10.000 events were acquired, and mean relative fluorescence intensity was determined after exclusion of debris events from the data set. All flow cytometric acquisitions and analyses were performed using FACSDiva software data acquisition (Becton Dickinson, Franklin Lakes, New Jersey) and FlowJo analysis software (Tree Star, San Carlos, California).

The obtained data were analyzed and plotted by density as a single-parameter histogram which shows the MTR fluorescence on the x-axis and the number of events on the y-axis.

During analyses, a marker indicating two cell population with low and high potential ($\Delta\Psi$) were applied to histograms of all samples.

2.8 Statistical Analysis

All data in this study are represented as the mean ± standard error of the mean. The unpaired two-tailed Student's *t* test was used to determine *p* values for all assays considering only two conditions. A multivariate analysis of variance (MANOVA) was used to compare the difference of means between the observations taken at various intervals with baseline. Significance levels for all measures were set at $p < 0.05$. *Statistical Package for the Social Sciences* software (SPSS, SPSS Inc. Chicago, IL, USA) version 23.0 was used for the statistical analyses.

3. Results

3.1 Fever induced by LPS

Figure 1 shows that intravenous injection of LPS (5 $\mu g.kg^{-1}$) produced a significant rise in body temperature when compared to that observed in the control group. To investigate the mitochondrial alterations in LPS-induced fever, animals were euthanized at 2.5 h (150 min), when the stimulus had induced significant increase in core body temperature (LPS: $\Delta T = 1.50 \pm 0.14$ °C, $p < 0.05$).

3.2 Impairment in mitochondrial respiratory chain activity in BAT but not in HT in LPS-induced fever

In BAT, LPS induced a significant reduction in complex I + III activity (around 30%) in comparison to saline group (**Figure 2A**). No differences were observed in complexes II and

IV activities (**Figure 2B and C**). Considering HT, no differences were observed between LPS and control group for all mitochondrial complexes (**Figure 2**).

Moreover, analysis showed that, as expected, BAT presented higher activities than hypothalamus for all complexes measured, evidencing the main role of this tissue, probably because the great number of mitochondria present in BAT tissue (**Figure 2**).

3.3 LPS-induced fever does not change the mitochondrial membrane potential

Flow cytometry was used to detect mitochondrial membrane potential ($\Delta\Psi$) in hypothalami and BAT cells through MTR labeling (**Figure 3**). Cells from both tissues comprised a subset of cells that shifted from a population with high (**Figure 3A**) mitochondrial $\Delta\Psi$ to a population of cells with less (**Figure 3B**) polarized mitochondrial membranes. No significant differences were observed in $\Delta\Psi$ in any of the tissues when comparing the LPS group with the control saline group. (**Figure 3**).

4. Discussion

Mitochondria are essential for maintenance of cellular homeostasis. Over 90 % of intracellular energy generation takes place in the mitochondria. This organelle also plays a role in Ca^{2+} metabolism and signaling, controls the fever response by modulation of thermogenesis, generates ROS and regulates apoptosis. Given its importance in cellular physiology, Manoli argues that it is obvious that the mitochondrion is among the first responders to various stressors able to invade the organism [43]. In the present study, some mitochondrial alterations during LPS-induced fever were investigated.

The results demonstrated that BAT mitochondria showed an overall higher activity than hypothalamus. This can be explained due to large quantity of mitochondria present in this tissue compared to hypothalamus. BAT also seems more sensitive to LPS-induced fever, since an

impairment in the activity of electron transport chain, more specifically in the electron flux from complex I to III, were detected in mitochondria from BAT compared to their controls 2.5 h after stimulus injection.

Under normal physiological conditions, cell respiration is accompanied by electron escape, that reduces oxygen molecules with single electrons yielding superoxide anion radicals [44]. The NADH-ubiquinone oxidoreductase is considered the main source of ROS formation in mitochondria since the electron transfer from complex I to ubiquinone is always accompanied by formation of semiquinone radical. The slow active/deactive state transition characteristic of complex I is implicated in conformational rearrangements that can be relevant in ROS production [45,46]. In neurodegenerative disease models it was observed that a small inhibition in complex 1 activity is sufficient to enhance ROS generation [47].

BAT produces heat by oxidation of fatty acids, an ability attributed to the tissue-specific presence of UCP1 [48]. The activation of BAT UCP1-dependent thermogenesis is defined by a substantial increase in mitochondrial ROS levels [49], evidencing the special role of mitochondrial derived ROS in sensitization of UCP1 to fatty acids activation [50]. During fever, BAT works as an effector organ, producing heat especially during the onset phase of the fever [48]. The impairment in electron flux from mitochondrial complex I-III observed here may suggest an onset in ROS production, sufficient to induce BAT heat production with no $\Delta\Psi$ consequences. In fact, recent published data from our research group detected BAT ROS formation by EPR spectroscopy 5 h after LPS stimuli, but not at 2.5 h [29]. It is possible that the first phase of febrile response represents an initial disturbance in mitochondrial energy metabolism capable to activate BAT thermogenesis, with a progressive increase in electron flux impairment and, consequently, ROS formation, detected at the second phase of fever [29].

Electrons from reduced substrates are passed through four protein complexes up to oxygen, forming water and causing protons to be pumped across the mitochondrial inner

membrane. This process generates an electrochemical gradient in the intermembrane space, referred as ΔΨ [25,43,51]. Mitochondrial potential is considered an important indicator of mitochondrial function, health and metabolic activity [25]. Loss of ΔΨ can lead to a functional collapse that can promote opening of the mitochondrial permeability transition pore, resulting in mitochondria swelling, release of cytochrome *c* and apoptosis [52].

In order to evaluate whether a depressed activity of the respiratory chain could affect ΔΨ , mitochondria were stained with MTR dye and subsequently analyzed by flow cytometry. In BAT samples, the inhibition of respiratory chain was not accompanied by alteration in ΔΨ. Acute inhibition of CI activity by rotenone over mitochondria from human skin fibroblasts failed to alter ΔΨ, evidencing that CI activity is not a major determinant of ΔΨ, and that $O_2^{\bullet-}$ generation is not strictly coupled to ΔΨ in this cells [25]. The impairment in activity of Complex I-III induced by LPS with intact ΔΨ in BAT reveals that, despite of fever response and mitochondrial alterations, the stability of mitochondrial membrane is preserved, possibly preventing a proapoptotic response leading to cell death.

In brain cells, mitochondria regulate fundamental aspects of brain structure and function such as synaptic transmission and cognition [53,54]. In general, the brain appears to be mostly vulnerable to mitochondrial defects, suggesting that neurons are particularly sensitive to bioenergetic fluctuations [54]. Since moderate fevers clinically do not produce brain injury, it is not surprising the absence of alterations in mitochondria from hypothalamus at the 2.5 h timepoint. On the other hand, increased ROS levels was detected in hypothalamus and BAT 5 h after LPS administration in a previous study [29], demonstrating that ROS are produced during the time course of the febrile response. Differently from hypothalamus, the great number of mitochondria in BAT make this tissue the main site of heat production in the body [48]. Based on this, it would be expected a minimum alteration in mitochondria function, as we indeed observed. More studies are needed to identify changes in mitochondrial function along

the whole time course of fever response. Also, how hypothalamus and BAT contribute to the generation of heat as well as how this response is physiologically controlled to avoid pathological consequences are worthwhile to be further investigated.

5. Conclusions

The present study reports for the first time that fever induced by LPS produces alterations in the activity of mitochondrial electron transport chain activity, without mitochondrial membrane potential changes. Since mitochondria is the organelle that has the unique capacity to produce heat, understanding the alterations produced during fever can contribute to the development of more specific and effective therapeutic agents.

Acknowledgments

This work was partly supported by grant 407321/2013-6 from the Brazilian National Council for Scientific and Technological Development (CNPq) to M.V.S. M.F. is recipient of a scholarship from CNPq (146256/2013-1), and S.N.W. is recipient of a fellowship from the Coordination for the Improvement of Higher Education Personnel (CAPES) (PNPD20132991).

Conflicts of Interest

The authors reports no conflict of interest.

References

[1] J. Roth, C.M. Blatteis, Mechanisms of fever production and lysis: lessons from experimental LPS fever., Compr. Physiol. 4 (2014) 1563–604. doi:10.1002/cphy.c130033.

[2] B. Andersson, B. Larsson, Influence of Local Temperature Changes in the Preoptic Area

and Rostral Hypothalamus on the Regulation of Food and Water Intake, Acta Physiol. Scand. 52 (1961) 75–89. doi:10.1111/j.1748-1716.1961.tb02203.x.

[3] S. Yu, M. François, C. Huesing, H. Münzberg, At the Cutting Edge The Hypothalamic Preoptic Area and Body Weight Control, Neuroendocrinology. 106 (2018) 187–194. doi:10.1159/000479875.

[4] S. Verma, V.M. Kumar, G. Gopinath, R. Sharma, P.N. Tandon, Recovery of preoptic–anterior hypothalamic functions after transplantation, Restor. Neurol. Neurosci. 1 (1989) 77–81. doi:10.3233/RNN-1989-1108.

[5] R.G. Paredes, Medial preoptic area/anterior hypothalamus and sexual motivation, Scand. J. Psychol. 44 (2003) 203–212. doi:10.1111/1467-9450.00337.

[6] A.A. Romanovsky, Thermoregulation: some concepts have changed. Functional architecture of the thermoregulatory system, Am. J. Physiol. Integr. Comp. Physiol. 292 (2007) R37–R46. doi:10.1152/ajpregu.00668.2006.

[7] K. Nakamura, Central circuitries for body temperature regulation and fever, AJP Regul. Integr. Comp. Physiol. 301 (2011) R1207–R1228. doi:10.1152/ajpregu.00109.2011.

[8] K. Nakamura, T. Kaneko, Y. Yamashita, H. Hasegawa, H. Katoh, A. Ichikawa, M. Negishi, Immunocytochemical localization of prostaglandin EP3 receptor in the rat hypothalamus, Neurosci. Lett. 260 (1999) 117–120. doi:10.1016/S0304-3940(98)00962-8.

[9] K. Nakamura, T. Kaneko, Y. Yamashita, H. Hasegawa, H. Katoh, M. Negishi, Immunohistochemical localization of prostaglandin EP3 receptor in the rat nervous system, J. Comp. Neurol. 421 (2000) 543–569. doi:10.1002/(SICI)1096-9861(20000612)421:4<543::AID-CNE6>3.0.CO;2-3.

[10] S.F. Morrison, Central control of body temperature, F1000Research. 5 (2016) 880. doi:10.12688/f1000research.7958.1.

[11] J. Roth, C. Rummel, S.W. Barth, R. Gerstberger, T. Hübschle, Molecular aspects of fever and hyperthermia., Immunol. Allergy Clin. North Am. 29 (2009) 229–45. doi:10.1016/j.iac.2009.02.005.

[12] B. Cannon, J. Nedergaard, Brown adipose tissue: function and physiological significance., Physiol. Rev. 84 (2004) 277–359. doi:10.1152/physrev.00015.2003.

[13] R. Oelkrug, E.T. Polymeropoulos, M. Jastroch, Brown adipose tissue: physiological function and evolutionary significance, J. Comp. Physiol. B. 185 (2015) 587–606. doi:10.1007/s00360-015-0907-7.

[14] A. Fenzl, F.W. Kiefer, Brown adipose tissue and thermogenesis, Horm. Mol. Biol. Clin. Investig. 19 (2014) 25–37. doi:10.1515/hmbci-2014-0022.

[15] K.A. Virtanen, M.E. Lidell, J. Orava, M. Heglind, R. Westergren, T. Niemi, M. Taittonen, J. Laine, N.-J. Savisto, S. Enerbäck, P. Nuutila, Functional Brown Adipose Tissue in Healthy Adults, N. Engl. J. Med. 360 (2009) 1518–1525. doi:10.1056/NEJMoa0808949.

[16] C. Contreras, F. Gonzalez, J. Fernø, C. Diéguez, K. Rahmouni, R. Nogueiras, M. López, The brain and brown fat, Ann. Med. 47 (2015) 150–168. doi:10.3109/07853890.2014.919727.

[17] D. Tupone, C.J. Madden, S.F. Morrison, Autonomic regulation of brown adipose tissue thermogenesis in health and disease: potential clinical applications for altering BAT thermogenesis, Front. Neurosci. 8 (2014) 1–14. doi:10.3389/fnins.2014.00014.

[18] M.D. Brand, The proton leak across the mitochondrial inner membrane, Biochim. Biophys. Acta - Bioenerg. 1018 (1990) 128–133. doi:10.1016/0005-2728(90)90232-S.

[19] G.C. Brown, M.D. Brand, On the nature of the mitochondrial proton leak, Biochim. Biophys. Acta - Bioenerg. 1059 (1991) 55–62. doi:10.1016/S0005-2728(05)80187-2.

[20] M.D. Brand, L.F. Chien, E.K. Ainscow, D.F. Rolfe, R.K. Porter, The causes and

functions of mitochondrial proton leak., Biochim. Biophys. Acta. 1187 (1994) 132–9. http://www.ncbi.nlm.nih.gov/pubmed/8075107 (accessed April 18, 2018).

[21] M.D. Brand, K.M. Brindle, J.A. Buckingham, J.A. Harper, D.F. Rolfe, J.A. Stuart, The significance and mechanism of mitochondrial proton conductance., Int. J. Obes. Relat. Metab. Disord. 23 Suppl 6 (1999) S4-11. http://www.ncbi.nlm.nih.gov/pubmed/10454114 (accessed April 18, 2018).

[22] R. Oelkrug, N. Goetze, C.W. Meyer, M. Jastroch, Antioxidant properties of UCP1 are evolutionarily conserved in mammals and buffer mitochondrial reactive oxygen species, Free Radic. Biol. Med. 77 (2014) 210–216. doi:10.1016/j.freeradbiomed.2014.09.004.

[23] K.S. Echtay, Mitochondrial uncoupling proteins-What is their physiological role?, Free Radic. Biol. Med. 43 (2007) 1351–1371. doi:10.1016/j.freeradbiomed.2007.08.011.

[24] D.B. Zorov, M. Juhaszova, S.J. Sollott, Mitochondrial Reactive Oxygen Species (ROS) and ROS-Induced ROS Release, Physiol. Rev. 94 (2014) 909–950. doi:10.1152/physrev.00026.2013.

[25] W.J.H. Koopman, L.G.J. Nijtmans, C.E.J. Dieteren, P. Roestenberg, F. Valsecchi, J.A.M. Smeitink, P.H.G.M. Willems, Mammalian Mitochondrial Complex I: Biogenesis, Regulation, and Reactive Oxygen Species Generation, Antioxid. Redox Signal. 12 (2010) 1431–1470. doi:10.1089/ars.2009.2743.

[26] A. Rimessi, M. Previati, F. Nigro, M.R. Wieckowski, P. Pinton, Mitochondrial reactive oxygen species and inflammation: Molecular mechanisms, diseases and promising therapies, Int. J. Biochem. Cell Biol. 81 (2016) 281–293. doi:10.1016/J.BIOCEL.2016.06.015.

[27] E. Naik, V.M. Dixit, Mitochondrial reactive oxygen species drive proinflammatory cytokine production: Figure 1., J. Exp. Med. 208 (2011) 417–420. doi:10.1084/jem.20110367.

[28] M. Mittal, M.R. Siddiqui, K. Tran, S.P. Reddy, A.B. Malik, Reactive oxygen species in inflammation and tissue injury., Antioxid. Redox Signal. 20 (2014) 1126–67. doi:10.1089/ars.2012.5149.

[29] B.R.B. Gomes, M. Firmino, J.S. Jorge, M.L.O. Ferreira, T.M. Rodovalho, S.N. Weis, G.E.P. Souza, P.C. Morais, M. V. Sousa, P.E.N. Souza, F.H. Veiga-Souza, Increase of reactive oxygen species in different tissues during lipopolysaccharide-induced fever and antipyresis: an electron paramagnetic resonance study, Free Radic. Res. (2018) 1–11. doi:10.1080/10715762.2018.1425549.

[30] E. Edition, Guide, 2011. doi:10.1163/1573-3912_islam_DUM_3825.

[31] C.J. Gordon, Thermal biology of the laboratory rat., Physiol. Behav. 47 (1990) 963–91. doi:10.1016/0031-9384(90)90025-Y.

[32] D.M. Soares, F. Hiratsuka Veiga-Souza, A. Sueli Coelho Fabrício, F. Javier Miñano, G.E. Petto Souza, CCL3/Macrophage inflammatory protein-1α induces fever and increases prostaglandin E2 in cerebrospinal fluid of rats: Effect of antipyretic drugs, Brain Res. 1109 (2006) 83–92. doi:10.1016/j.brainres.2006.06.026.

[33] D.M. Soares, R. Cristofoletti, M.C.C. Melo, C.J. Lindsey, F.H. Veiga-Souza, A.S.C. Fabricio, G.E.P. Souza, Cyclooxygenase-independent mechanism of ibuprofen-induced antipyresis: the role of central vasopressin V1 receptors, Fundam. Clin. Pharmacol. 25 (2011) 670–681. doi:10.1111/j.1472-8206.2010.00894.x.

[34] S.N. Weis, L.F. Pettenuzzo, R. Krolow, L.M. Valentim, C.S. Mota, C. Dalmaz, A.T.S. Wyse, C.A. Netto, Neonatal hypoxia–ischemia induces sex-related changes in rat brain mitochondria, Mitochondrion. 12 (2012) 271–279. doi:10.1016/j.mito.2011.10.002.

[35] L.F. Pettenuzzo, G. da C. Ferreira, A.L. Schmidt, C.S. Dutra-Filho, A.T.S. Wyse, M. Wajner, Differential inhibitory effects of methylmalonic acid on respiratory chain complex activities in rat tissues, Int. J. Dev. Neurosci. 24 (2006) 45–52.

doi:10.1016/j.ijdevneu.2005.10.005.

[36] J.S. Orr, A.J. Kennedy, A.H. Hasty, Isolation of adipose tissue immune cells., J. Vis. Exp. (2013) e50707. doi:10.3791/50707.

[37] J.C. Fischer, W. Ruitenbeek, J.A. Berden, J.M.F. Trijbels, J.H. Veerkamp, A.M. Stadhouders, R.C.A. Sengers, A.J.M. Janssen, Differential investigation of the capacity of succinate oxidation in human skeletal muscle, Clin. Chim. Acta. 153 (1985) 23–36. doi:10.1016/0009-8981(85)90135-4.

[38] A.H. Schapira, J.M. Cooper, D. Dexter, J.B. Clark, P. Jenner, C.D. Marsden, Mitochondrial complex I deficiency in Parkinson's disease., J. Neurochem. 54 (1990) 823–7. http://www.ncbi.nlm.nih.gov/pubmed/2154550 (accessed February 4, 2018).

[39] P. Rustin, D. Chretien, T. Bourgeron, B. Gérard, A. Rötig, J.M. Saudubray, A. Munnich, Biochemical and molecular investigations in respiratory chain deficiencies., Clin. Chim. Acta. 228 (1994) 35–51. http://www.ncbi.nlm.nih.gov/pubmed/7955428 (accessed February 4, 2018).

[40] K. Gilmore, M. Wilson, The use of chloromethyl-X-rosamine (Mitotracker Red) to measure loss of mitochondrial membrane potential in apoptotic cells is incompatible with cell fixation, Cytometry. 36 (1999) 355–358. doi:10.1002/(SICI)1097-0320(19990801)36:4<355::AID-CYTO11>3.0.CO;2-9.

[41] J.F. Keij, C. Bell-Prince, J.A. Steinkamp, Staining of mitochondrial membranes with 10-nonyl acridine orange, MitoFluor Green, and MitoTracker Green is affected by mitochondrial membrane potential altering drugs., Cytometry. 39 (2000) 203–10. http://www.ncbi.nlm.nih.gov/pubmed/10685077 (accessed February 7, 2018).

[42] W. Pendergrass, N. Wolf, M. Poot, Efficacy of MitoTracker Green? and CMXrosamine to measure changes in mitochondrial membrane potentials in living cells and tissues, Cytometry. 61A (2004) 162–169. doi:10.1002/cyto.a.20033.

[43] I. Manoli, S. Alesci, M.R. Blackman, Y.A. Su, O.M. Rennert, G.P. Chrousos, Mitochondria as key components of the stress response, Trends Endocrinol. Metab. 18 (2007) 190–198. doi:10.1016/j.tem.2007.04.004.

[44] M.D. Brand, J.A. Buckingham, T.C. Esteves, K. Green, A.J. Lambert, S. Miwa, M.P. Murphy, J.L. Pakay, D.A. Talbot, K.S. Echtay, Mitochondrial superoxide and aging: uncoupling-protein activity and superoxide production., Biochem. Soc. Symp. (2004) 203–13. http://www.ncbi.nlm.nih.gov/pubmed/15777023 (accessed May 5, 2018).

[45] E.. Gavrikova, A.. Vinogradov, Active/de-active state transition of the mitochondrial complex I as revealed by specific sulfhydryl group labeling, FEBS Lett. 455 (1999) 36–40. doi:10.1016/S0014-5793(99)00850-9.

[46] A.D. Vinogradov, Catalytic properties of the mitochondrial NADH-ubiquinone oxidoreductase (complex I) and the pseudo-reversible active/inactive enzyme transition., Biochim. Biophys. Acta. 1364 (1998) 169–85. http://www.ncbi.nlm.nih.gov/pubmed/9593879 (accessed May 20, 2018).

[47] V. Adam-Vizi, Production of reactive oxygen species in brain mitochondria: contribution by electron transport chain and non-electron transport chain sources., Antioxid. Redox Signal. 7 (2005) 1140–9. doi:10.1089/ars.2005.7.1140.

[48] B. Cannon, J. Houstek, J. Nedergaard, Brown adipose tissue. More than an effector of thermogenesis?, Ann. N. Y. Acad. Sci. 856 (1998) 171–187. doi:10.1111/j.1749-6632.1998.tb08325.x.

[49] E.T. Chouchani, L. Kazak, M.P. Jedrychowski, G.Z. Lu, B.K. Erickson, J. Szpyt, K.A. Pierce, D. Laznik-Bogoslavski, R. Vetrivelan, C.B. Clish, A.J. Robinson, S.P. Gygi, B.M. Spiegelman, Mitochondrial ROS regulate thermogenic energy expenditure and sulfenylation of UCP1., Nature. 532 (2016) 112–6. doi:10.1038/nature17399.

[50] D.G. Nicholls, E. Rial, A novel regulatory mechanism for the brown-fat uncoupling

protein?, Nat. Struct. Mol. Biol. 23 (2016) 364–365. doi:10.1038/nsmb.3221.

[51] M.D. Brand, C. Affourtit, T.C. Esteves, K. Green, A.J. Lambert, S. Miwa, J.L. Pakay, N. Parker, Mitochondrial superoxide: production, biological effects, and activation of uncoupling proteins, Free Radic. Biol. Med. 37 (2004) 755–767. doi:10.1016/j.freeradbiomed.2004.05.034.

[52] W.I. Sivitz, M.A. Yorek, Mitochondrial Dysfunction in Diabetes: From Molecular Mechanisms to Functional Significance and Therapeutic Opportunities, Antioxid. Redox Signal. 12 (2010) 537–577. doi:10.1089/ars.2009.2531.

[53] Y. Hara, F. Yuk, R. Puri, W.G.M. Janssen, P.R. Rapp, J.H. Morrison, Presynaptic mitochondrial morphology in monkey prefrontal cortex correlates with working memory and is improved with estrogen treatment, Proc. Natl. Acad. Sci. 111 (2014) 486–491. doi:10.1073/pnas.1311310110.

[54] M. Picard, B.S. McEwen, Mitochondria impact brain function and cognition, Proc. Natl. Acad. Sci. 111 (2014) 7–8. doi:10.1073/pnas.1321881111.

Captions:

Figure 1. Time course of changes in body temperature following LPS injection.

(A) The time course of the change in body temperature of the rats, measured by telemetry, following an intravenous LPS (5 $\mu g/kg^{-1}$) injection. The control group received saline (0.9%). Values are represented as mean ± S.E.M of the body temperature (°C) of 10-11 animals, until 2.5 h after the stimulus injection. (B) The bars represent the means ± S.E.M of the change in body temperature ΔT (°C) with respect to the basal temperature at the moment of euthanasia of the animals. *$p < 0.05$ compared with the saline group. Student's *t*-test. A half of the animals were assigned to the measure of activity of mitochondrial complex and another half were used for cytometry analyses.

Figure 2. Mitochondrial respiratory chain activity in hypothalamus and brown adipose tissue.

The activities of mitochondrial electron transport chain complexes were determined in hypothalamus and brown adipose tissues of rats 2.5 h after LPS injection. (A) complex I-III, (B) complex II and (C) complex IV. Data are expressed as nmol/min/mg protein (mean ± S.E.M) of five to six animals in each group. Significant differences between HT/BAT *versus* LPS/saline were revealed by Student's *t*-test. $^{\#}$ illustrates *tissue* main effect, **LPS x saline* interaction ($p < 0.05$).

Figure 3. Mitochondrial membrane potential measurement in hypothalamus and brown adipose tissue. Flow cytometry analysis of MitoTracker Red fluorescence intensity from hypothalamus and brown adipose tissues of rats 2.5 h after LPS injection. Data are expressed as percentage of number of cells (mean ± S.E.M) of five animals in each group and were plotted as a histogram producing two populations with high and low mitochondrial $\Delta\Psi$. Statistic analysis were performed using Student's *t*-test. ($p < 0.05$).

Figure 1

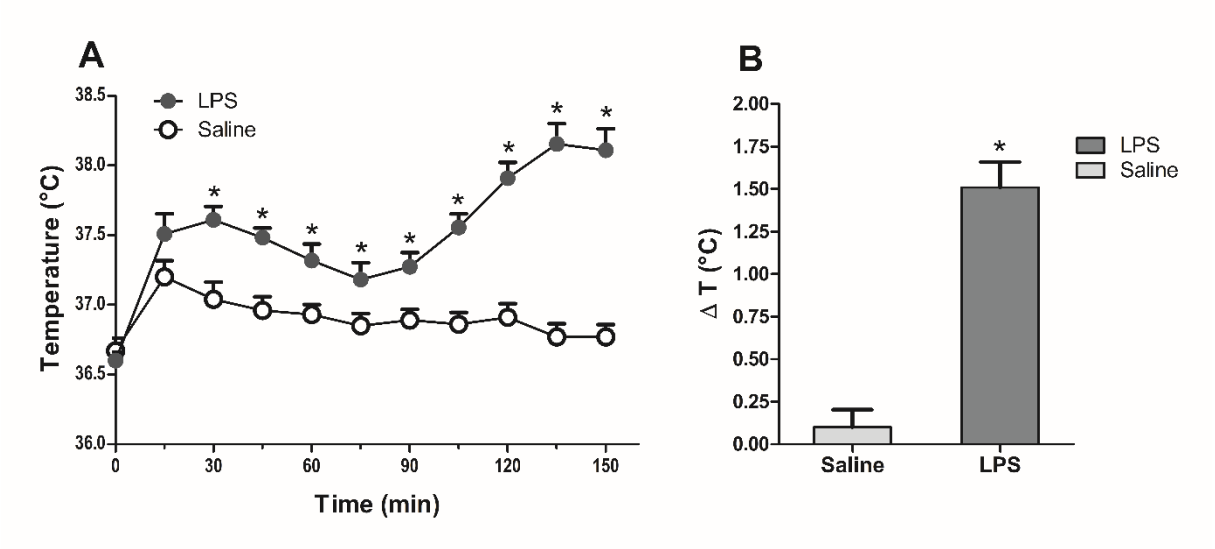
A
LPS
Saline
Temperature (°C)
38.5
38.0
37.5
37.0
36.5
36.0
0
30
60
90
120
150
Time (min)
B
2.00
1.75
1.50
1.25
1.00
0.75
0.50
0.25
0.00
Δ T (°C)
LPS
Saline
Saline
LPS

Figure 2

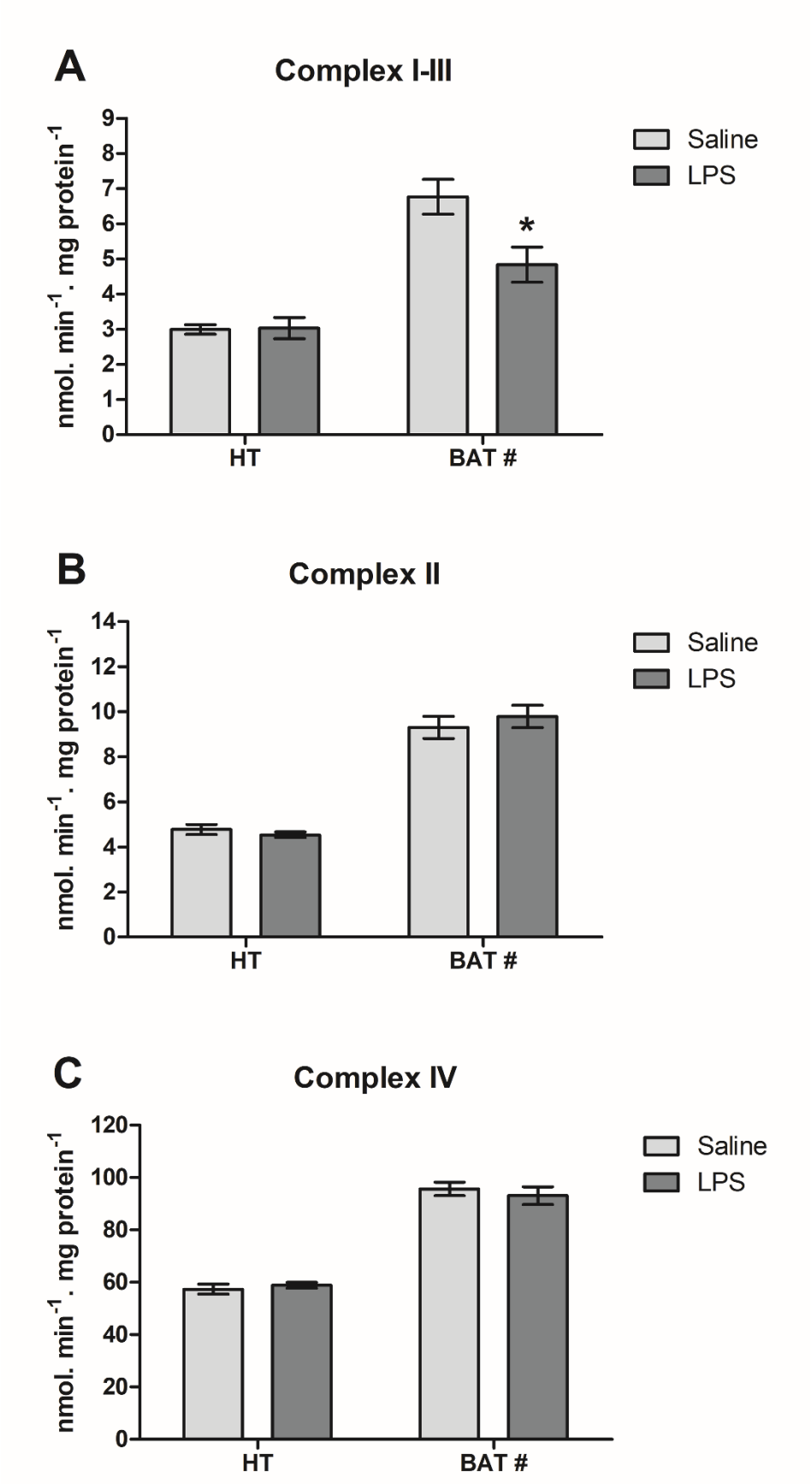
A
Complex I-III
nmol. min-1. mg protein-1
9
8
7
6
5
4
3
2
1
0
*
HT
BAT #
Saline
LPS
B
Complex II
nmol. min-1. mg protein-1
14
12
10
8
6
4
2
0
HT
BAT #
Saline
LPS
C
Complex IV
nmol. min-1. mg protein-1
120
100
80
60
40
20
0
HT
BAT #
Saline
LPS

Figure 3

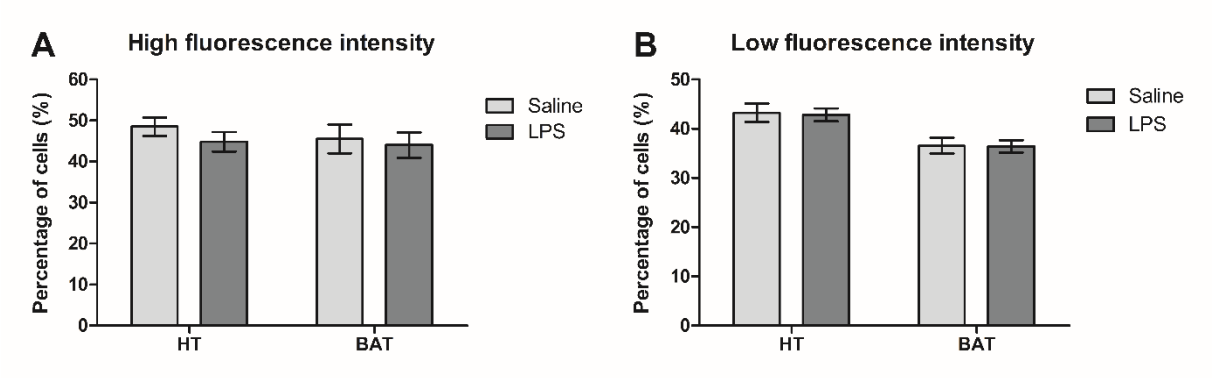
A
High fluorescence intensity
Percentage of cells (%)
60
50
40
30
20
10
0
HT
BAT
Saline
LPS
B
Low fluorescence intensity
Percentage of cells (%)
50
40
30
20
10
0
HT
BAT
Saline
LPS

5. Capítulo 3

Inibição farmacológica das proteínas cinases, PKA e PKC – **Dados não publicados**

1. Introdução

Durante processos infecciosos o aumento da temperatura corporal não ocorre como um evento isolado, mas sim, como parte de uma complexa resposta de defesa controlada pelo cérebro, que se desenvolve em resposta a invasão do organismo por agentes patogênicos. Esta resposta é mediada pela ativação de processos fisiológicos, imunológicos e neuroendócrinos que levam ao desenvolvimento da resposta febril (EVANS; REPASKY; FISHER, 2015; ROTH; BLATTEIS, 2014). A administração de LPS em roedores representa o modelo clássico para estudo dos mecanismos de indução de febre (ROTH; BLATTEIS, 2014).

A resposta febril que se desenvolve em decorrência da administração do LPS é iniciada pelo reconhecimento desta molécula pelo seu receptor (TLR4), e consequente indução de uma série de eventos intracelulares que culminam na ativação do fator de transcrição NFκB (CONTI et al., 2004; KLUGER, 1991; ROTH et al., 2009; ZEISBERGER, 1999). Além desta via clássica, associada ao NFκB, a estimulação do receptor TLR4 pelo LPS desencadeia outras vias de sinalização intracelular, onde estão envolvidos segundos mensageiros como adenosina 3',5'-monofosfato cíclico (AMPc), guanosina monofosfato cíclico (GMPc), diacilglicerol (DAG), inositol trifosfato (IP3) e cálcio (Ca^{2+}) (YAN et al., 2016). Estes segundos mensageiros, por sua vez, amplificam os sinais extracelulares através da ativação de proteínas cinases como, por exemplo, proteína cinase C (PKC) e proteína cinase dependente de AMPc (PKA), que atuam fosforilando outras proteínas da cascata de sinalização até a ativação de fatores de transcrição (LOEGERING; LENNARTZ, 2011; YAN et al., 2016).

A prostaglandina E_2 (PGE_2) é um mediador lipídico sintetizado por macrófagos ativados por pirogênios exógenos e endógenos, que exerce seus efeitos pela ligação aos receptores EP (OKA, 2004). Evidências sugerem que o receptor EP3 seja o principal responsável pelo desenvolvimento de febre em resposta a PGE_2 (USHIKUBI et al., 1998). Especificamente para o receptor EP3 foram descritas diferentes isoformas (SUGIMOTO; NARUMIYA, 2007). Em

roedores foram identificadas 3 isoformas (α; β e γ) e em humanos são descritas pelo menos 8 isoformas deste receptor (HATA; BREYER, 2004; KALINSKI, 2012). A sinalização mediada pelos receptores EP3 envolve a participação de segundos mensageiros como AMPc, IP3 e Ca^{2+}, e, dependendo da isoforma ativada, pode-se observar aumento ou diminuição de AMPc e aumento de IP3/Ca^{2+} (OKA, 2004).

Considerando a participação de proteínas cinases em vias de sinalização intracelular, incluindo àquelas desencadeadas por LPS e PGE_2, buscou-se neste trabalho investigar a participação das cinases PKC e PKA, através do uso de inibidores farmacológicos na sinalização responsável pela produção de febre induzida por LPS e PGE_2 no hipotálamo.

2. Materiais e Métodos

2.1 Animais

Os experimentos foram realizados utilizando-se ratos (*Rattus novergicus*), variedade *Wistar*, machos, pesando entre 180 e 200 g. Os animais foram fornecidos pelo Biotério do Instituto de Biologia (IB) da Universidade de Brasília (UnB) e mantidos em sala com temperatura (24 ± 1 °C) e umidade (50 %) controladas, com ciclo claro/escuro de 12 h e livre acesso à ração e água durante todo o experimento. Os procedimentos cirúrgicos e experimentos farmacológicos foram realizados no Laboratório de Bioquímica e Química de Proteínas do IB/UnB, no período entre 8:00 e 18:00 h. Este trabalho foi aprovado pelo comitê de ética no uso animal do IB/UNB sob o número: 30652/2014.

2.2 Drogas

Foram utilizadas as seguintes drogas:

- Estímulos pirogênicos: LPS (endotoxina de *E. coli* 0111:B4, Sigma-Aldrich, St. Louis, EUA) e PGE_2 (prostaglandina E_2 P5640 Sigma-Aldrich, St. Louis, EUA);
- Antiinflamatório: dexametasona (Azium®, Mantecorp Ind. Quím. e Farm. Ltda., Rio de Janeiro, Brasil);
- Antibiótico: cloridrato de oxitetraciclina (Terramicina®, Pfizer, São Paulo, Brasil);
- Anestésicos: cetamina (Ketamin®, Cristália, São Paulo, Brasil); lidocaína e fenilefrina (Novocol 100®, S. S. White Artigos Dentários Ltda, Rio de Janeiro, Brasil); xilazina (Calmiun®, Agener União, São Paulo, Brasil).
- Inibidor não seletivo de PKC: celeritrina (chelerythrine chloride C2932, Sigma-Aldrich, St. Louis, EUA);
- Inibidor não seletivo de PKA: H-89 (H-89 dihydrochloride hydrate B1427, Sigma – Aldrich, St. Louis, EUA);

2.3 Procedimentos Cirúrgicos

2.3.1 Implante de transmissores de temperatura na cavidade peritoneal

Os ratos foram anestesiados com uma mistura de cetamina e xilazina nas doses de 60 mg/kg^{-1} e 10 mg/kg^{-1}, respectivamente, pela via intraperitoneal (i.p.). Após a tricotomia e assepsia da pele, uma incisão de aproximadamente 2 cm na pele e músculos peritoneais foi feita para inserção do transmissor (Subcue dataloggers, Calgary, Canadá), previamente esterilizado em álcool 70% e lavado com solução salina estéril, na cavidade peritoneal. Em seguida, os músculos e a pele foram suturados separadamente.

2.3.2 Implante de cânulas no ventrículo lateral direito

Imediatamente após a cirurgia para implante dos transmissores de temperatura, procedeu-se o implante de cânulas no ventrículo lateral cerebral. Os animais foram tricotomizados, posicionados e fixados em aparelho estereotáxico (Insight, Ribeirão Preto, SP). Após a assepsia da pele da parte superior da cabeça, os animais receberam uma injeção local (subcutânea) de lidocaína 2% e fenilefrina 0,04% (0,2 mL), e uma incisão de aproximadamente 1 cm foi feita para a exposição da calota craniana, a fim de permitir a introdução da cânula intracerebroventricular (i.c.v.). Os parâmetros estereotáxicos utilizados para a perfuração do crânio e posterior implantação da cânula, tendo o bregma como referência, foram: -1,5 mm antero-posterior e -1,6 mm lateralmente ao bregma, sendo a inclinação da barra incisal de -2,5 mm.

As cânulas esterilizadas, constituídas de um segmento de agulha hipodérmica BD-7, com 10 mm de comprimento e 0,7 mm de diâmetro, foram introduzidas no tecido cerebral com coordenada ventral de 2,5 mm abaixo da superfície craniana. Todas as coordenadas utilizadas foram determinadas com base no Atlas de Paxinos e Watson (PAXINOS; WATSON, 2007).

A fixação das cânulas foi feita por meio de uma prótese de acrílico auto-polimerizável com o auxílio de dois parafusos rosqueados à calota craniana. Ao fim da cirurgia, os animais receberam injeção intramuscular de cloridrato de oxitetraciclina (400 mg/kg^{-1} intramuscular) e dexametasona (1 mg/kg^{-1} intramuscular) para uso veterinário. Os animais recém-operados foram, então, mantidos por 2 h sob aquecimento controlado para manutenção da temperatura corporal em uma caixa moradia até a completa recuperação da cirurgia. Após, os animais retornaram ao biotério onde permaneceram, por no mínimo 7 dias, para completa recuperação pós-cirúrgica.

2.4 Aferição da temperatura corporal dos ratos

O processo de aferição da temperatura corporal foi realizado por transmissores implantados na cavidade peritoneal, como descrito anteriormente. Para a ambientação, os ratos permaneceram na sala de experimentação, por pelo menos 12 h, antes do início dos experimentos. Para os experimentos de febre, a temperatura corporal foi monitorada e registrada em intervalos de 10 a 15 min, com início da aferição 2 h antes dos experimentos, prosseguindo por até 6 h após a injeção do estímulo pirogênico. O intervalo entre as medidas e o tempo total de análise variou de acordo com o estímulo utilizado (LPS ou PGE_2). O procedimento experimental foi realizado dentro da zona termoneutra para ratos, ou seja, com a sala experimental sob temperatura controlada a 28 ± 1 °C (GORDON, 1990). A temperatura basal de cada animal foi determinada pela média das aferições 2 h antes de qualquer tratamento. O índice de febre foi calculado subtraindo-se o valor da temperatura basal das medidas individuais (registradas a cada 10 ou 15 min) obtidas após a injeção de LPS ou PGE_2, durante o período total de observação. Foi calculada a área sob a curva (ASC) para cada animal, usando para isto, o índice de febre expresso em unidades arbitrárias.

2.5 Experimentos Farmacológicos

Os animais receberam celeritrina (3 µg em 2 µL de solução salina estéril), um inibidor de PKC, ou H-89 (30 µg em 2 µL de solução salina estéril), um inibidor de PKA, ou somente solução salina (0,9 %, 2 µL) por via intracerebroventricular (i.c.v), 30 min antes da administração dos estímulos pirogênicos. As doses dos inibidores farmacológicos foram selecionadas com base em experimentos prévios (SILVA, 2013). O LPS (5 $\mu g.kg^{-1}$ em solução salina 2 mL.kg) foi administrado por via endovenosa (i.v.) e a PGE_2 (100 ng em 2 µL 0,5 % etanol em salina) foi administrada por via i.c.v. Os animais controle receberam, respectivamente, injeções i.v de solução salina e i.c.v. de veículo (0,5 % etanol em salina). Após

a administração dos estímulos, cada animal teve sua temperatura corporal aferida, por 2 ou 6 h, em intervalos de 10-15 min, dependendo do estímulo pirogênico.

2.6 Análise Estatística

Os dados são apresentados como a média ± EPM (erro padrão da média). As comparações estatísticas foram efetuadas por análise de variância de uma via (ANOVA), ou análise de variância multivariada (MANOVA), seguidas pelo teste de Bonferroni. Para calcular o índice de febre, a temperatura corporal basal média (4 medidas anteriores a qualquer tratamento) foi determinada para cada animal, o valor basal médio foi subtraído de cada medida obtida durante o procedimento experimental, após a injeção dos estímulos. Esta abordagem permitiu o cálculo da área sob a curva (ASC) para cada animal, utilizada como um índice de febre e expresso em unidades arbitrárias. Todas as análises estatísticas foram realizadas utilizando-se o programa *Statistical Package for the Social Sciences* software (SPSS, SPSS Inc. Chicago, IL, USA) versão 23.0. O nível de significância considerado foi de 5 % ($p < 0,05$).

3. Resultados

3.1 Efeito da administração de celeritrina sobre as respostas febris induzidas por LPS e PGE_2

Com o objetivo de investigar a participação da PKC na resposta febril, administrou-se celeritrina (3 µg/2 µL), 30 min antes da injeção dos estímulos. A dose de celeritrina foi selecionada com base em experimentos prévios (SILVA, 2013).

Como pode ser observado na **Figura 1 (A e B)**, os animais pré-administrados com salina, que receberam LPS desenvolveram febre prolongada com início aproximadamente 1,5 h após a injeção e com duração de pelo menos 6 h, período total de observação. Os animais

controle (SAL/SAL e CEL/SAL) não apresentaram resposta febril. A pré-administração de celeritrina promoveu redução (36 %) da resposta febril induzida pelo LPS. Considerando-se a análise estatística de todas as medidas, está redução só foi significativa nos tempos de 4,25; 4,5 e 5,25 h.

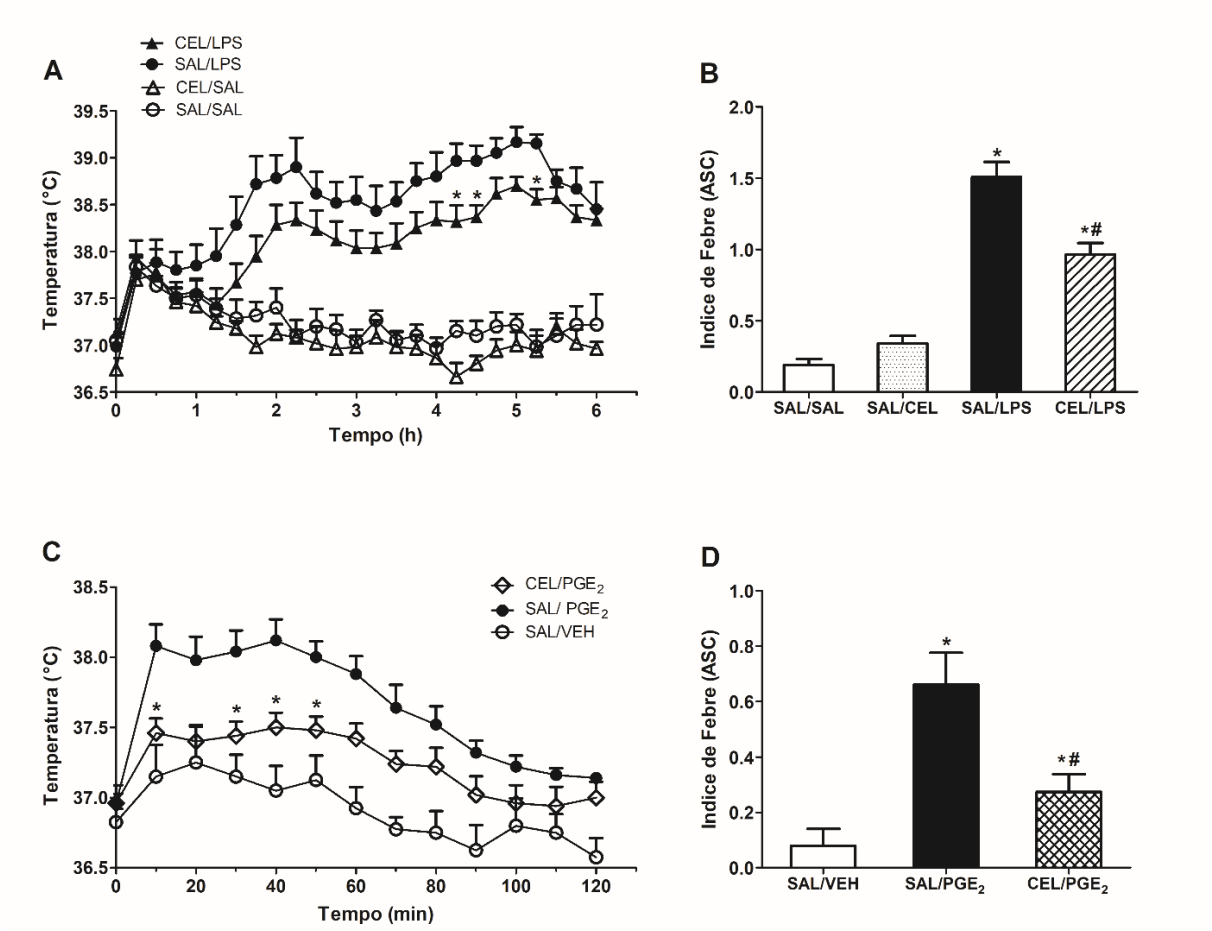

Figura 1: Efeito do pré-tratamento com celeritrina sobre a febre induzida por LPS ou PGE_2 em ratos. Celeritrina (3 µg/2 µL) ou solução salina (0,9 %/ 2 µL) foram administradas 30 min antes das injeções de LPS (5 $\mu g.kg^{-1}$) (A e B); PGE_2 (100 ng/ 2 µL 0,5 % etanol em salina) (C e D), ou seus respectivos controles. Nos painéis A e C, os pontos representam a média ± E.P.M da temperatura corporal (em °C) de 5 a 6 animais, * $p < 0,05$ comparando os grupos CEL/LPS e SAL/LPS ou CEL/PGE_2 e SAL/PGE_2. Nos painéis B e D, as barras representam o índice de febre (ASC em unidades arbitrárias) de 5 a 6 animais. * $p < 0,05$ em comparação aos grupos SAL/SAL ou SAL/VEH, e # $p < 0,05$ em comparação aos grupos SAL/LPS ou SAL/PGE_2.

Ainda na **Figura 1 (C e D)**, podemos observar que os animais pré-administrados com salina que receberam PGE_2 desenvolveram febre com uma duração total de pouco mais de uma

hora. A administração do veículo não induziu resposta febril. A administração de celeritrina promoveu uma redução significativa (58,6 %) da febre induzida por PGE_2. Esta redução é evidenciada nos tempos de 30, 40 e 50 min.

3.2 Efeito da administração de H-89 sobre as respostas febris induzidas por LPS e PGE_2

A participação da PKA na resposta febril também foi investigada. Para isso, utilizou-se o inibidor H-89 (30 µg/2 µL) administrado 30 min antes da injeção dos estímulos pirogênicos. A dose de H-89 também foi selecionada com base em uma curva dose-resposta realizada previamente (SILVA, 2013).

Na **Figura 2 (A e B)**, pode-se observar que os animais pré-administrados com salina que receberam LPS desenvolveram febre prolongada com início aproximadamente 1,5 h após a injeção e com duração total de aproximadamente 6 h. Os animais controle (SAL/SAL e H-89/SAL) não desenvolveram febre. A pré-administração de H-89 promoveu uma significativa redução (57,6 %) da resposta febril induzida pelo LPS. Esta redução se iniciou 2 h após a injeção do estímulo pirogênico e permaneceu por todo o período de observação (6 h).

Quando analisamos o efeito da administração de H-89 sobre a febre induzida pela PGE_2 **(Figura 2, C e D)**, podemos observar que este inibidor não foi capaz de reduzi-la.

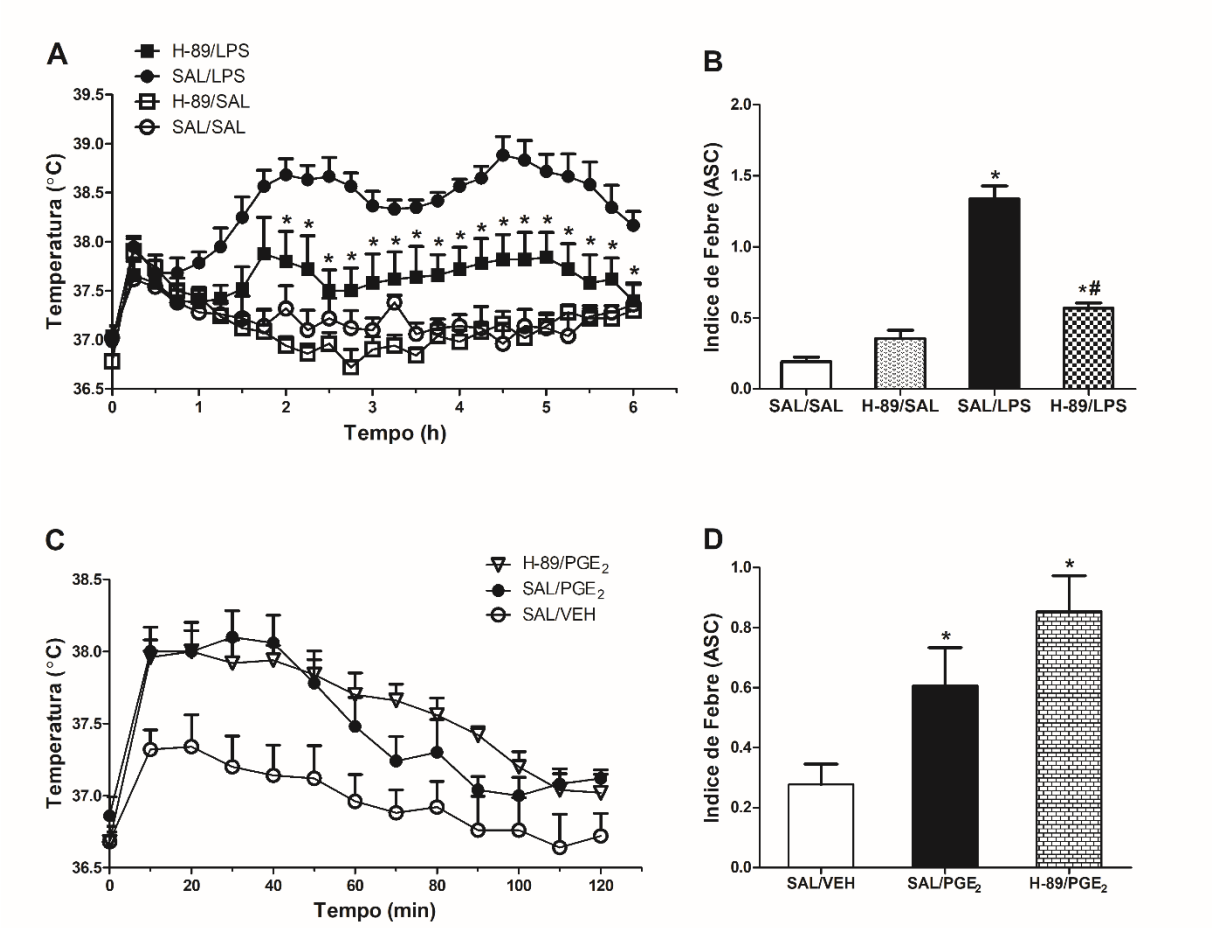

Figura 2: Efeito do pré-tratamento com H-89 sobre a febre induzida por LPS ou PGE_2 em ratos. H-89 (30 µg/2 µL) ou solução salina (0,9 %/ 2 µL) foram administradas 30 min antes das injeções de LPS (5 $\mu g.kg^{-1}$) (A e B); PGE_2 (100 ng/ 2 µL 0,5 % etanol em salina) (C e D), ou seus respectivos controles. Nos painéis A e C, os pontos representam a média ± E.P.M da temperatura corporal (em °C) de 5 a 6 animais, * $p < 0,05$ comparando os grupos H-89/LPS e SAL/LPS ou H-89/PGE_2 e SAL/PGE_2. Nos painéis B e D, as barras representam o índice de febre (ASC em unidades arbitrárias) de 5 a 6 animais. * $p < 0,05$ em comparação aos grupos SAL/SAL ou SAL/VEH, e # $p < 0,05$ em comparação aos grupos SAL/LPS ou SAL/PGE_2.

4. Discussão

Evidências iniciais do envolvimento de PKC e PKA na sinalização do receptor TLR4, vem de experimentos demonstrando que a inibição dessas cinases reduzem a secreção de citocinas e mediadores inflamatórios após a administração de LPS, em células do sistema imune (AVNI et al., 2010; DÍAZ-MUÑOZ et al., 2012; FRONHOFER; LENNARTZ; LOEGERING, 2006; KONTNY et al., 2000; ZHOU; YANG; LI, 2006).

A PKC pertence a uma família de cinases de serina e treonina envolvidas na transdução de sinais intracelulares. As isoformas de PKC são estruturalmente relacionadas, mas possuem padrões distintos de distribuição e função nos tecidos. São divididas em 3 subfamílias com base nos seus padrões de ativação: 1) convencionais ou clássicas (PKC-α, -βI, -βII e –γ) que requerem cálcio, diacilglicerol e fosfatidilserina para sua ativação; 2) novas (PKC-δ, -ε, -η e –θ) que requerem diacilglicerol e fosfatidilserina, mas são independentes de cálcio; e 3) atípicas (PKC-ζ e –λ) que requerem apenas fosfatidilserina para sua ativação (NEWTON, 2003; NISHIZUKA, 1992).

Diversos estudos têm apontado a participação de isoformas de PKC na sinalização mediada pelo TLR4. Em macrófagos, a *down-regulation* de PKC-δ diminui, de maneira expressiva, a ativação de p38 MAPK e NFκB mediada pela ativação de TLR4 (KUBO-MURAI et al., 2007). Em camundongos nocaute para PKC-ε observou-se que diversos aspectos da resposta imune permaneciam normais, entretanto os macrófagos apresentavam deficiência na produção de TNF-α, IL-1β, PGE_2 e óxido nítrico, e na ativação de MAPK e NFκB, após estimulação por LPS (CASTRILLO et al., 2001). A PKC-ε tem sido referida como um componente essencial na via de sinalização relacionada a ativação de macrófagos e células dendrítricas após estimulação por LPS (AKSOY; GOLDMAN; WILLEMS, 2004).

Neste trabalho observou-se que a celeritrina reduziu parcialmente a resposta febril induzida por LPS, demonstrando a participação de PKC na via de sinalização relacionada a produção de febre. De maneira semelhante, Kozak e colaboradores também demonstraram o envolvimento de PKC na resposta febril induzida por LPS. Foram utilizados dois inibidores de PKC, com diferentes constantes de inibição, e verificou-se que o pré-tratamento (via subcutânea) com esses inibidores reduziu, tanto a febre, quanto o aumento da concentração plasmática de IL-6, induzida pela injeção intraperitoneal de LPS em ratos (KOZAK et al., 1997).

A PKA altera as atividades de proteínas-alvo fosforilando grupos específicos de serina e treonina. Na sua forma inativa, a PKA apresenta-se como uma holoenzima, formada por duas subunidades catalíticas e duas subunidades regulatórias. Quando há aumento dos níveis intracelulares de AMPc, duas moléculas de AMPc se ligam as duas subunidades regulatórias da PKA, promovendo a liberação das subunidades catalíticas e a ativação da proteína. São descritos 2 subtipos de PKA, sendo identificadas diferentes isoformas para as subunidades regulatória (RIα; RIβ; RIIα; e RIIβ) e catalíticas (Cα; Cβ e Cγ) (CADD; STANLEY MCKNIGHT, 1989).

Sabe-se que a via de sinalização intracelular do AMPc contribui para indução de COX-2 e ativação da transcrição de mPGES-1 após administração do LPS (DÍAZ-MUÑOZ et al., 2012). Neste estudo, a administração do inibidor H-89 reduziu de maneira significativa a resposta febril induzida por LPS.

Fortes evidencias sugerem que a resposta febril mediada pela PGE_2 depende da ligação aos receptores EP3, presentes na AH/POA (LAZARUS, 2006; NAKAMURA et al., 2000; USHIKUBI et al., 1998). A principal via de sinalização atribuída a este receptor envolve a inibição de adenilil ciclase, por meio da sinalização mediada por uma proteína G inibitória (Gi), reduzindo, desta forma, a formação de AMPc e, por consequência, a atividade de PKA. A ativação dos receptores EP3 pela PGE_2 promove a redução dos níveis de AMPc e consequentemente a ativação de PKA, estando esse mecanismo intimamente associado ao desenvolvimento de febre. Esta sinalização diminui as taxas de disparo dos neurônios sensíveis ao calor na AH/POA, desencadeando parte da sinalização necessária para aumento da temperatura corporal (STEINER; BRANCO, 2003). Os resultados apresentados demonstram que o H-89 não foi capaz de inibir a febre induzida pela administração de PGE_2. De acordo com a hipótese de que a sinalização desencadeada pela PGE_2 levaria a diminuição da atividade de PKA, é esperado que a inibição desta cinase não tenha efeito sobre a febre induzida pela PGE_2.

Em contrapartida, outros estudos afirmam que a PGE_2 estimularia a produção de AMPc no hipotálamo por meio da ativação de receptores EP1. Dessa forma, o AMPc atuaria de forma semelhante a uma molécula neurotransmissora/sinalizadora nos neurônios ativando a sinalização necessária para o desenvolvimento de febre (DINARELLO, 2004).

Apesar de o H-89 ser frequentemente utilizado como inibidor especifico de PKA, tem sido demonstrado que ele inibe pelo menos outras 8 cinases (LOCHNER; MOOLMAN, 2006), assim, a possível existência de efeitos independentes de PKA podem dificultar a análise da participação desta proteína na sinalização da resposta febril. A inibição adicional de MAPKs pode ajudar a explicar a significativa redução observada na febre induzida pelo LPS, quando da pré-administração de H-89.

Diferentes isoformas para o receptor EP3 são descritas na literatura. Estas isoformas possuem a capacidade de acoplar-se a múltiplas proteínas G e desencadear diferentes vias de sinalização. Quando ativado por um agonista, o receptor EP3 pode promover a morte por necrose de neutrófilos pela ativação de PKC, uma via de sinalização diferente da tipicamente conhecida para necrose e apoptose (LIU et al., 2000). Nossos dados sugerem o envolvimento parcial da PKC na sinalização induzida por PGE_2. Entretanto, mais estudos são necessários para compreender os mecanismos envolvidos nesta resposta.

Espera-se que a inibição de proteínas cinases esteja relacionada à produção de efeitos colaterais, visto que estas proteínas desempenham diversas funções em processos fisiológicos. No entanto, vários inibidores de cinases tem demonstrado ser bem tolerados durante ensaios clínicos (COHEN, 2002; GERALDES; KING, 2010; ROFFEY et al., 2009). Os resultados aqui apresentados contribuem para compreensão dos mecanismos envolvidos na gênese da resposta febril, bem como para delinear possíveis alvos para controle farmacológico da febre.

5. Referências Bibliográficas

AKSOY, E.; GOLDMAN, M.; WILLEMS, F. Protein kinase C epsilon: a new target to control inflammation and immune-mediated disorders. **The International Journal of Biochemistry & Cell Biology**, v. 36, n. 2, p. 183–188, fev. 2004.

AVNI, D. et al. Role of CREB in modulation of TNFα and IL-10 expression in LPS-stimulated RAW264.7 macrophages. **Molecular Immunology**, v. 47, n. 7–8, p. 1396–1403, abr. 2010.

CADD, G.; STANLEY MCKNIGHT, G. Distinct patterns of cAMP-dependent protein kinase gene expression in mouse brain. **Neuron**, v. 3, n. 1, p. 71–79, 1 jul. 1989.

CASTRILLO, A. et al. Protein kinase Cepsilon is required for macrophage activation and defense against bacterial infection. **The Journal of experimental medicine**, v. 194, n. 9, p. 1231–42, 5 nov. 2001.

COHEN, P. Protein kinases — the major drug targets of the twenty-first century? **Nature Reviews Drug Discovery**, v. 1, n. 4, p. 309–315, 1 abr. 2002.

CONTI, B. et al. Cytokines and fever. **Frontiers in bioscience : a journal and virtual library**, v. 9, n. 4, p. 1433–49, 1 maio 2004.

DÍAZ-MUÑOZ, M. D. et al. Involvement of PGE2 and the cAMP signalling pathway in the up-regulation of COX-2 and mPGES-1 expression in LPS-activated macrophages. **The Biochemical journal**, v. 443, n. 2, p. 451–61, 15 abr. 2012.

DINARELLO, C. A. Infection, fever, and exogenous and endogenous pyrogens: some concepts have changed. **Journal of endotoxin research**, v. 10, n. 4, p. 201–22, 2004.

EVANS, S. S.; REPASKY, E. A.; FISHER, D. T. Fever and the thermal regulation of immunity: the immune system feels the heat. **Nature Reviews Immunology**, v. 15, n. 6, p. 335–349, 15 jun. 2015.

FRONHOFER, V.; LENNARTZ, M. R.; LOEGERING, D. J. Role of PKC isoforms in the Fc(gamma)R-mediated inhibition of LPS-stimulated IL-12 secretion by macrophages. **Journal of leukocyte biology**, v. 79, n. 2, p. 408–15, 19 fev. 2006.

GERALDES, P.; KING, G. L. Activation of Protein Kinase C Isoforms and Its Impact on Diabetic Complications. **Circulation Research**, v. 106, n. 8, p. 1319–1331, 30 abr. 2010.

GORDON, C. J. Thermal biology of the laboratory rat. **Physiology & behavior**, v. 47, n. 5, p. 963–91, maio 1990.

HATA, A. N.; BREYER, R. M. Pharmacology and signaling of prostaglandin receptors: multiple roles in inflammation and immune modulation. **Pharmacology & therapeutics**, v. 103, n. 2, p. 147–66, ago. 2004.

KALINSKI, P. Regulation of Immune Responses by Prostaglandin E2. **The Journal of Immunology**, v. 188, n. 1, p. 21–28, 1 jan. 2012.

KLUGER, M. J. Fever: role of pyrogens and cryogens. **Physiological reviews**, v. 71, n. 1, p. 93–127, jan. 1991.

KONTNY, E. et al. Rottlerin, a PKC isozyme-selective inhibitor, affects signaling events and

cytokine production in human monocytes. **Journal of leukocyte biology**, v. 67, n. 2, p. 249–58, fev. 2000.

KOZAK, W. et al. Attenuation of lipopolysaccharide fever in rats by protein kinase C inhibitors. **The American journal of physiology**, v. 273, n. 3 Pt 2, p. R873-9, set. 1997.

KUBO-MURAI, M. et al. Protein kinase Cδ binds TIRAP/Mal to participate in TLR signaling. **Molecular Immunology**, v. 44, n. 9, p. 2257–2264, mar. 2007.

LAZARUS, M. The differential role of prostaglandin E2 receptors EP3 and EP4 in regulation of fever. **Molecular nutrition & food research**, v. 50, n. 4–5, p. 451–5, abr. 2006.

LIU, J. et al. Induction of neutrophil death resembling neither apoptosis nor necrosis by ONO-AE-248, a selective agonist for PGE2 receptor subtype 3. **Journal of leukocyte biology**, v. 68, n. 2, p. 187–93, ago. 2000.

LOCHNER, A.; MOOLMAN, J. A. The many faces of H89: a review. **Cardiovascular drug reviews**, v. 24, n. 3–4, p. 261–74, 2006.

LOEGERING, D. J.; LENNARTZ, M. R. Protein Kinase C and Toll-Like Receptor Signaling. **Enzyme Research**, v. 2011, p. 1–7, 2011.

NAKAMURA, K. et al. Immunohistochemical localization of prostaglandin EP3 receptor in the rat nervous system. **The Journal of Comparative Neurology**, v. 421, n. 4, p. 543–569, 12 jun. 2000.

NEWTON, A. C. Regulation of the ABC kinases by phosphorylation: protein kinase C as a paradigm. **The Biochemical journal**, v. 370, n. Pt 2, p. 361–71, 1 mar. 2003.

NISHIZUKA, Y. Intracellular signaling by hydrolysis of phospholipids and activation of protein kinase C. **Science (New York, N.Y.)**, v. 258, n. 5082, p. 607–14, 23 out. 1992.

OKA, T. Prostaglandin E2 as a mediator of fever: the role of prostaglandin E (EP) receptors. **Frontiers in bioscience : a journal and virtual library**, v. 9, p. 3046–57, 1 set. 2004.

PAXINOS, G.; WATSON, C. **The rat brain in stereotaxic coordinates**. [s.l.] Elsevier, 2007.

ROFFEY, J. et al. Protein kinase C intervention—the state of play. **Current Opinion in Cell Biology**, v. 21, n. 2, p. 268–279, abr. 2009.

ROTH, J. et al. Molecular aspects of fever and hyperthermia. **Immunology and allergy clinics of North America**, v. 29, n. 2, p. 229–45, maio 2009.

ROTH, J.; BLATTEIS, C. M. Mechanisms of fever production and lysis: lessons from experimental LPS fever. **Comprehensive Physiology**, v. 4, n. 4, p. 1563–604, out. 2014.

STEINER, A. A.; BRANCO, L. G. S. Fever and anapyrexia in systemic inflammation: intracellular signaling by cyclic nucleotides. **Frontiers in bioscience : a journal and virtual library**, v. 8, p. s1398-408, 1 set. 2003.

SUGIMOTO, Y.; NARUMIYA, S. Prostaglandin E receptors. **The Journal of biological chemistry**, v. 282, n. 16, p. 11613–7, 20 abr. 2007.

USHIKUBI, F. et al. Impaired febrile response in mice lacking the prostaglandin E receptor subtype EP3. **Nature**, v. 395, n. 6699, p. 281–4, 17 set. 1998.

YAN, K. et al. The cyclic AMP signaling pathway: Exploring targets for successful drug discovery (Review). **Molecular medicine reports**, v. 13, n. 5, p. 3715–23, maio 2016.

ZEISBERGER, E. From humoral fever to neuroimmunological control of fever. **Journal of Thermal Biology**, v. 24, n. 5–6, p. 287–326, 1999.

ZHOU, X.; YANG, W.; LI, J. Ca2+- and protein kinase C-dependent signaling pathway for nuclear factor-kappaB activation, inducible nitric-oxide synthase expression, and tumor necrosis factor-alpha production in lipopolysaccharide-stimulated rat peritoneal macrophages. **The Journal of biological chemistry**, v. 281, n. 42, p. 31337–47, 20 out. 2006.

6. Discussão

Nesta tese, investigamos vias de sinalização e alterações bioquímicas envolvidas na gênese da resposta febril induzida pelos estímulos de LPS e PGE_2. Mais especificamente, investigamos alterações proteômicas e sinalizações desencadeadas por administrações sistêmica de LPS e intracerebroventricular de PGE_2, assim como alterações mitocondriais induzidas por LPS no hipotálamo e tecido adiposo marrom. Este trabalho foi realizado com o objetivo de obtermos uma melhor compreensão a respeito dos mecanismos relacionados ao desenvolvimento da febre, e quais os efeitos desta resposta nos tecidos mencionados.

O LPS é um pirogênio exógeno conhecido por ser amplamente utilizado em estudos experimentais para caracterização dos processos fisiológicos, imunológicos e neuroendócrinos que constituem a base da resposta febril (ROTH; BLATTEIS, 2014). A administração sistêmica deste estímulo mimetiza uma resposta infecciosa sendo, portanto, acompanhada de um complexo processo inflamatório, acompanhado do desenvolvimento de febre (DINARELLO, 2004). O LPS é capaz de estimular diferentes vias de sinalização que levam a produção de citocinas pró-inflamatórias e outros mediadores que podem, direta ou indiretamente, produzir febre pela estimulação da produção de PGE_2 na AH/POA (DINARELLO, 2004; ROTH et al., 2009; ROTH; BLATTEIS, 2014). A PGE_2 é um pirogênio endógeno que se liga aos receptores termossensíveis na AH/POA e desencadeia os mecanismos necessários para o aumento da temperatura corporal (TANSEY; JOHNSON, 2015). Considerando a natureza destes estímulos, e sua inter-relação, decidimos avaliar as alterações promovidas por eles para melhor compreender o desenvolvimento da resposta febril.

O **capítulo 1** desta tese teve por objetivo, investigar as principais alterações proteômicas induzidas no hipotálamo durante a resposta febril induzida por LPS e PGE_2. Um total de 1.388 proteínas diferencialmente expressas foram identificadas no grupo LPS, e 895 no grupo PGE_2. Podemos observar que ambos os estímulos induzem alterações significativas no proteoma do hipotálamo. Entretanto, o LPS promove alterações na abundância de uma quantidade maior de

proteínas, fato este esperado considerando a complexidade da resposta induzida por este estímulo e o tempo selecionado para as análises.

Para o grupo LPS, selecionamos o tempo de 150 min, após a administração do estímulo para a coleta do hipotálamo, momento onde podemos visualizar uma diferença significativa entre o grupo LPS e o seu respectivo controle. Segundo dados da literatura, em 150 min é possível observar a ativação do fator de transcrição NFκB, a produção de diversas citocinas, dentre elas TNF-α, IL-1β e IL-6, além da ativação da sinalização das MAPKs (JANSKÝ et al., 1995; LEE et al., 2003; PARNET; POUSSET; LAYE, 2003; ROTH; DE SOUZA, 2001; SABIO; DAVIS, 2014). Neste estudo foi possível identificar um aumento na abundância de várias proteínas relacionadas a sinalização das MAPKs e NFκB, corroborando a hipótese da ativação destas vias em células hipotalâmicas durante a febre. Entretanto, como mencionado anteriormente, na resposta febril induzida pelo LPS ocorre a produção de diversas citocinas, de modo que os efeitos observados no proteoma hipotalâmico podem ser devidos, em parte, a ação desses mediadores e seus subprodutos e não somente pela ação direta do LPS. Quando o estímulo utilizado foi a PGE_2, não foram observadas alterações significativas na sinalização do NFκB. Por outro lado, acredita-se que a via da JNK seja ativada por este estímulo em função do aumento na abundância de proteínas envolvidas nesta sinalização.

O papel da PGE_2 como mediador final da resposta febril está bem estabelecido e documentado (IVANOV; ROMANOVSKY, 2004; ROTH; BLATTEIS, 2014; SAPER; ROMANOVSKY; SCAMMELL, 2012). Contudo, o local de produção da PGE_2 que atua sobre a AH/POA produzindo febre é ainda um tema controverso. Outro ponto de discussão está na discrepância entre o tempo necessário para indução das enzimas que catalisam a produção de PGE_2 e o início da primeira fase da febre induzida por LPS. Diversos estudos indicam que a ativação genômica das células endoteliais cerebrais e a subsequente formação de PGE_2 através das isoformas COX-2/mPGES-1 está melhor relacionado a manutenção da febre do que ao seu

início (ROTH; BLATTEIS, 2014). Nossos resultados demonstram o aumento na expressão da enzima cPGES em ambos estímulos, sugerindo um possível mecanismo para rápida produção central de PGE_2 durante a primeira fase da resposta febril, por meio da sinalização de COX-1/cPGES. Em macrófagos, foi demonstrado que a PGE_2 estimula a expressão de COX-2 e m-PGES-1 (DÍAZ-MUÑOZ et al., 2012), assim sendo a PGE_2 produzida durante a primeira fase da resposta febril via COX-1/cPGES, poderia contribuir ainda para síntese de COX-2/m-PGES-1 e consequentemente produção de PGE_2 e manutenção da resposta febril.

Alterações significativas foram observadas nas vias de sinalização do AMPc e cálcio provocadas pela administração de ambos os estímulos. No **capítulo 3** desta tese, descrevemos o resultado da inibição farmacológica de PKA e PKC. Estas análises foram realizadas com o objetivo de melhor compreender como estas proteínas se relacionam com o desenvolvimento da resposta febril. Pela análise proteômica do hipotálamo, observamos que LPS e PGE_2 induziram aumento na abundância de diferentes isoformas de AC e PKA.

Nos testes farmacológicos observamos que o H-89, um inibidor de PKA, reduziu de maneira significativa a febre induzida por LPS, sem qualquer alteração na febre induzida pela PGE_2. A interpretação destes dados foi dificultada pelo fato de H-89 inibir outras cinases além de PKA (LOCHNER; MOOLMAN, 2006). A significativa inibição observada na febre, induzida por LPS, pode ser devido a inibição de outras MAPKs, que reconhecidamente participam desta via de sinalização (AHMED; WILLIAMS; HANNIGAN, 2015; ROUX; BLENIS, 2004; SUN; NAN, 2016). Considerando a sinalização relacionada à PGE_2, os dados proteômicos demonstram aumento na abundância de uma proteína G estimulatória (Gs), proteína esta que pode se ligar a uma das isoformas do receptor EP3 ou mediar a sinalização de outros subtipos do receptor EP. Pelo aumento na abundância das proteínas envolvidas na sinalização mediada por Gs/AC/PKA sugere-se que esta via pode estar relacionada à produção de febre. Entretanto, mais estudos precisam ser realizados para observar qual o receptor seria

responsável pela ativação desta via, e ainda se existe aumento de atividade da via em resposta à PGE_2.

Em relação à PKC, ambos os estímulos provocaram aumento de sua abundância no hipotálamo. No grupo LPS, mais de uma isoforma de PKC (β e γ), apresentou abundância aumentada. Além disso, tanto em LPS quanto em PGE_2 houve a redução na abundância de uma proteína referida como substrato de PKC (*PKC substrate 80K-H* – Prkcsh). Os resultados farmacológicos mostraram que a celeritrina, um inibidor não seletivo de PKC, reduziu a resposta febril produzida por ambos os estímulos.

Em células eucarióticas, as vias de sinalização do Ca^{2+} e AMPc atuam de forma cooperativa. Foi observado que em células tratadas com agentes que aumentam simultaneamente os níveis de Ca^{2+} e AMPc há o desenvolvimento de respostas sinérgicas (VAJANAPHANICH et al., 1995; YAN et al., 2016). Este trabalho demonstrou o aumento na abundância de diversas proteínas associadas a via do AMPc e Ca^{2+}, além de redução da febre quando foram utilizados inibidores de PKA e PKC. Desta forma, sugere-se que estas vias possam atuar de maneira conjunta durante a resposta febril.

Em relação às vias metabólicas, os dados proteômicos demonstram que a maioria das proteínas associadas ao metabolismo tiveram sua abundância diminuída nos grupos LPS e PGE_2, em comparação aos respectivos controles. Em geral, observamos uma diminuição na abundância de proteínas envolvidas na glicólise, via das pentoses-fosfato, ciclo de Krebs e complexos mitocondriais.

Uma vez que as mitocôndrias são as organelas responsáveis pela produção de calor, decidimos avaliar as possíveis alterações na função mitocondrial do hipotálamo (HT) e tecido adiposo marrom (BAT), durante a resposta febril induzida por LPS (**Capítulo 2**). No HT, apesar dos dados proteômicos evidenciarem a redução na abundância de diversas proteínas dos complexos da cadeia de transporte de elétrons mitocondrial, isso não comprometeu a função

dos complexos, nem afetou o potencial de membrana, 2,5 h após a administração do LPS. Entretanto, em trabalhos anteriores do nosso grupo foi observado aumento na produção de espécies reativas de oxigênio (ROS; de *Reactive Oxygen Species*) 5 h após a administração do LPS (GOMES et al., 2018). Assim sendo, é possível que esta redução na abundância das proteínas mitocondriais na fase inicial da resposta febril possa representar o início de alterações moderadas que irão contribuir para produção de ROS durante a segunda fase desta resposta. A análise proteômica demonstrou ainda, redução de diversas proteínas antioxidantes, em resposta a administração de LPS, o que pode contribuir para o estresse oxidativo observado em 5 h (GOMES et al, 2018). Apesar destas alterações a nível mitocondrial, observamos aumento na abundância de proteínas anti-apoptóticas e diminuição na abundância de proteínas pró-apoptóticas, sugerindo uma possível resposta adaptativa das células para evitar a morte celular e consequentemente a injúria neuronal.

Durante a febre, o BAT funciona como um órgão efetor, produzindo calor principalmente na primeira fase da resposta febril (CANNON; HOUSTEK; NEDERGAARD, 1998). Assim sendo, neste tecido observamos diminuição do fluxo de elétrons entre os complexos I e III, sem alteração do potencial de membrana mitocondrial. Esta redução pode contribuir para o maior escape de elétrons e formação de ROS, que por sua vez contribui com a sensibilização de UCPs e indução da termogênese.

Por fim, o metabolismo de lipídeos também foi impactado pela administração dos estímulos no hipotálamo. O ácido araquidônico, liberado a partir de glicerofosfolipídeos de membrana, é um importante precursor para produção de prostaglandinas. Após administração do LPS, foi observado aumento na abundância de proteínas associadas a síntese de glicerofosfolipídeos contendo ácido araquidônico, assim como de proteínas que viabilizam a reincorporação de ácido araquidônico livre. Após a administração de PGE_2, observou-se redução na abundância da maioria das proteínas relacionadas ao metabolismo de lipídeos.

O conhecimento das vias metabólicas envolvidas na resposta febril é importante não somente para melhor compreender os mecanismos pelos quais esta resposta se desenvolve, mas também para avaliar efeitos metabólicos decorrentes dela. A análise destas vias pode ainda acelerar o desenvolvimento de agentes terapêuticos mais específicos e com menor incidência de efeitos colaterais.

7. Conclusão

Os resultados obtidos nestes estudos nos permitem concluir que:

1. Os estímulos pirogênicos, LPS e PGE_2, produzem significativas alterações na abundância de diversas proteínas hipotalâmicas. Estas proteínas estão principalmente associadas a vias inflamatórias e metabólicas. De maneira geral, grande parte das proteínas relacionadas a glicólise, via das pentoses-fosfato e ciclo de Krebs apresentaram redução na abundância. Ocorreram também alterações em proteínas dos complexos mitocondriais, com maior redução na abundância de proteínas dos complexos I e IV. O LPS, em especial, foi capaz de reduzir a abundância de diversas proteínas do sistema antioxidante, bem como alterar a abundância de proteínas associadas ao metabolismo de lipídeos.

2. O tecido adiposo marrom (BAT) apresenta maior atividade mitocondrial em comparação ao hipotálamo. Este tecido mostrou-se mais susceptível a administração de LPS, apresentando comprometimento do fluxo de elétrons entre os complexos I e III, sem, entretanto, alterar o potencial de membrana. Nenhuma alteração, nem na atividade dos complexos nem no potencial de membrana mitocondrial, foi observada no hipotálamo em 2,5 h após a administração de LPS. Estes dados sugerem que a febre induzida por LPS causa uma inibição parcial da atividade mitocondrial no BAT, que pode contribuir para o desenvolvimento da primeira fase da resposta febril.

3. A celeritrina reduziu parcialmente as respostas febris induzidas por LPS e PGE_2, demonstrando a participação de PKC na via de sinalização relacionada à produção de febre em resposta a administração destes estímulos. Entretanto, mais estudos são necessários para compreender os mecanismos envolvidos nesta resposta. O H-89

promoveu uma maior redução da resposta febril induzida por LPS, em comparação com celeritrina. Já na resposta febril induzida pela PGE_2 observamos que o H-89 não teve efeito algum. Apesar de ser utilizado como inibidor específico de PKA, sabe-se que o H-89 pode inibir outras cinases como, por exemplo, as MAPKs. A inibição adicional de MAPKs pode ajudar a explicar a significativa redução observada na febre induzida pelo LPS, quando da pré-administração de H-89.

8. Perspectivas

1. Selecionar as principais proteínas alteradas em resposta aos dois estímulos pirogênicos e investigar o papel delas de maneira específica, a fim de tentar identificar marcadores moleculares da resposta febril.

2. Realizar análise metabolômica para identificar os mediadores lipídicos envolvidos na resposta febril, correlacionando-os com as alterações proteômicas identificadas neste trabalho.

3. Avaliar a presença de alterações mitocondriais durante a segunda fase da resposta febril induzida por LPS, bem como durante a febre induzida por PGE_2.

9. Referências Bibliográficas

ABBAS ABUK K.; LICHTMAN ANDREW H. H.; PILLAI SHIV. **Imunologia Celular e Molecular**. 8. ed. 2016.

AHMED, A. U.; WILLIAMS, B. R. G.; HANNIGAN, G. E. Transcriptional Activation of Inflammatory Genes: Mechanistic Insight into Selectivity and Diversity. **Biomolecules**, v. 5, n. 4, p. 3087–111, 11 nov. 2015.

AKIRA, S.; TAKEDA, K. Toll-like receptor signalling. **Nature Reviews Immunology**, v. 4, n. 7, p. 499–511, jul. 2004.

AKIRA, S.; UEMATSU, S.; TAKEUCHI, O. Pathogen Recognition and Innate Immunity. **Cell**, v. 124, n. 4, p. 783–801, 24 fev. 2006.

ARONOFF, D. M.; NEILSON, E. G. Antipyretics: mechanisms of action and clinical use in fever suppression. **The American journal of medicine**, v. 111, n. 4, p. 304–15, set. 2001.

BARACOS, V. E.; WHITMORE, W. T.; GALE, R. The metabolic cost of fever. **Canadian journal of physiology and pharmacology**, v. 65, n. 6, p. 1248–54, jun. 1987.

BASTOS-PEREIRA, A. L. et al. Central mediators involved in the febrile response induced by polyinosinic–polycytidylic acid: Lack of involvement of endothelins and substance P. **Journal of Neuroimmunology**, v. 278, p. 100–107, 15 jan. 2015.

BERNHEIM, H. A.; KLUGER, M. J. Fever: effect of drug-induced antipyresis on survival. **Science (New York, N.Y.)**, v. 193, n. 4249, p. 237–9, 16 jul. 1976.

BLATTEIS, C. M. Endotoxic fever: New concepts of its regulation suggest new approaches to its management. **Pharmacology & Therapeutics**, v. 111, n. 1, p. 194–223, jul. 2006.

BOUILLAUD, F. et al. Molecular approach to thermogenesis in brown adipose tissue: cDNA cloning of the mitochondrial uncoupling protein. **Proceedings of the National Academy of Sciences of the United States of America**, v. 82, n. 2, p. 445–8, jan. 1985.

BOULANT, J. A. Role of the preoptic-anterior hypothalamus in thermoregulation and fever. **Clinical infectious diseases : an official publication of the Infectious Diseases Society of America**, v. 31 Suppl 5, n. Supplement 5, p. S157-61, 1 out. 2000.

BOULANT, J. A.; DEAN, J. B. Temperature receptors in the central nervous system. **Annual review of physiology**, v. 48, n. 1, p. 639–54, out. 1986.

BOULANT, J. A.; SILVA, N. L. Neuronal sensitivities in preoptic tissue slices: interactions among homeostatic systems. **Brain research bulletin**, v. 20, n. 6, p. 871–8, jun. 1988.

BROWN, J. et al. TLR-signaling networks: an integration of adaptor molecules, kinases, and cross-talk. **Journal of dental research**, v. 90, n. 4, p. 417–27, 12 abr. 2011.

CANNON, B.; HOUSTEK, J.; NEDERGAARD, J. Brown adipose tissue. More than an effector of thermogenesis? **Annals of the New York Academy of Sciences**, v. 856, n. 1 MOLECULAR MEC, p. 171–187, set. 1998.

CANNON, B.; NEDERGAARD, J. Brown adipose tissue: function and physiological significance. **Physiological reviews**, v. 84, n. 1, p. 277–359, jan. 2004.

CAO, W. et al. β-Adrenergic Activation of p38 MAP Kinase in Adipocytes. **Journal of Biological Chemistry**, v. 276, n. 29, p. 27077–27082, 20 jul. 2001.

COLEMAN, R. A.; SMITH, W. L.; NARUMIYA, S. International Union of Pharmacology classification of prostanoid receptors: properties, distribution, and structure of the receptors and their subtypes. **Pharmacological reviews**, v. 46, n. 2, p. 205–29, jun. 1994.

CONTRERAS, C. et al. The brain and brown fat. **Annals of Medicine**, v. 47, n. 2, p. 150–168, 17 fev. 2015.

DANTZER, R. Cytokine-induced sickness behaviour: a neuroimmune response to activation of innate immunity. **European journal of pharmacology**, v. 500, n. 1–3, p. 399–411, 1 out. 2004.

DEMON, D.; VANDE WALLE, L.; LAMKANFI, M. Sensing the enemy within: how macrophages detect intracellular Gram-negative bacteria. **Trends in biochemical sciences**, v. 39, n. 12, p. 574–6, 1 dez. 2014.

DERIJK, R. H. et al. Fever and thermogenesis in response to bacterial endotoxin involve macrophage-dependent mechanisms in rats. **The American journal of physiology**, v. 265, n. 5 Pt 2, p. R1179-83, nov. 1993.

DÍAZ-MUÑOZ, M. D. et al. Involvement of PGE2 and the cAMP signalling pathway in the up-regulation of COX-2 and mPGES-1 expression in LPS-activated macrophages. **The Biochemical journal**, v. 443, n. 2, p. 451–61, 15 abr. 2012.

DINARELLO, C. A. Infection, fever, and exogenous and endogenous pyrogens: some concepts have changed. **Journal of endotoxin research**, v. 10, n. 4, p. 201–22, 2004.

ENGSTRÖM, L. et al. Lipopolysaccharide-Induced Fever Depends on Prostaglandin E2 Production Specifically in Brain Endothelial Cells. **Endocrinology**, v. 153, n. 10, p. 4849–4861, out. 2012.

ESKILSSON, A. et al. Immune-Induced Fever Is Dependent on Local But Not Generalized Prostaglandin E2 Synthesis in the Brain. **The Journal of neuroscience : the official journal of the Society for Neuroscience**, v. 37, n. 19, p. 5035–5044, 10 maio 2017.

EVANS, S. S.; REPASKY, E. A.; FISHER, D. T. Fever and the thermal regulation of immunity: the immune system feels the heat. **Nature Reviews Immunology**, v. 15, n. 6, p. 335–349, 15 jun. 2015.

FORTIER, M.-E. The viral mimic, polyinosinic:polycytidylic acid, induces fever in rats via an interleukin-1-dependent mechanism. **AJP: Regulatory, Integrative and Comparative Physiology**, v. 287, n. 4, p. R759–R766, 27 maio 2004.

FRAIFELD, V.; KAPLANSKI, J. Brain eicosanoids and LPS fever: species and age differences. **Progress in brain research**, v. 115, p. 141–57, 1998.

GOMES, B. R. B. et al. Increase of reactive oxygen species in different tissues during lipopolysaccharide-induced fever and antipyresis: an electron paramagnetic resonance study. **Free Radical Research**, p. 1–11, 26 jan. 2018.

HARDEN, L. M. et al. Interleukin-6 and leptin mediate lipopolysaccharide-induced fever and

sickness behavior. **Physiology & Behavior**, v. 89, n. 2, p. 146–155, 30 set. 2006.

HARDEN, L. M. et al. Fever and sickness behavior: Friend or foe? **Brain, Behavior, and Immunity**, v. 50, p. 322–333, nov. 2015.

HASDAY, J. D.; FAIRCHILD, K. D.; SHANHOLTZ, C. The role of fever in the infected host. **Microbes and infection**, v. 2, n. 15, p. 1891–904, dez. 2000.

HASDAY, J. D.; THOMPSON, C.; SINGH, I. S. Fever, Immunity, and Molecular Adaptations. In: **Comprehensive Physiology**. Hoboken, NJ, USA: John Wiley & Sons, Inc., 2014. v. 4p. 109–148.

HATAE, N.; SUGIMOTO, Y.; ICHIKAWA, A. Prostaglandin receptors: advances in the study of EP3 receptor signaling. **Journal of biochemistry**, v. 131, n. 6, p. 781–4, jun. 2002.

IVANOV, A. I.; ROMANOVSKY, A. A. Prostaglandin E2 as a mediator of fever: synthesis and catabolism. **Frontiers in bioscience : a journal and virtual library**, v. 9, n. 1–3, p. 1977–93, 1 maio 2004.

JANSKÝ, L. et al. Production of systemic and hypothalamic cytokines during the early phase of endotoxin fever. **Neuroendocrinology**, v. 62, n. 1, p. 55–61, jul. 1995.

KANASHIRO, A. et al. Characterization and pharmacological evaluation of febrile response on zymosan-induced arthritis in rats. **AJP: Regulatory, Integrative and Comparative Physiology**, v. 296, n. 5, p. R1631–R1640, 1 maio 2009.

KAWAI, T.; AKIRA, S. TLR signaling. **Cell Death and Differentiation**, v. 13, p. 816–825, 2006.

KAWAI, T.; AKIRA, S. The role of pattern-recognition receptors in innate immunity: update on Toll-like receptors. **Nature Immunology**, v. 11, n. 5, p. 373–384, 20 maio 2010.

KAWASAKI, T.; KAWAI, T. Toll-like receptor signaling pathways. **Frontiers in immunology**, v. 5, n. SEP, p. 461, 2014.

KLUGER, M. J. Phylogeny of fever. **Federation proceedings**, v. 38, n. 1, p. 30–4, jan. 1979.

KLUGER, M. J. Fever: role of pyrogens and cryogens. **Physiological reviews**, v. 71, n. 1, p. 93–127, jan. 1991.

KLUGER, M. J. et al. The adaptive value of fever. **Infectious disease clinics of North America**, v. 10, n. 1, p. 1–20, mar. 1996.

KONG, Y.; LE, Y. **Toll-like receptors in inflammation of the central nervous systemInternational Immunopharmacology**, out. 2011. Disponível em: <http://www.ncbi.nlm.nih.gov/pubmed/21600311>. Acesso em: 2 out. 2017

KOTANI, M. et al. Molecular cloning and expression of multiple isoforms of human prostaglandin E receptor EP3 subtype generated by alternative messenger RNA splicing: multiple second messenger systems and tissue-specific distributions. **Molecular pharmacology**, v. 48, n. 5, p. 869–79, nov. 1995.

KRAUSS, S.; ZHANG, C.-Y.; LOWELL, B. B. The mitochondrial uncoupling-protein homologues. **Nature Reviews Molecular Cell Biology**, v. 6, n. 3, p. 248–261, 1 mar. 2005.

KREGEL, K. C. Invited Review: Heat shock proteins: modifying factors in physiological stress responses and acquired thermotolerance. **Journal of Applied Physiology**, v. 92, n. 5, p. 2177–2186, maio 2002.

KUROSAWA, S. et al. Effects of antipyretics in rinderpest virus infection in rabbits. **The Journal of infectious diseases**, v. 155, n. 5, p. 991–7, maio 1987.

LAUNEY, Y. et al. Clinical review: fever in septic ICU patients--friend or foe? **Critical care (London, England)**, v. 15, n. 3, p. 222, 2011.

LEE, J.-J. et al. Blocking NF-kappaB activation may be an effective strategy in the fever therapy. **The Japanese journal of physiology**, v. 53, n. 5, p. 367–75, out. 2003.

LI, Z. et al. Kupffer cell-generated PGE2 triggers the febrile response of guinea pigs to intravenously injected LPS. **American journal of physiology. Regulatory, integrative and comparative physiology**, v. 290, n. 5, p. R1262-70, 22 maio 2006.

LOCHNER, A.; MOOLMAN, J. A. The many faces of H89: a review. **Cardiovascular drug reviews**, v. 24, n. 3–4, p. 261–74, 2006.

LU, Z.; XU, S. ERK1/2 MAP kinases in cell survival and apoptosis. **IUBMB Life**, v. 58, n. 11, p. 621–631, 2006.

LUHESHI, G.; ROTHWELL, N. Cytokines and fever. **International archives of allergy and immunology**, v. 109, n. 4, p. 301–7, abr. 1996.

MANTHOUS, C. A. et al. Effect of cooling on oxygen consumption in febrile critically ill patients. **American journal of respiratory and critical care medicine**, v. 151, n. 1, p. 10–4, jan. 1995.

MARTINS, J. M. et al. Involvement of PGE2 and RANTES in Staphylococcus aureus-induced fever in rats. **Journal of Applied Physiology**, v. 113, n. 9, p. 1456–1465, 1 nov. 2012.

MATTHIAS, A. et al. Thermogenic Responses in Brown Fat Cells Are Fully UCP1-dependent. **Journal of Biological Chemistry**, v. 275, n. 33, p. 25073–25081, 18 ago. 2000.

MEDZHITOV, R.; HORNG, T. Transcriptional control of the inflammatory response. **Nature reviews. Immunology**, v. 9, n. 10, p. 692–703, out. 2009.

MOLTENI, M.; GEMMA, S.; ROSSETTI, C. The Role of Toll-Like Receptor 4 in Infectious and Noninfectious Inflammation. **Mediators of Inflammation**, v. 2016, p. 1–9, 2016.

MORRISON, S. F. Central control of body temperature. **F1000Research**, v. 5, n. 0, p. 880, 12 maio 2016.

MORRISON, S. F.; MADDEN, C. J.; TUPONE, D. Central Neural Regulation of Brown Adipose Tissue Thermogenesis and Energy Expenditure. **Cell Metabolism**, v. 19, n. 5, p. 741–756, 6 maio 2014.

NAGAI, Y. et al. Essential role of MD-2 in LPS responsiveness and TLR4 distribution. **Nature Immunology**, v. 3, n. 7, p. 667–72, 10 jun. 2002.

NAKAMURA, K. et al. Immunocytochemical localization of prostaglandin EP3 receptor in the rat hypothalamus. **Neuroscience Letters**, v. 260, n. 2, p. 117–120, 29 jan. 1999.

NAKAMURA, K. et al. Immunohistochemical localization of prostaglandin EP3 receptor in the rat nervous system. **The Journal of Comparative Neurology**, v. 421, n. 4, p. 543–569, 12 jun. 2000.

NAKAMURA, K. Central circuitries for body temperature regulation and fever. **AJP: Regulatory, Integrative and Comparative Physiology**, v. 301, n. 5, p. R1207–R1228, 1 nov. 2011.

NAMBA, T. et al. Alternative splicing of C-terminal tail of prostaglandin E receptor subtype EP3 determines G-protein specificity. **Nature**, v. 365, n. 6442, p. 166–170, 9 set. 1993.

NARUMIYA, S.; SUGIMOTO, Y.; USHIKUBI, F. Prostanoid receptors: structures, properties, and functions. **Physiological reviews**, v. 79, n. 4, p. 1193–226, out. 1999.

OELKRUG, R.; POLYMEROPOULOS, E. T.; JASTROCH, M. Brown adipose tissue: physiological function and evolutionary significance. **Journal of Comparative Physiology B**, v. 185, n. 6, p. 587–606, 13 ago. 2015.

OGOINA, D. Fever, fever patterns and diseases called 'fever'--a review. **Journal of infection and public health**, v. 4, n. 3, p. 108–24, ago. 2011.

PÅLSSON-MCDERMOTT, E. M.; O'NEILL, L. A. J. Signal transduction by the lipopolysaccharide receptor, Toll-like receptor-4. **Immunology**, v. 113, n. 2, p. 153–162, 2004.

PARNET, P.; POUSSET, F.; LAYE, S. NF kappa B activation in mouse pituitary: comparison of response to interleukin-1 beta and lipopolysaccharide. **Journal of neuroendocrinology**, v. 15, n. 3, p. 304–14, mar. 2003.

PECCHI, E. et al. Prostaglandins and sickness behavior: Old story, new insights. **Physiology & Behavior**, v. 97, n. 3–4, p. 279–292, 22 jun. 2009.

RAETZ, C. R. H. et al. Lipid A Modification Systems in Gram-Negative Bacteria. **Annual Review of Biochemistry**, v. 76, n. 1, p. 295–329, 7 jun. 2007.

RAETZ, C. R. H.; WHITFIELD, C. Lipopolysaccharide Endotoxins. **Annual Review of Biochemistry**, v. 71, n. 1, p. 635–700, jun. 2002.

RAHIMIFARD, M. et al. Targeting the TLR4 signaling pathway by polyphenols: A novel therapeutic strategy for neuroinflammation. **Ageing research reviews**, v. 36, p. 11–19, jul. 2017.

ROTH, J. et al. Fever and production of cytokines in response to repeated injections of muramyl dipeptide in guinea-pigs. **Pflugers Archiv European Journal of Physiology**, v. 434, n. 5, p. 525–533, 11 ago. 1997.

ROTH, J. et al. Molecular aspects of fever and hyperthermia. **Immunology and allergy clinics**

of North America, v. 29, n. 2, p. 229–45, maio 2009.

ROTH, J.; BLATTEIS, C. M. Mechanisms of fever production and lysis: lessons from experimental LPS fever. **Comprehensive Physiology**, v. 4, n. 4, p. 1563–604, out. 2014.

ROTH, J.; DE SOUZA, G. E. Fever induction pathways: evidence from responses to systemic or local cytokine formation. **Brazilian journal of medical and biological research = Revista brasileira de pesquisas medicas e biologicas**, v. 34, n. 3, p. 301–14, mar. 2001.

ROTONDO, D. et al. Pyrogenic immunomodulators increase the level of prostaglandin E2 in the blood simultaneously with the onset of fever. **European journal of pharmacology**, v. 154, n. 2, p. 145–52, 13 set. 1988.

ROUX, P. P.; BLENIS, J. ERK and p38 MAPK-activated protein kinases: a family of protein kinases with diverse biological functions. **Microbiology and molecular biology reviews : MMBR**, v. 68, n. 2, p. 320–44, 1 jun. 2004.

RUMMEL, C. Inflammatory transcription factors as activation markers and functional readouts in immune-to-brain communication. **Brain, Behavior, and Immunity**, v. 54, p. 1–14, maio 2016.

RYAN, M.; LEVY, M. M. Clinical review: fever in intensive care unit patients. **Critical care (London, England)**, v. 7, n. 3, p. 221–5, jun. 2003.

SABIO, G.; DAVIS, R. J. TNF and MAP kinase signalling pathways. **Seminars in Immunology**, v. 26, n. 3, p. 237–245, jun. 2014.

SAPER, C. B.; ROMANOVSKY, A. A.; SCAMMELL, T. E. Neural circuitry engaged by prostaglandins during the sickness syndrome. **Nature Neuroscience**, v. 15, n. 8, p. 1088–1095, 26 jul. 2012.

SCHILTZ, J. C.; SAWCHENKO, P. E. Distinct brain vascular cell types manifest inducible cyclooxygenase expression as a function of the strength and nature of immune insults. **The Journal of neuroscience : the official journal of the Society for Neuroscience**, v. 22, n. 13, p. 5606–18, 1 jul. 2002.

SCHMID, A. et al. Splice variants of the human EP3 receptor for prostaglandin E2. **European journal of biochemistry**, v. 228, n. 1, p. 23–30, 15 fev. 1995.

SILVA, M. F.*Efeito de inibidores de proteínas quinases sobre a resposta febril e a expressão de proteínas em ratos.* 2013. 62 folhas. Dissertação (Mestrado em Patologia Molecular) - Faculdade de Medicina, Universidade de Brasília, Brasília, 2013.

SINGH, I. S.; HASDAY, J. D. Fever, hyperthermia and the heat shock response. **International Journal of Hyperthermia**, v. 29, n. 5, p. 423–435, 17 ago. 2013.

STITT, J. T. Differential sensitivity in the sites of fever production by prostaglandin E1 within the hypothalamus of the rat. **The Journal of physiology**, v. 432, p. 99–110, jan. 1991.

SUGIMOTO, Y.; NARUMIYA, S. Prostaglandin E receptors. **The Journal of biological chemistry**, v. 282, n. 16, p. 11613–7, 20 abr. 2007.

SUN, J.; NAN, G. The Mitogen-Activated Protein Kinase (MAPK) Signaling Pathway as a Discovery Target in Stroke. **Journal of molecular neuroscience : MN**, v. 59, n. 1, p. 90–8, 3 maio 2016.

TANSEY, E. A.; JOHNSON, C. D. Recent advances in thermoregulation. **Advances in Physiology Education**, v. 39, n. 3, p. 139–148, set. 2015.

TAO, C. et al. Short-Term Versus Long-Term Effects of Adipocyte Toll-Like Receptor 4 Activation on Insulin Resistance in Male Mice. **Endocrinology**, v. 158, n. 5, p. 1260–1270, 1 maio 2017.

TAYLOR, K. R. et al. Hyaluronan Fragments Stimulate Endothelial Recognition of Injury through TLR4. **Journal of Biological Chemistry**, v. 279, n. 17, p. 17079–17084, 23 abr. 2004.

TORTORA, C. L. C.; GERARD J. BERDELL R. FUNKE. **Micro biologia**. 12a. ed. Porto Alegre: Artmed, 2017.

TSENG, P. et al. Different modes of ubiquitination of the adaptor TRAF3 selectively activate the expression of type I interferons and proinflammatory cytokines. **Nature immunology**, v. 11, n. 1, p. 70–5, jan. 2010.

TUPONE, D.; MADDEN, C. J.; MORRISON, S. F. Autonomic regulation of brown adipose tissue thermogenesis in health and disease: potential clinical applications for altering BAT thermogenesis. **Frontiers in Neuroscience**, v. 8, n. 8 FEB, p. 1–14, 2014.

USHIKUBI, F. et al. Impaired febrile response in mice lacking the prostaglandin E receptor subtype EP3. **Nature**, v. 395, n. 6699, p. 281–4, 17 set. 1998.

VAJANAPHANICH, M. et al. Cross-talk between calcium and cAMP-dependent intracellular signaling pathways. Implications for synergistic secretion in T84 colonic epithelial cells and rat pancreatic acinar cells. **Journal of Clinical Investigation**, v. 96, n. 1, p. 386–393, 1 jul. 1995.

VASILACHE, A. M.; ANDERSSON, J.; NILSBERTH, C. Expression of PGE2 EP3 receptor subtypes in the mouse preoptic region. **Neuroscience Letters**, v. 423, n. 3, p. 179–183, 23 ago. 2007.

VAUGHN, L. K.; VEALE, W. L.; COOPER, K. E. Antipyresis: Its effect on mortality rate of bacterially infected rabbits. **Brain Research Bulletin**, v. 5, n. 1, p. 69–73, 1980.

VAURE, C.; LIU, Y. A comparative review of toll-like receptor 4 expression and functionality in different animal species. **Frontiers in immunology**, v. 5, n. JUL, p. 316, 10 jul. 2014.

WANG, X.; QUINN, P. J. Lipopolysaccharide: Biosynthetic pathway and structure modification. **Progress in lipid research**, v. 49, n. 2, p. 97–107, abr. 2010.

YAMAGATA, K. et al. Coexpression of microsomal-type prostaglandin E synthase with cyclooxygenase-2 in brain endothelial cells of rats during endotoxin-induced fever. **The Journal of neuroscience : the official journal of the Society for Neuroscience**, v. 21, n. 8, p. 2669–77, 15 abr. 2001.

YAN, K. et al. The cyclic AMP signaling pathway: Exploring targets for successful drug discovery (Review). **Molecular medicine reports**, v. 13, n. 5, p. 3715–23, maio 2016.

ZAMPRONIO, A. R.; SOARES, D. M.; SOUZA, G. E. P. Central mediators involved in the febrile response: effects of antipyretic drugs. **Temperature**, v. 2, n. 4, p. 506–521, 2 out. 2015.

ZANONI, I. et al. CD14 controls the LPS-induced endocytosis of toll-like receptor 4. **Cell**, v. 147, n. 4, p. 868–880, 11 nov. 2011.

ZEISBERGER, E. From humoral fever to neuroimmunological control of fever. **Journal of Thermal Biology**, v. 24, n. 5–6, p. 287–326, 1999.

10. Anexos

Anexo 1 – Declaração de Aprovação pelo Comitê de Ética no Uso Animal.

Universidade de Brasília
Instituto de Ciências Biológicas
Comitê de Ética no Uso Animal

Brasília, 11 de abril de 2014.

UNIVERSIDADE DE BRASÍLIA INSTITUTO DE CIÊNCIAS BIOLÓGICAS -UnB-

DECLARAÇÃO

Declaramos que o projeto intitulado "**VIAS DE SINALIZAÇÃO E PROTEÍNAS HIPOTALÂMICAS ENVOLVIDAS NA RESPOSTA FEBRIL INDUZIDA POR LPS/PGE2 EM RATOS**", UnBDOC n.º 30652/2014, sob responsabilidade da Professora Fabiane Hiratsuka Veiga de Souza foi avaliado e aprovado pela Comissão de Ética no Uso Animal (CEUA) do Instituto de Ciências Biológicas da Universidade de Brasília.

UNIVERSIDADE DE BRASÍLIA Comitê de Ética no Uso Animal - UnB -

Prof. Dr. Fernando Pacheco Rodrigues
Coordenador da CEUA

*Este documento se restringe à avaliação ética do projeto supracitado e não substitui outras licenças e permissões que porventura se façam necessárias.

Anexo 2 – Aceite do Manuscrito "Label-free quantitative proteomics of rat hypothalamus under fever induced by LPS and PGE_2" pelo periódico *Journal of Proteomics* com *Minor Revison*.

Journal of PROTEOMICS

Contact us | Help | ?

Username: mvsousa@unb.br
Switch To: Author | Go to: My EES Hub

Version: EES 2018.5

home | main menu | submit paper | guide for authors | register | change details | log out

Submissions Needing Revision for Author Marcelo Valle de Sousa, Ph.D.

A submission has been returned to you for revision. To revise the submission, click 'File Inventory' in the Actions menu to download any files requiring revision. When you are ready to submit the revised files, click 'Revise Submission' and then 'OK' to begin the submission process.

For more information, click here, or view this short tutorial on submitting a revision.

If you do not want to submit a revised version, click 'Decline to Revise' and then 'OK'. Your submission will be moved to the Declined Revisions folder.

Page: 1 of 1 (1 total submissions) Display 10 results per page.

Action	Manuscript Number	Title	Initial Date Submitted	Date Revision Due	Status Date	Current Status	View Decision
Action Links	JPROT-D-18-00183	Label-free quantitative proteomics of rat hypothalamus under fever induced by LPS and PGE2	Apr 16, 2018	Jul 14, 2018	Jun 14, 2018	Revise	Minor Revision

Page: 1 of 1 (1 total submissions) Display 10 results per page.

<< Author Main Menu

Anexo 3 – Publicação nos anais do congresso "6th International Conference on the Physiology and Pharmacology of Temperature Regulation (PPTR)" realizado na Eslovênia em 2016.

Proteomic profiling of hypothalamus reveals common and differential proteins associated with LPS and PGE_2-induced fever

Marina Lima de Oliveira[1], Bruna Gomes[1], Jaques Sousa[1], Alan Mól[1], Simone Weis[1], Wagner Fontes[1], Carlos André Ricart[1], Marcelo Valle de Sousa[1], Fabiane Veiga-Souza[1,2]

[1]Laboratory of Protein Chemistry and Biochemistry, Departament of Cell Biology, University of Brasilia, Brasília, DF, Brazil, [2]Faculty of Ceilândia, University of Brasília, Brasília, DF, Brazil

Introduction

Fever is defined as the increase in body temperature that occurs as a component of the acute phase response triggered in reaction to injury, trauma or invasion by infectious agents. Systemic administration of lipopolysaccharide (LPS) to experimental animals produces a biphasic fever, accompanied by increase in PGE_2 brain levels. PGE_2 is considered to be the final mediator of pyrogen fever. Previous studies have addressed the molecular pathogenesis of fever, but there have not been any comprehensive mass spectrometry-based proteomic studies to reveal common and differential proteins associated with LPS and PGE_2-induced fevers.

Methods

Experiments were conducted on male Wistar rats (180-200g b.w). The body temperature was measured using intraperitoneally implanted data loggers. The animals received intracerebroventricular (i.c.v.) injection of PGE_2 (100 ng/rat) or intravenous (i.v.) LPS (5 µg/Kg). Control animals received i.c.v. and i.v. injections of vehicle. At the time corresponding to the fever peak induced by each stimulus (30 min for PGE_2 and 150 min for LPS) the animals were euthanized and their hypothalami dissected. Protein extracts prepared from the rats hypothalami were subjected to mass spectrometry-based proteomics (label-free approach) for identification and quantification of differentially abundant proteins.

Results

We identified a total of 6.847 proteins with one unique peptide and a protein FDR of ≤1%. Differentially abundant proteins (fold change ≥1.5) revealed 280 up and 246 down-regulated proteins (LPS/control group) and 158 up and 101 down-regulated proteins (PGE_2/control group). The bioinformatics analysis of proteins linked to immune and inflammatory responses reveals proteins related with oxidative stress, nuclear factor κB, MAPK-signaling and calcium signaling. LPS and PGE_2 treatments evoked 21 common proteins (15 up and 6 down-regulated).

Conclusion: These results improve our knowledge about fever associated signaling pathways and provide a basis for identification of novel therapeutics targets for fever control.

Financial Support: CAPES, CNPq, FINEP and FAPDF.

Anexo 2 – Artigo: Increase of reactive oxygen species in different tissues during lipopolysaccharide-induced fever and antipyresis: an electron paramagnetic resonance study.

FREE RADICAL RESEARCH, 2018
https://doi.org/10.1080/10715762.2018.1425549

Taylor & Francis
Taylor & Francis Group

ORIGINAL ARTICLE

Increase of reactive oxygen species in different tissues during lipopolysaccharide-induced fever and antipyresis: an electron paramagnetic resonance study

Bruna R. B. Gomes[a], Marina Firmino[a], Jardeson S. Jorge[b], Maria L. O. Ferreira[b], Thays M. Rodovalho[b], Simone N. Weis[a], Gloria E. P. Souza[c], Paulo C. Morais[d,e], Marcelo V. Sousa[a], Paulo E. N. Souza[e] and Fabiane H. Veiga-Souza[a,b]

[a]Department of Cell Biology, Laboratory of Protein Chemistry and Biochemistry, Institute of Biology, University of Brasilia, Brasília, Brazil; [b]School of Ceilandia, University of Brasilia, Brasília, Brazil; [c]Laboratory of Pharmacology, School of Pharmaceutical Sciences of Ribeirão Preto, University of São Paulo, Ribeirão Preto, Brazil; [d]School of Chemistry and Chemical Engineering, Anhui University, Hefei, China; [e]Laboratory of Electron Paramagnetic Resonance, Institute of Physics, University of Brasilia, Brasília, Brazil

ABSTRACT

Fever is a regulated increase in body temperature and a component of the acute-phase response, triggered mainly after the invasion of pathogens in the body. Reactive oxygen species (ROS) are generated during the physiological and pathological processes, and can act as both signalling molecules as well as promoters of oxidative stress. Male Wistar rats, pretreated with oral doses of acetaminophen, celecoxib, dipyrone, or ibuprofen 30 min before an intravenous lipopolysaccharide (LPS) or sterile saline injection, showed a reduced febrile response in all animals tested. The formation of ROS in the fresh blood, liver, brown adipose tissue (BAT), and hypothalamus of febrile and antipyretic-treated animals was assessed by electron paramagnetic resonance using the spin probe 1-hydroxy-3-methoxycarbonyl-2,2,5,5-tetramethylpyrrolidine (CMH). While the $CM^{\bullet}$ concentrations remained unaltered in the blood samples examined 5 h after the induction of fever, we found increased $CM^{\bullet}$ levels in the liver (in μM, saline: 290 ± 42; LPS: 512 ± 34), BAT (in μM, saline: 509 ± 79, LPS: 855 ± 79), and hypothalamus (in μM, saline: 292 ± 35; LPS: 467 ± 8) at the same time point. Importantly, none of the antipyretics were seen to alter the $CM^{\bullet}$ accumulation profile. Data from this study suggest that there is an increased formation of ROS in the different tissues during fever, which may cause oxidative stress, and that the antipyretics tested do not interfere with ROS production.

ARTICLE HISTORY
Received 4 September 2017
Revised 21 December 2017
Accepted 5 January 2018

KEYWORDS
Antipyretics; reactive oxygen species (ROS); oxidative stress; EPR; fever

Introduction

Fever is a brain-mediated increase in the body temperature (Tb), usually triggered by the infectious or aseptic stimuli [1]. It is a clinical hallmark of the acute phase response, indicating the occurrence of processes related to infection, inflammation, drug reaction, autoimmune diseases, or neoplasia [2,3]. The preoptic area (POA) of the hypothalamus is generally considered the most important region for temperature homeostasis. It contains the key integrative circuitry for the thermoregulation and fever, being able to detect the temperature changes of local blood flow and activate the thermoregulatory responses required for the maintenance of a constant Tb [4].

Administration of the lipopolysaccharide (LPS), derived from the Gram-negative bacterial cell wall, is a widely used technique to induce fever in the experimental models. LPS acts by binding to the toll-like receptor (TLR) member TLR4, which is known to be present on neurons, microglia, astrocytes and endothelial cells of brain [5–7]. LPS stimulates the different cells to release cytokines (also known as endogenous pyrogens) which, in turn, induce the synthesis of prostaglandins (PG) [5]. Prostaglandin E_2 (PGE_2) is considered to be the final mediator of febrile response. It activates the E prostanoid receptors in the preoptic neurons, thereby altering their intrinsic firing rate, and finally triggers the effector responses, such as vasoconstriction, shivering, and brown adipose tissue (BAT) thermogenesis to increase Tb [1,8].

Antipyretic drugs are widely used in the treatment of fever. The antipyretic action of nonsteroidal anti-inflammatory drugs (NSAIDs), such as ibuprofen and celecoxib, is generally believed to be mediated via the inhibition of cyclooxygenases (COX) 1/2. However, the

CONTACT Fabiane H. Veiga-Souza fhveiga@unb.br Faculdade de Ceilândia, Universidade de Brasília, Centro Metropolitano, Brasília, DF, Brazil